LOCAL SCOUR DUE TO SUBMERGED HORIZONTAL JETS

M.Sc. Thesis

in

Department of Civil Engineering
University of Gaziantep

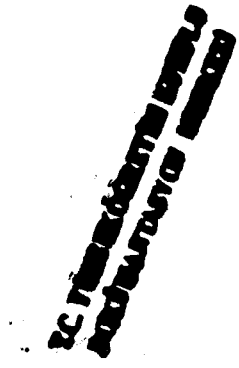

by
Aytaç GÜVEN

June 2003

Approval of the Garduate School of Natural and Applied Sciences

Prof. Dr. Bülent GÖNÜL
Director

I certify that this thesis satisfies all the requirements as a thesis for the degree of Master of Science.

Prof. Dr. Mustafa ÖZAKÇA
Chairman of the Department

This is to certify that we have read this thesis and that in our opinion it is fully adequate, in scope and quality, as a thesis for the degree of Master of Science.

Assist. Prof. Dr. Mustafa GÜNAL
Supervisor

Examining Committee Members:

Prof. Dr. Melda ÇARPINLIOĞLU (Chairman)

Assist. Prof. Dr. Mazen KAVVAS

Assist. Prof. Dr. Mustafa GÜNAL

ABSTRACT

LOCAL SCOUR DUE TO SUBMERGED HORIZONTAL JETS

GÜVEN, Aytaç
M.Sc. in Civil Engineering
Supervisor : Assist Prof. Dr. Mustafa Günal
June 2003, 114 pages

In this thesis, three major studies were done on local scour due to horizontal jets. They are : (i) a detailed literature survey on local scour due to horizontal jets, (ii) investigation on mean and turbulent characteristics of local scour due to horizontal jet and (iii) k-ε turbulence modelling of submerged horizontal jet .

In this thesis, no experimental studies were performed. A wide range of numerical and experimental studies in the literature have been inspected and it was decided to deal with the studies on "frozen scoured beds". This makes it possible to take one scour profile and find the mean characteristics in it for various conditions of flow such as sluice opening, tailwater depth, upstream submerged jet Froude number, and the quantity of flow.

k-ε turbulence modelling of submerged horizontal jet using boundary fitted coordinates is developed to predict the mean and turbulent characteristics within the flow. Two dimensional continuity, momentum and transport equations for turbulence quantities are solved numerically by the finite volume method in boundary fitted coordinates. The SIMPLE algorithm is adapted for the computation. The non-rectangular domain of submerged horizontal jet with scoured bed is transformed to

rectangular computational plane. The transformed equations are then solved initially with a guess that the free surface is flat. After each iteration, the new surface profile is then transformed and mesh is generated again.

The numerical results of this study were presented and compared with the experimental and numerical results of other researchers. It was especially noticed that the distributions of turbulent intensities, Reynolds stresses and bed shear stresses have had peak values in maximum scour depth region. Also reverse flow was observed in maximum scour depth region. The highest deviation of pressure from hydrostatic was also observed in this region. Basicly, strict agreements were obtained between both the experimental and numerical studies of other researchers and the numerical results of this present study.

Keywords: Local scour, submerged horizontal jet, k-ε turbulence modelling, finite volume method, boundary-fitted coordinate system.

ÖZ

BATIK YATAY JETLER ALTINDA LOKAL EROZYON

GÜVEN, Aytaç
Yüksek Lisans Tezi, naat Müh. Bölümü
Tez Yöneticisi : Yrd. Doç. Dr. Mustafa Günal
Haziran 2003, 113 sayfa

Bu tezde, yatay jetler altnda oluan lokal erozyon ile ilgili üç önemli çalma yaplmtr. Bunlar : (i) yatay jetler altnda ouan lokal erozyon hakknda geni bir literatür aratrmas, (ii) yatay jetler altnda oluan lokal erozyonun ortalama ve türbülans karaktersitikleri üzerine aratrma ve (iii) batk yatay jetin k-ε türbülans modellemesi.

Bu tezde deneysel çalma yaplmamtr. Literatürdeki geni kapsaml deneysel ve nümerik çalmalar incelenmi ve "dondurulmu- erozyona uram tabanlar" üzerine çalmaya karar verilmitir. Bu, kapak alt aral, kuyruksuyu derinlii, ak yukar batk jet Froude says ve ak miktar gibi çeitli ak durumlar için tek bir erozyon profilini alp ortalama karakteristiklerinin ölçülebilmesini salamtr.

Ak boyunca ortalama ve türbülans karakteristiklerinin tahmin edilebilmesi için batk yatay jetin, snr-uyumlu koordinat sistemi kullanarak, türbülans modellemesi gelitirilmitir. Türbülans niceliklerinin iki boyutlu süreklilik, momentum ve tama denklemlerinin, snr-uyumlu koordinat sisteminde sonlu hacim metodu kullanlarak, nümerik çözümü yapld. Hesaplamalar için SIMPLE algoritmas adapte edildi. Dikdörtgen eklinde olmayan batk yatay jet ve erozyon nüfuz alan, dikdörtgen hesaplama nüfuz alanna dönütürülmütür. Dönüüm denklemleri daha sonra,

balangçta düz bir serbest yüzey varsaym ile çözümlendi. Her iterasyondan sonra yeni yüzey profili tekrar dönütürüldü ve a tekrar meydana getirildi.

Mevcut çalmann nümerik sonuçlar sunuldu ve bakalarnn deneysel ve nümerik sonuçlaryla karlatrld. Türbülans iddeti, Reynolds gerilmesi ve taban kayma gerilmesi dalmnn, özellikle, maksimum erozyon derinlii bölgesinde en yüksek deerlere sahip olduunun farkna varlmtr. Ayrca, maximum erozyon derinlii bölgesinde ters yönde aka da rastlanmtr. Yine bu bölgede, hidrostatik basnçtan en yüksek derecede sapmalar gözlenmitir. Esas olarak, dier çalmalarn deneysel ve nümerik sonuçlar ile mevcut çalmann nümerik sonuçlar arasnda sk bir uyum elde edilmitir.

Anahtar Kelimeler: Lokal erozyon, batk yatay jet, k-ε türbülans modelleme, sonlu hacim metodu, snr uyumlu koordinat sistemi.

ACKNOWLEDGEMENTS

Firstly, I would like to express my deep gratitude to my supervisor, Assist. Prof. Dr. Mustafa Günal, for his invaluable guidance, continous advice and providing encontinous encouragement. He provided me stimulation and constructive criticism throughout the development of this research.

I would like to sincerely thank to the Scientific and Technical Research Council of Turkey for their financial and moral support throughout my study. Particularly, the University of Gaziantep is gratefully acknowledged.

Sincere thanks to Dr. Adhy Kurniawan, Dr. Simon Gant and Prof.Dr. Rambala Balachandar for their guidance and constructive discussion on internet throughout completion of this thesis. They gave me invaluable advices while dealing with problems during this study.

Lastly, but by no means least, I would like to thank to my family for their continous encouragement and stimulation during the period of this study.

TABLE OF CONTENTS

LIST OF FIGURES

LIST OF TABLES

LIST OF SYMBOLS /ABREVIATIONS

$C_\mu, C_1, C_2, \sigma_k, \sigma_\varepsilon$	empirical constants
c_s	a dimensional coefficient
d	mean size of particles of bed material
d_{50}	mean particle diameter
E	a wall roughness parameter
f	turbulence frequency
F_1	upstream Froude number
F_0	the densimetric Froude number
f_c	roughness coefficient
g	gravitational acceleration
G	turbulence production term
h	depth of water in the channel
J	Jacobian
k	kinetic energy
κ	Von Karman constant
K	a parameter
L, L_s	length scale
l_m	mixing length
N	number of data
n	trial value of power of the relative magnitude of kinetic enrgy to the potential energy
p	instantenous pressure
$\overline{p}$	mean value of fluctuating pressures
p_c	pressure correction
Pe	Peclet number
P_k	the volumetric production rate of k
Q	discharge in m^3s^{-1}

q	discharge per unit width
q_1 to q_9	tranformation coefficients given in Equation 4.25
R	the jet area divided by the perimeter of the jet
Re	Reynolds number
S	submergence factor
s	specific gravity of sand
s_k	skewness coefficient
S_u, S_v, S_k, S_e, S_p	source terms in transformed plane
t	time
u	streamwise component of velocity
u_c, v_c	velocity corrections
$\left(\sqrt{\overline{u'^2}}\right)$	longitudinal turbulent intensity
$-\overline{u'v'}$	turbulent shear stress
U, V	velocities in boundary fitted coordinates
V_s	volume of scour hole per unith width
u*	friction velocity
u_o	surface velocity
u1	upstream velocity
u2	downstream velocity
u_m	streamwise maximum mean velocity
u', v' and p'	fluctuating components of u, v and p
v	vertical component of velocity
$\left(\sqrt{\overline{v'^2}}\right)$	vertical turbulent intensity
x, y	Cartesian coordinate axis in the horizontal and vertical directions
x_ξ, x_η	differentiation of x with respect to ξ, η
y_ξ, y_η	differentiation of y with respect to ξ, η
y_1	upstream depth of water
y_2	downstream depth of water

y'	distance between the maximum velocity and corresponding mean velocity
y_t	tailwater depth
z	pressure deviation from the mean divided by the standard deviation of the pressure
$\dot{\alpha}$	relaxation factor
β	correction factor
β_l	length scale for inner layer
γ	unit weight of water
δij	Kronecker delta, =1 for i=j and =0 for ij
ε	dissipation rate of kinetic energy
η, ξ	curvilinear coordinate axis
ν_t	turbulent kinematic viscosity
ρ	density of water
ρ_s	the density of sediment particle
δ_{la}	length scale for outer layer
σ	standard deviations or r.m.s value of data
τ	Reynolds turbulent shear stress
τ_w	wall shear stress
Φ	dependent variable stands for u, v, k and ε

Chapter 1

Introduction

Horizontal jets are one of the most popular agents of local scour that are extensively investigated by many researchers in the past. Considerable research has been done on two- and three-dimensional wall jets. Rajaratnam (1976) presented a comprehensive bibliography on wall jets. More recent works on turbulent jets were carried out by Altnbilek and Okay (1973), Lim (1985), Salehi-Neyshaboury (1990), Ali and Walley (1992) , Karim and Ali (2000) and Ead and Rajaratnam (2002).

As the water jet is diffused on erodible bed, the scouring potential of the jet, created by high incoming velocity, is usually so strong that the sand grains are immediately dislodged from the surface and transported downstream at a rapid rate. The vertical dimension of scour profile begins to increase at a faster rate than the horizontal dimensions of the scour and the bed material is transported mainly as bed load. But the rate of scouring decreases as the depth of hole increases and the bed velocity reduces to a value that it no more capable of moving the bed material. At this point, we can say that the scour geometry reached its " equilibrium" or "asymptotic" condition.

Scouring is the natural phenomenon caused by the flow of water in rivers and streams. Local scour is the erosion of bed surface and the hydraulic structures due to the impact effect of flowing water. Depending on whether sediment is being supplied from upstream to the scour zone, localized scour can occur in two ways

(a) Clear water scour
(b) Live bed scour

Clear water scour refers to the situation where no sediment is supplied from upstream into the scour zone. Live bed scour, in contrast, occurs where there is general bed load transport by the stream. In this case, sediment is continously being supplied to the areas subjected to scour.

In hydraulic engineering, the prediction and control of erosion are important considerations in the safe design of hydraulic structures, for example, near cooling pools of power plants, bridge piers, in spillway outlets, culvert outlets and spur dikes. Large scale erosion caused by fluid flow local to hydraulic structures is of obvious concern because the foundations can be undermined leading to structural failure. (Nik Hassan and Narayanan, 1985).

Local scour has been also extensively investigated due to its complexity besides its hazardous effects on hydraulic structures by many researchers in the past. The earliest investigation on scour is known to be performed by Rouse (1939). Scour due to horizontal jet was studied by Laursen (1952). Cartens (1966), Rajaratnam and Berry (1977), Altnbilek and Okyay (1973), Ali and Lim (1986) are some of the most important development in understanding the characteristics of local scour due to different conditions.

In the present study, the mean characteristics of the submerged horizontal jets occured on frozen bed profile are investigated numerically by k-ε turbulence model using boundary fitted coordinate system. Fortran 77 compiler is used for iterative running purpose.

Turbulence models are the numerical methods to achieve closure of the time-averaged governing fluid flow equations by providing a scheme for the evaluation of the Reynolds stress terms (Straw, 2000). The aim of any turbulence model is that it can be applied to a wide range of fluid flow situations and provide realistic solutions to mean flow patterns and scalar transport. The numerical studies are preferred by the researchers rather than the experimental studies because the experimental studies are much more expensive and more time consuming. The developments and high capabilities of computers are another factor that numerical studies are preferred. Turbulence models are classified according to the number of equations they add to

the system, and this means adding more complication to the system (El Hadidi, 1998). The types of turbulence modelling is presented in Chapter 2.

k-ε turbulence modelling is one of the most popular and most efficient turbulence models. The succes enjoyed by the k-ε model depends on the application of the wall functions that relate the surface boundary conditions to points in the fluid away from the boundaries. (Straw, 2000). The basic assumption of this method is that the local state of turbulence is characterized by the two parameters k and ε , which are equivalent to the parameter pair k and L because ε is proportional to $k^{3/2}/L$. But this model suffers from rough assumptions and defficiencies in modelling two- and three-dimensional turbulent flows.

In fact, it is more realistic to implement the free surface conditions in Cartesian coordinates (x,y) when we choose a very fine mesh. But it is computationally expensive and needs more computer memory and it is not practical. The boundary fitted cordinate system which is applied in the present thesis, makes this problem far simpler. The main idea of boundary fitted coordinate system is to extend the capabilities of finite difference methods by transforming the complex flow domain (x,y) in the physical space to a simple rectangular flow domain (ζ , η) in the computational space. Boundary conditions are then implemented naturally in the rectangular computational domain. By this method the governing equations look complicated but they are easy to discretize in the rectangular computational domain. In this thesis, transformed governing equations are solved with a finite volume method in the computational domain (ζ , η) to compute the mean flow and turbulence characteristics of submerged horizontal jet occuring on frozen erodible bed.

Because of its popularity and efficiency, several modified k-ε models have been proposed in the literature (the Yap k-ε model (1987), the RNG k-ε model (1986), the Chen-Kim modified k-ε model (1987), etc.). The common objective of different modified k-ε models is to develop the deficiencies of the standard model in dissipation, turbulent viscosity, modelling three-dimensional turbulent flows and improving the time-scale to characterize the dynamic processes in turbulent flows.

In this thesis, no experimental studies were performed. A wide range of numerical and experimental studies in the literature have been inspected and some most relevant studies have been chosen to make comparison with the present study's numerical predictions. Most of the studies have been performed on " local scour due to horizontal jets ", and the author decided to work on the studies on scouring due to horizontal jets. The basic data that are needed for comparison are the initial jet velocity, width of sluice gate opening, the tailwater depth of submerged horizontal jet and the scoured bed profile in equilibrium state.

It is extremely difficult to make measurements of flow characteristics within the fast growing scour hole if it is wanted to relate some mean characteristics (mean velocity distribution, maximum scour depth, etc.) measured at each time increments to the whole scouring process. In deed the early studies proved the similarity of scour profiles at different time increments (Nik Hassan and Narayanan, 1985). This makes it possible to take one scour profile and find the mean characteristics in it for various conditions of flow such as sluice opening, the length of apron, and the quantity of flow. For this reason the researchers used the scour profile at asymptotic (equilibrium) state and relate the measured mean characteristics to the whole scouring process. Nik Hassan and Narayanan (1985), Ali and Lim (1986), Chatterjee and Ghosh (1980) and Karim and Ali (2000) are some of the studies that dealt with local scour in asymptotic state.

One of the basic goals of this study is to investigate the mean and hydrodynamic characteristics of water jet issuing on erodible beds. The mean velocity distribution of jet along the scour profile , the turbulent intensity distributions, Reynolds stress distributions, pressure deviation from hydrostatic distribution and the bed shear stress distribution along the scoured bed are basicly studied in this thesis. The second goal is pointing out some clear results that can be made use of by the researchers as a guide in their studies, also for the designers of hydraulic structures (spillways, cooling pools, culvert outlets, etc.) while predicting the mean characteristics of scouring process and minimize the risk of structural failures due to undermining effect of scouring process.

Chapter 2

Literature Survey

2.1 Local Scour by submerged horizontal jets

2.1.1 General

In hydraulic engineering, the prediction and control of the erosion are of important considerations in the safe design of many structures. The localised scour phenomenon has been the subject of extensive investigations by many researchers and numerous literature exists for scour due to variable conditions. Most of these studies have been empirical because of the complexity of the physical processes of scouring.

Starting with the pioneering investigation by Rouse in 1939, a number of studies have been conducted on erosion caused by jets. Following Rouse, Rao and Sarma (1967), and Altnbilek and Okyay (1973) studied erosion by impinging plane jets. Doddiah et al (1953), Pereh and Hefez (1967), Sarma (1967), Sarma and Sivasankar (1967), Westrich and Kobus (1973), Rajaratnam and Beltaos (1977) studied erosion produced by circular impinging jets. Erosion by plane wall jets was studied by Laursen (1952), Tarapore (1956), Basmaci (1971) and Johnston (1990). Erosion by circular wall jets in cross flow was studied by Rajaratnam (1980). Local scour caused by submerged wall jets was studied by Chatterjee and Ghosh (1980), Ali and Lim (1986,1987), Ali and Neyshaboury (1991), and Balachandar et al. (1999). Ade and Rajaratnam(1999) made a generalised study of erosion by circular horizontal turbulent jets. Ali and Salehi-Neyshabouri (1991) and Ali and Walley (1992) conducted experiments on local scour downstream of offset jets and Salehi-Neyshaboury et al. (2000) performed a numerical simulation of scour by a wall jet.

2.1.2 Local Scour Due To Turbulent Jets

Local erosions of the alluvial rivers near solid structures have been studied largely by many investigators to determine the maximum depth of an erosion hole. In some problems it is desirable to extrapolate data such as the rate at which the grains are removed from model erosion studies to the event in the prototype river. The geometry of the boundaries and other features of water flow can be reproduced but the scaling laws for sand transport are not so well known.(Chatterjee and Ghosh, 1980).

One of the earliest formulas defining the scour depth ,proposed by Schoklitsch (1932), is

$$y_{m,e} + h_t = c_s \frac{q^{0.57H^{0.2}}}{d_{90}^{0.32}} \qquad \textbf{(2.1)}$$

where; c_s :dimensional coefficient; d_{90} :particle diameter, which is not exceeded by 90% of the sediment grains; h_t : tailwater depth; H : height between head and tailwater levels ; q :discharge per unit width ; and $y_{m,e}$: equilibrium scour depth.

The study by Chatterjee and Ghosh (1980) concerned the findings of an experimental investigation carried out to evaluate the hydraulic parameters for the computation of sediment transport due to a two-dimensional horizontal jet drowned in a relatively large depth of water and flowing over apartly rigid apron to an erodible sand bed. The classical wall jet solutions were not directly applicable to their problem because the existence of apron before the erodible bed causes the flow characteristics of the jet to alter significantly. Thus, Chatterjee and Ghosh studied the diffusion characteristics of such a jet following the procedure adopted by Albertson et al. (1950). They developed an expression for critical shear stress at equilibrium depth of scour from the solution of von Karman's integral equation. Comparison of the value of critical shear stress as estimated from the expression developed with that of conventional Shield's criteria showed rather good agreement in the case of gravel bed, whereas for the sand bed, a great deal of difference was observed.

Chatterjee and Ghosh (1980) found that the growth of the thickness of boundary layer for a rigid, mobile, and transition region on the boundary surface was dependent on the flow depth, length of rigid apron, grain size, and the distance from the sluice opening. The vertical velocity distribution over the apron showed a considerable amount of difference compared to that for a classical wall jet in the region beyond the boundary layer.

Nik Hassan and Narayanan (1985) studied on scour hole developments downstream of a rigid apron due to a jet of water issuing through a sluice opening. They performed several experiments for various sand sizes, sluice openings, efflux velocities, and lengths of apron. The mean velocity profiles along the rigid model of the scour hole showed similarity. Using the experimental results derived from measuring the mean velocities along the rigid scour hole, they presented an empirical formula that expresses tha mean velocity distribution along the scour hole:

$$\frac{U}{U_m} = e^{-0{,}693(y'/\delta_{1a})^{1.5}} \tag{2.2}$$

where; y' :distance between the maximum velocity and corresponding mean velocity

δ_{1a} : length scale for outer layer in boundary layer

U_m : max. mean velocity

Presenting the mean velocity profiles at various distances along the apron nondimensionally as U/U_m versus y'/δ_{1a} , Hassan and Narayanan observed that the mean velocity of the scour hole exhibit similarity as shown in Figure 2.1. They used the mean velocity distributions measured along the rigid scour hole to develop a semi-empirical theory to predict the temporal rate of scour depth for wall jets issuing on a bed of sand:

$$\frac{1}{n+1} = \frac{d}{dt}\left[h^{n+1}\right] = \beta_1 \left[\frac{U_m^2}{\rho(s-1)}\right]^n U_m \left[\frac{U_m^2}{\rho(s-1)D}\right] \tag{2.3}$$

where; β_1 = length scale for inner layer; D= sediment size; s= specific gravity of sand; t = time; h = maximum scour depth and n = trial value of power of the relative magnitude of kinetic energy to the potential energy.

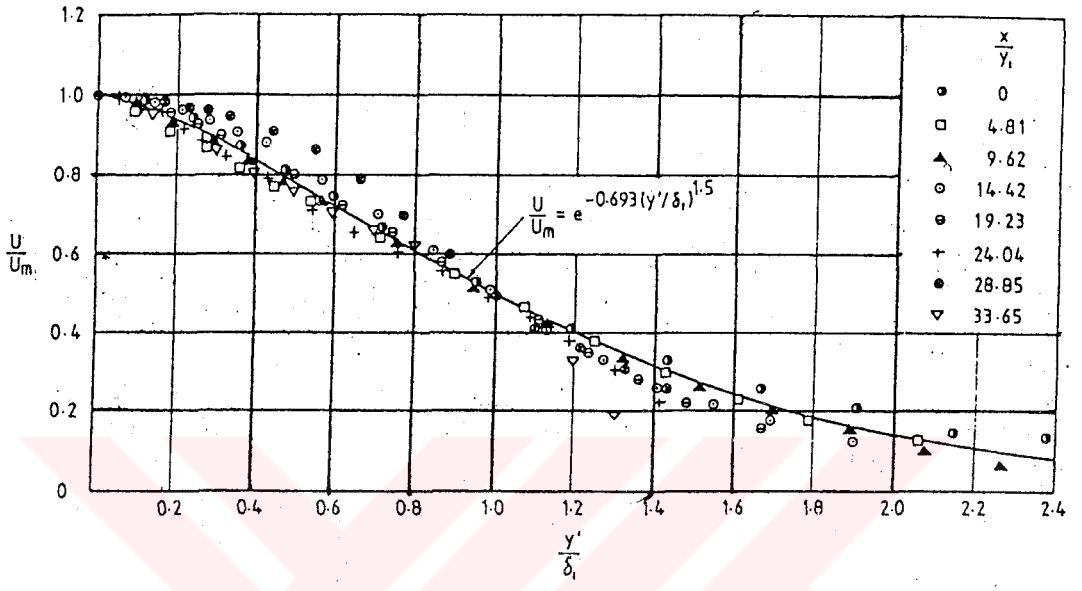

Figure 2.1 Mean Velocity Profiles Pertaining to the Outer Layer within Scour Hole (Nik Hassan and Narayanan, 1985)

In general, localised scour will occur whenever the local rate of sediment transport exceeds the rate of supply to the area under consideration. Depending on whether sediment is being supplied from upstream to the scour area, localised scour can occur in two ways:

1. Clear water scour
2. Live bed scour

Clear water scour refers to the situation where no sediment is supplied from upstream in to the scour zone. Live bed scour, in contrast, occurs where there is general bed load transported by the stream. In this case, sediment is continously being supplied to the areas subjected to scour. In other fields of sediment transport, there is no entirely satisfactory theoritical solution which describes scour completely.

The complexity of non-steady flow patterns and the mechanics by which the flow entrains an erodible sediment from the bed is not yet solvable analytically. Several solutions to this problem have been proposed. The work done by Laursen(1952), Cartens(1966), Altnbilek and Basmac(1980), and Rajaratnam et al(1977,1985) are examples of such investigations. (Ali and Lim, 1986)

Ali and Lim (1986) studied on clear water scour produced by two- and three-dimensional horizontal turbulent jets. They performed two types of experiments, as pipe experiments and sluice-gate experiments. The main aim of the both type of experiments was to measure the volume V_s and the maximum depth d_m of scour and the centreline scoured bed profiles. The time variations of these scour characteristics were studied for different rates of flow, jet sizes and tailwater depths.

During the experiments of two- and three-dimensional experiments, Ali and Lim plotted V_s / R^3 against d_m / R (Figure 2.2) for all experimental results. All the plotted data could satisfactorily be represented by two curves, for the two- and three-dimensional jets respectively.Using the figure, they obtained the following reletionships:

$$\frac{V_s}{R^3} = 187.72\left(\frac{d_m}{R}\right)^{2.28} \qquad \textbf{(2.4)}$$

for two-dimensional jets, and

$$\frac{V_s}{R^3} = 49.36\left(\frac{d_m}{R}\right)^{1.89} \qquad \textbf{(2.5)}$$

for three-dimensional jets.

where; R= the jet area divided by the perimeter of the jet.

Ali and Lim (1986) used Rossinskii (1961)'s method for the two-dimensional scour holes for predicting the velocity distributions and compared the resultant values with the experimental results. Reasonable agreement was obtained between the calculated and measured velocities. Finally, Ali and Lim (1986) developed a method for

calculating the boundary shear stress in a scour hole using the floor velocity and compared this method with that obtained using turbulent layer theory.

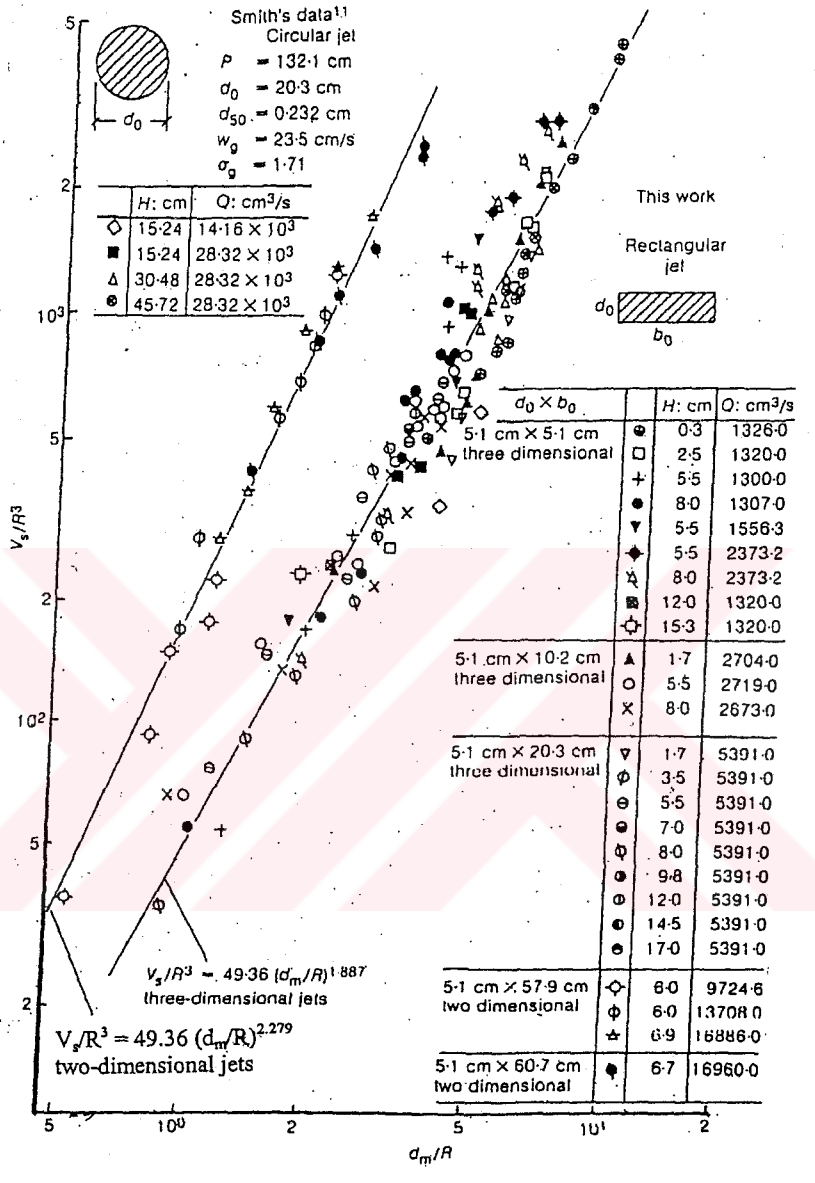

Figure 2.2 Correlation of volume and maximum depth of scour (Ali and Lim, 1986)

Johnston and Halliwell (1987) presented a discussion paper on the study of Ali and Lim(1986). They inspected the study from all aspects and made comparisons with the study of Johnston and Halliwell(1986). Johnston and Halliwell were particularly interested in a feature (see Figure 2.2) which describes the variation in geometric scour hole development which is possible if the densimetric Froude numbe of the depth of the tailwater is altered .

$$F_0 = U_0 / \sqrt{[gd(\rho_s - \rho)/\rho]} \qquad (2.6)$$

where; F_0 is the densimetric froude number; U_0 = the jet velociy; d = the median particle size; b_0 = the jet nozzle thickness or sluice gate opening; ρ_s = the density of sediment particle; ρ = the density of water; g = the acceleration of gravity

They made clear in their paper that different flow patterns are associated with different depths of tailwater (H), but they did not specifically argue or state that sometimes different flow patterns exist at the same tailwater depth. Johnston and Halliwell (1987) pointed out that although the experimental conditions in their early study (Johnston and Halliwell, 1986) involved a rigid flat horizontal bed, the densimetric Froude numbers and other flow characteristics are within the range of those of Ali and Lim.

Scour created by flow when water is passing through a sluice gate or falling over a weir has been investigated by many researchers (Cartens 1966; Hortung 1957; Schoklitch 1932; Veronese 1937). However, the scour originating when water is passing both under and over vertical gate has not been considered.(Breuser 1967; Farhoudi and Smith 1982; Jaeger 1939; Tusuchiya and Iwagaki 1967) (Ali, 1988).

Ali (1988) studied on the scour phenomenon in non-cohesive soils below the vertical gates in the case of simultaneous flow over and under the gate. Performing the experiments with two different bed materials of homogenous noncohesive soil, he observed that the length of scour and the maximum depth of scour are smaller for water passing both under and over the gate than for water passing only under the gate, even though it is possible to pass larger discharges throgh the gate.

Ali plotted the experimental results as d_0 (depth of scour) versus q (discharge) (Fig. 2.3) and observed that in the case of discharge over the gate the depth of scour is greater than in the case of discharge under the gate. But he also observed that in the case of simultaneous flow over and under the gate, scour is smaller compared with the two former cases. The reason for this case was that flows coming from under and

over the gate dissipate each other's energy while they are mixing below the gate. This shows that the overtopping of a sluice gate is not dangerous from the point of view of downstream scour.

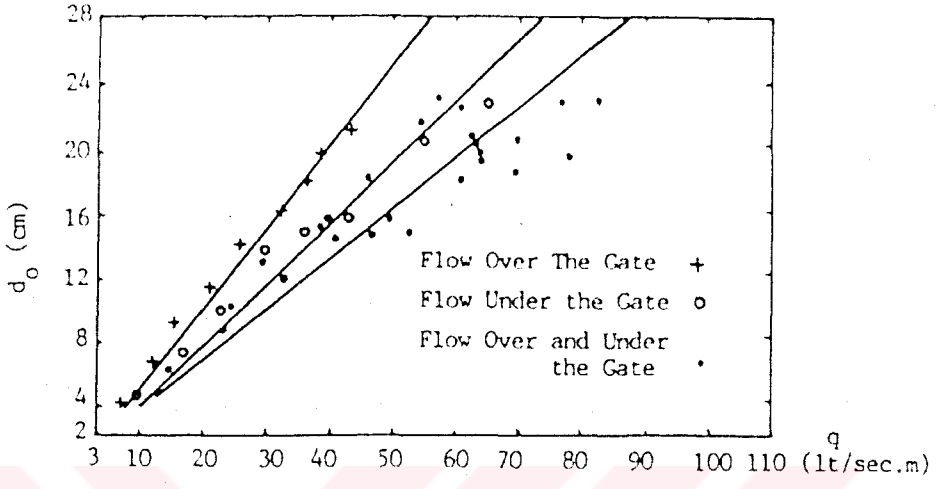

Figure 2.3 Change of depth of Scour with q (Ali, 1988)

Among different flow cases, the action of an offset jet can result in the erosion of bed material causing severe damage to the bed and nearby structures. For example, near cooling pools of power plants or in two-and three-dimensional jets whose invert is higher than the level of the downstream bed. Therefore it is esential that the erosive power of an offset jet is understood in order to enable adequate safety factor to be included in design of any structure where scour is to be expected.

An offset jet is usually a submerged jet, with its entrance level above the original bed (Figure 2.4) The combined action, on the erodible bed, of the attachment of jet, the pressure inside the vortex under the curved jet, and the wall jets flowing upstream and downstream of the attachment point cause a complicated process of sediment movement and localised scour.

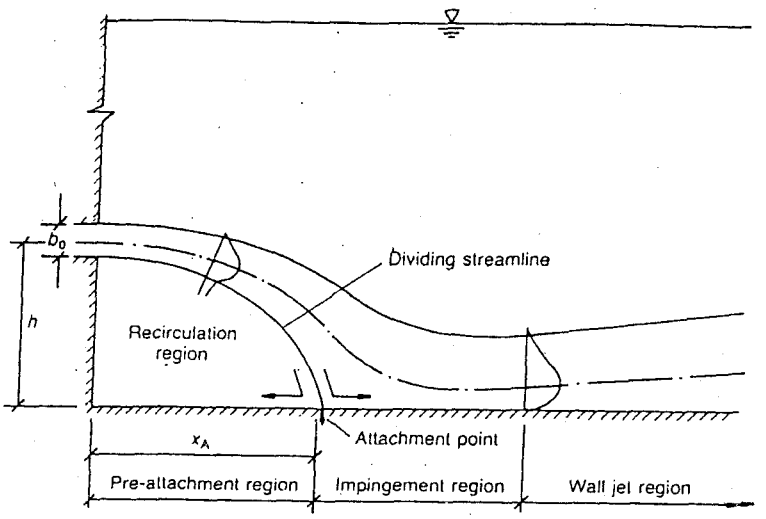

Figure 2.4 Definition sketch for an offset jet. (Ali and Neyshaboury, 1991)

Ali and Neyshaboury (1991) investigated experimentally the scour caused by an offset jet. To date, little research has been carried out on offset jets. Most of the studies dealt with two- and three-dimensional wall jets. (Ali and Neyshaboury, 1991). The development of scour in a uniform sand bed was monitored at set time intervals until the asymptotic state was reached. In all tests, the tailwater depth and the slot's thickness were kept constant. Particles of three different test sizes were used.

A new method for the measurement of scour profile, during its formation was developed. Accuracy of measurements by this method was confirmed by meausrements of the scour profile, using a depth gauge. Ali and Neyshaboury didn't find it necessary to freeze the scour hole in the same way that most of the previous investigators did and as they considered the flow conditions to be asymptotic state, they measured the horizontal and vertical velocity distributions along the scour hole.

The maximum depth of scour hole was found to be a function of the particle size, the densimetric Froude number, and the jet's height:

$$\frac{V_s}{b_0^2} \text{ or } \frac{d_m}{b_0} = f(F_0, \frac{tU_0}{b_0}, \frac{H}{b_0}, \frac{h}{b_0}) \qquad (2.7)$$

where (d_0 = scour depth; V_s = volume of scour hole per unith width; d_m = the maximum depth of scour; F_0 = the densimetric Froude number.

They measured the velocity distribution in one of the tests, at the asymptotic stages, and the velocity distributions along the centre-line bed profile revealed that, as in the case of offset jet impinging on a rigid bed, decay of maximum velocity was enhanced as the curvature effect increased in the pre-attachment region. Ali and Neyshaboury (1991) also observed that downstream of the impingement region, the maximum veocity increased for some distance and then continued to decrease.

The erosion of plunge pools downstream of dams has been increasingly popular subject in hydraulic energy disipation. Flood flows are issued from flip buckets, presure gates and dam spillway crests in the form of high enrgy jets. Plunge pools or scour holes are formed in the river bed downstream at the point of jet impact. Such scour developments can cause important problems. Many formulas have been developed over the years for predicting the depth of such scour holes. After a 30-year review against bodies of model and prototype data Mason and Arumugam (1985) observed a wide variation in the probable accuracy of these formulas.

They found the most potentially accurate expression as:

$$D = K\frac{q^x H^y}{d^z} \qquad \textbf{(2.8)}$$

where; D= scour depth; q = discharge per unit width; H = the head drop from reservoir to tailwater level; d = characteristic size of bed material; K, x, y and z are constant for any given formula, although K is not dimensionless and has to be adjusted according to the units being used.

John Mason (1989), dealt with plunge pool air entrainment as an alternative parameter other from the pre-mentioned major factors. He performed experiments both with and without air entrainment and observed that with the addition of air, scour profiles were generally flatter than those from the nonaerated tests.It was

found that in the absence of air, the scour depth was only dependent on q and independent of H. With the addition of air in proportions which it was calculated an equivalent free-falling jet would entrain naturally, the effect of q on the scour process appeared to be modified and scour also appeared to vary with H. Mason related the reason of this event to the case that scour may be dependent on only q and the percentage of the entrained air.

He explained the test results in terms of a characteristic force on the particles of bed material where plunge pool depth varies with flow, and with the percentage of entrained air needed to maintain that force. The equations produced were developed to give a three-dimensional scour approximation:

$$D = 3.39 \frac{q^{0.60}(1+\beta^{0.30}h^{0.16})}{g^{0.30}d^{0.06}} \qquad \textbf{(2.9)}$$

where; D= depth of scour measured from tailwater level β= water ratio; q= discharge per unit width; h = maximum tailwater depth above unscoured river bed; g = gravitational acceleration; d = mean size of particles of bed material.

Lastly, Mason concluded from his study that air entrainment on prototypes may not be significantly different from that is seen on reasonably sized models, given that there may be an upper limit on β of around 2-3 and that such figures can easily be approached on models.

The scour process in areas where loose sediments are located near the foundations of hydraulic structures must be understood well during analysis and design. Failures of bridges due to scouring at their supports emphasise the importance of an appreciation of the relevant scouring processes. Further scouring situations, such as occur in zones downstream of culverts, in areas upstream sluice gates, all require careful considerations. (Johnston, 1990)

Johnston (1990) studied on the scour hole developed by a plane jet entering shallow tailwater. His study can be considered as a literature survey in detail about the

scouring process in zones downstream of culverts, in areas upstream of intake structures an downstream of outlet structures of sluice gates. Johnston performed experiments with the aim of inspecting the local scour process under shallow and deeper tailwater conditions and observed that in certain shallow tailwater conditions the development of a scour hole downstream of a slot jet is more complicated than in relatively deep conditions. While in deep conditions the scour hole development is orderly and invariably reaches a well-defined asymptotic state, in shallow conditions such a state is sometimes not reached.

Johnston (1990) pointed out that submergence parameter (D/L_d), a bed offset parameter (P/L_d) and densimetric Froude number are the dominant influences on the flow pattern (where; D= vertical distance from jet centre line to the free surface; L_d = length scale= $d_0 F_d^{1.33}$; P= vertical distance from centre line to the bed).

He observed three types of jet regimes such as:

1. A surface jet scour hole regime where for fairly small depth values($D/L_d < 0.15$) and small densimetric Froude numbers (F_r <1).
2. A bed jet regime where large depth values($D/L_d < 0.6$) upto, and beyond, large offsets ($P/L_d = 0.70$).
3. A bed-surface jet regime where moderate depths (($D/L_d = 0.16 - 0.50$) and moderate bed offsets ($P/L_d = 0 - 0.55$).

One of the major characteristics of the form of scour hole is the upstream scour slope which must be less than the angle of internal friction has not been mentioned as often as the other characteristics such as the maximum scour depth. In fact, the magnitude of the maximum scour depth is not of importance as long as the geotechnical stability of the upstream scour slope is assured. In the equilibrium stage, the maximum scour depth as well as the upstream scour slope reach their maximum values. The instability of the upstream scour slope results in a shear failure or flow slide that is more significant when compared other scour phases. This emphasises the

importance of reliable predictions of the maximum scour depth and the upstream scour slope.

Hoffmans and Pilarczyk (1995) studied in detail on the semi-empirical relations of the scour process and the analysis of the stability of the upstream scour slope. Performing several flume experiments and taking the previous equations in consideration. They proposed the best equation as the best compromise between the measured and calculated angle of slope that resulted in (Hoffmans 1993):

$$\beta_\ell = \arcsin\left(2.9 \cdot 10^{-4} \frac{U_\ell^2}{\Delta g d_{50}} + (0.11 + 0.75 r_{0,\ell}) f_c \right) \qquad \textbf{(2.10)}$$

where; β_ℓ = local upstream scour slope; U_ℓ = local depth-averaged flow velocity; Δ = relative density; g = gravitational acceleration; d_{50} = mean particle diameter; $r_{o,\ell}$ =local relative turbulence intensity; f_c = roughness coefficient.

In spite of making simplifications in closure problems, this study shows a way to calculate the steepness of upstream slopes in the equilibrium phase of the scour process for noncohesive material. Hoffman and Pilarczyk also developed a criterion that is able to predict undermining at the end of bed protection because of small-scale failures. They suggest that more authorative criterions should be developed and applied as a part of overall design.

Many empirical and semi-empirical relationships for some aspect of the equilibrium scour condition (asymptotic state) have been suggested. Unfortunately, these relationships provide a wide range of scour prediction for similar flow conditions. Some investigators report that the time to achieve equilibrium scour may be long, in some instances may never be attained.

The importance of time-scale problem was pointed out by Balachandar and Kells (1997). They discussed the importance of time-scale during the local scour of uniformly graded sediments and the dynamics of the erosion process in the context of the scour which takes place downstream of a submerged sluice gate. During the

empirical studies, they obtained the scour profiles using video-imaging process. The dynamic nature of the scour profile downstream of submerged sluice gate was clearly established by presenting scour profiles at various instants in time from the start of the erosion process.

The similarity parameters describing the scour hole as identified in previous studies were not found to be valid, however, as found in related studies, some of the major variables (maximum scour depth) during phase A did show a linear increasing trend in a logarithmic time scale. In deed, Balachandar and Kells couldn't observe an equilibrium state by the end of the 144 hours test period.

The mechanism of local scour downstream of hydraulic structures is directly related to the type of flow over and through those structures. Such flows are generally of jet type with different regimes (plunging jets or horizontal jets) (Hoffmans, 1998). The term "plunging jet" refers to jets of water that impinge on the free surface due to the discharge from an outlet above the free surface or overflow through an opening as shown in Figure 2.5

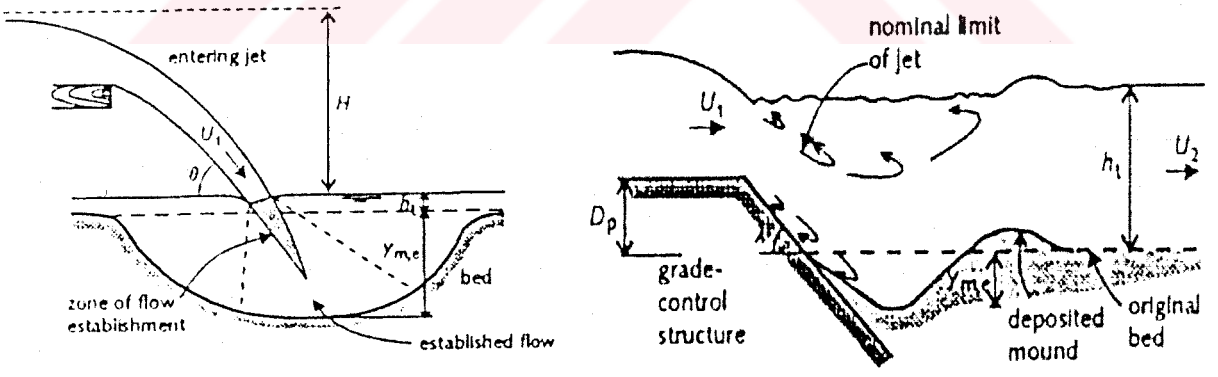

Figure 2.5 Plunging jets (Hoffmans, 1998)

The term "horizontal jets" refers to flows under barriers or gates that are infinitely, i.e., suficiently wide (Fig 2.6). The horizontal flows cases are two-dimensional along the width of the barrier and usually have a considerable potential of scour.

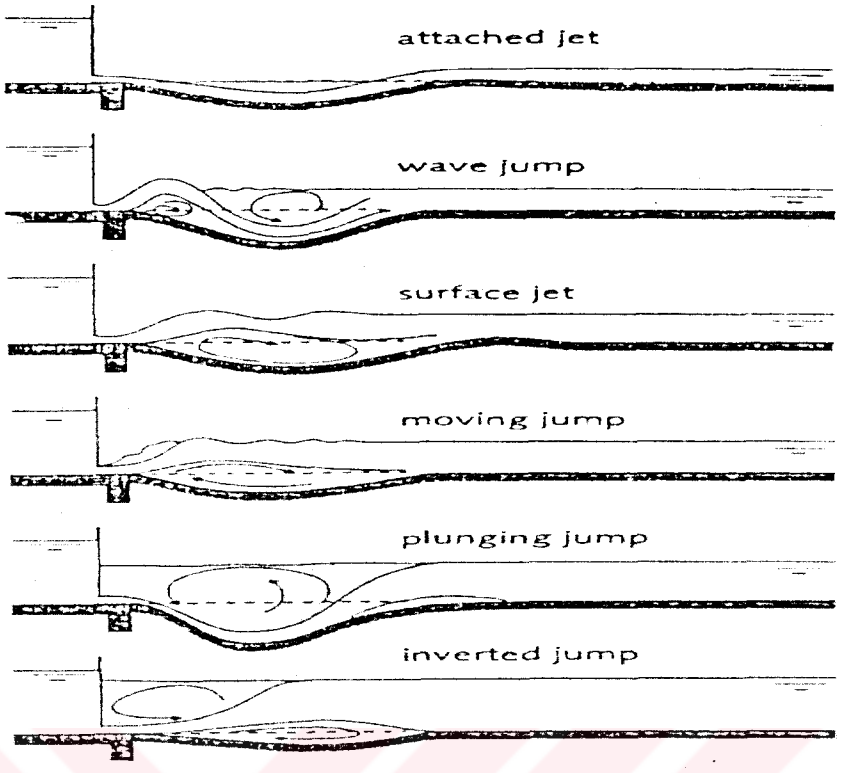

Figure 2.6 Different Horizontal Jet Forms (Hoffmans, 1998)

Hoffmans (1998) used a different approach to compute the practical equilibrium scour process caused by plunging or horizontal jets when no bed protection is present. He applied Newton's second law of motion to mass of particles of fluid to derive relations for the maximum scour depth in the equilibrium phase (no sediment is tranported downstream anymore).

Hoffman used the equations found previously by other researchers and the accuracy of these equations were evaluated using numerous of data of both prototype situations and flume experiments. He used a significant amount of work from other researchers by drawing them together to calibrate and verify the predictors for the scour depth caused by horizontal jets. Although the simplifications were made in applying the momentum principle to a short horizontal reach of a scour hole, reasonable results were obtained for both 2-D and 3-D jet scour compared with other scour relations.

Hoffman (1998) suggested that desk studies as well as detailed physical models should be carried out to increase the accuracy of predictions made about the local scour event and he claimed that the second law of Newton and new developments in the modelling of coherent structure will help to accomplish this goal.

In the field of hydraulic engineering , erosion by circular horizontal jets is perhaps one of the most common types of erosion by jets. It can be found at the outlets of circular culverts or storm drainage pipes, which may be either submerged or unsubmerged depending on tailwater conditions.

Ade and Rajaratnam (1998) performed a study on an experimental and exploratory study that can be taken as a useful literature review of the studies about the circular wall jets. They also performed an anlysis of over three hundred and fifty experimental results of scour at pipe outlets obtained from thirteen sources including the experimental results of the mentioned paper. Their experimental study consisted of air jets on canola seeds and water jets on sand and gravel beds. In one of the experiments, the study of scour growth at high densimetric Froude number (F_o=88.2) revealed that, it could take over a week for the asymptotic (equilibrium) state to be reached. They also noticed that the equilibrium state was reached earlier at section nearer to nozzle.

Some resesarchers have reported of the presence of an equilibrium scour condition. (Rajaratnam and Macdoughal 1983; Ade and Rajaratnam 1998, etc.), while the investigation by Balachandar and Kells (1997), conducted with one tailwater depth, indicated the absence of an equilibrium state even after five or more days of testing in laboratory setting. The absence of an equilibrium scour condition is a serious design problem. The study of Balachandar and Kells showed that local scour can be cyclic, in a nature, with alternate digging and filling of the scour hole.

Following the previous study (Balachandar and Kells 1997), Balachandar et al. (2000) studied on two-dimensional local scour occuring downstream from a submerged sluice gate for various tailwater depths using video imaging technique and a Laser-Doppler anemometer.

Performing several experiments, Balachandar and co-workers did not observe an equilibrium state as already mentioned in Balachandar and Kells (1997), that contrasts with the study of Rajaratnam and Macdougall(1983), in which an asymptotic state was reached after about 0.5 h (hour) from the start of test for the case of plane wall jets. The suggested specific time an length scale laws ($\sqrt{A_s^3}$ and y^3) , based on volume of scour and the time evaluated from the start of the erosion process, are very useful for predicting the tailwater effects on the scour profile when a state of equilibrium is not reached.

As a continuation of earlier work in local scour dynamic (Balachandar and Kells 1997,1998; Thiessen et al 1997), Balachandar and Kells (1999) issued a paper on the erosion of loose bed of non-cohesive granular material by a two-dimensional jet issuing from a submerged sluice gate. Whereas the previous work focussed on the understanding and quantifying the flow pattern, this study was directred toward the devlopment of local scour counter-measures.

Balachandar and Kells performed the experiments with and without the presence of rigid apron and observed that the amount of scour was significantly reduced with the apron in place. The maximum depth of scour was reduced with a rate of 60% in the presence of apron. The presence of apron also served to move the location of the point of maximum scour further downstream from the gate and thus, it provides an increased margin of safety against structure failure from undermining.

Ushijima et al. (1992) considered two- and three-dimensional scouring by warmed jets. The unsteady continuity and momentum equations along with the k-ε turbulence closure model were solved using a finite difference method. Both bed-load and suspended-load were considered in the solution of continuity equation for sediment at the bed. The convection-diffusion equation for suspended load concentration was solved numerically. They compared their predicted bed profiles with Ashida et al. (1978). Although the results were generally in good agreement, they observed some undulations in computed bed profiles which were not present in the experimental results.

To solve these problems, Ushijima et al (1992) used an arbitrary Langrangian-Eularian approach in which three-dimensional body-fitted coordinates are generated for the sand bed profile unsteadily deformed by flow.

Salehi Neyshabouri et al. (2000) presented a numerical simulation of scour by wall jet using k-ε turbulence model. They assumed the flow to be two-dimensional, and the alluvium is cohensionless (sand) . They used three basic steps :

1. simulation of a turbulent wall jet flow
2. solution of the convection-diffusion of sand concentration
3. prediction of the bed deformation.

Salehi Neyshabouri et al. (2000) solved the governing equations for momentum, mass balance and turbulent parameters (k and ε) in a general two- dimensional non-orthogonal curvilinear domain by finite volume method. A non-staggered grid arrangement was used. The SIMPLE scheme was used for pressure correction and a diffusion equation was solved for sediment concentration. All the aforementiond steps were repeated at each stage of scouring process. Comparison of simulation results with experimental data showed favorable agreement on the evolution of the scour with time. They also pointed out that the shape and position of scour hole that they predicted were realistic.

Prediction of local scour holes that develop downstream of hydraulic structures has a very important role in their design. Excessive local scour can progressively undermine the foundation of the structure. Because complete protection against scour is too expensive, generally, the maximum scour depth and upstream scour slope of the scour hole have to be predicted to minimize the risk of failure.

Karim and Ali (2000) proposed a procedure for investigating the Fluent CFD package program in simulating fow patterns generated by a turbulent water jet impinging on rigid horizontal and scoured beds. Fluent is a multipurpose computer software for modelling fluid flow, heat transfer and chemical reaction which enables a rapid analysis of complex flow.

They used Fluent to predict the 2-D flow velocity disribution and the bed shear stress for both flat and scoured bed. They investigated the experimental studies of Ali and Lim (1986) and Wu and Rajaratnam (1995) to compare the calculated values by the software with the experimental results. Figure 2.7 (from Ali and Lim,1986) shows that the line of maximum velocity was deflected towards the water surface and that negative velocities were present near the section of maximum scour. In general, these resultant figures of the velocity vectors by the FLUENT are close to the experimental distributions made by Ali and Lim(1986), Rosiinski (1961), Breusers (1967) and other researchers in their experiments.

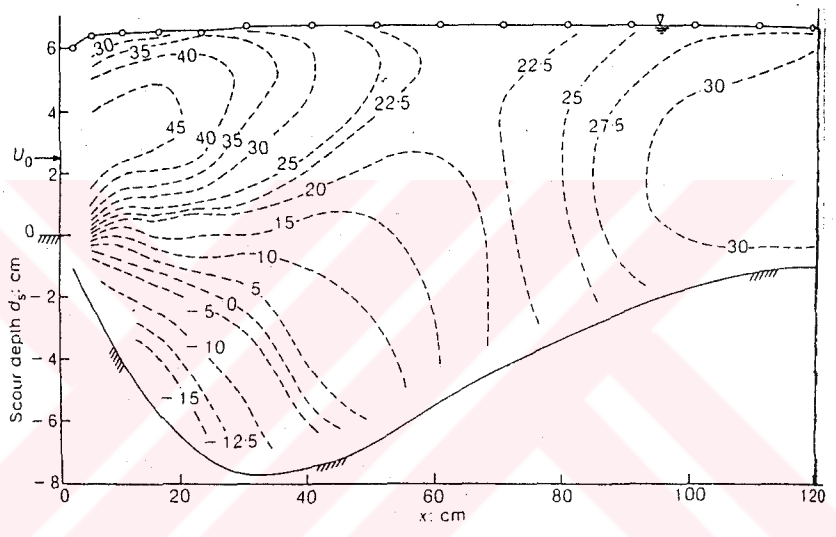

Figure 2.7 Experimental Velocity Contours (Ali and Lim, 1986)

The three closure models (Standard k-ε model, RNG k-ε model and RSM k-ε model) available in Fluent were tested using scoured bed by Ali and Lim (1986) and there were no significant variations in the computed values between the Standard k-M model and the RNG k-M model. However the RNG k-M model converged twice as fast as other models. The RSM model yielded good agreement except at sections beyond that of maximum scour. In general, flowfields, velocities and shear stresses predicted by Fluent showed a close agreement with relevant experimental results.

Culverts are engineering structures that allow water to be diverted to permit the flow to continue whilst the land above may be developed for other uses. If poorly designed, the culvert structure can be undermined due to scouring at both

downstream and upstream ends which lead to damage of the culvert structure and nearby structure. This means high rebuild costs and repairs from possible flood damage. A valuable prediction of scouring downstream of such outlet structures can only be achieved if both the turbulent flow structure and the sediment transport mechanism are well understood.

Liriano et al. (2002) studied on the measurement of the turbulent flow structure within scour hole downstream of pipe culvert outlets at different stages of development. The figures below show the centreline mean velocity vectors the mentioned progressive stages of scour hole development.

The analysis of the mean velocity and turbulence intensity, showed that near-bed velocities decrase as the scour hole develops. Areas of high turbulence intensity and low Reynolds stresses were observed close to the dune crest in addition to a large number of inward and outward interaction events being present in this area of the scour hole (see Figure 3 and 4 in Liriano et al., 2002).

No recirculating flow was observed along the centreline of scour holes downstream or pipe culvert outlets. Peak values of turbulence intensities over the fixed bed coincided with the location of the maximum scour depth for the fully (99%) developed scour holes as seen from Fig. 2.8.

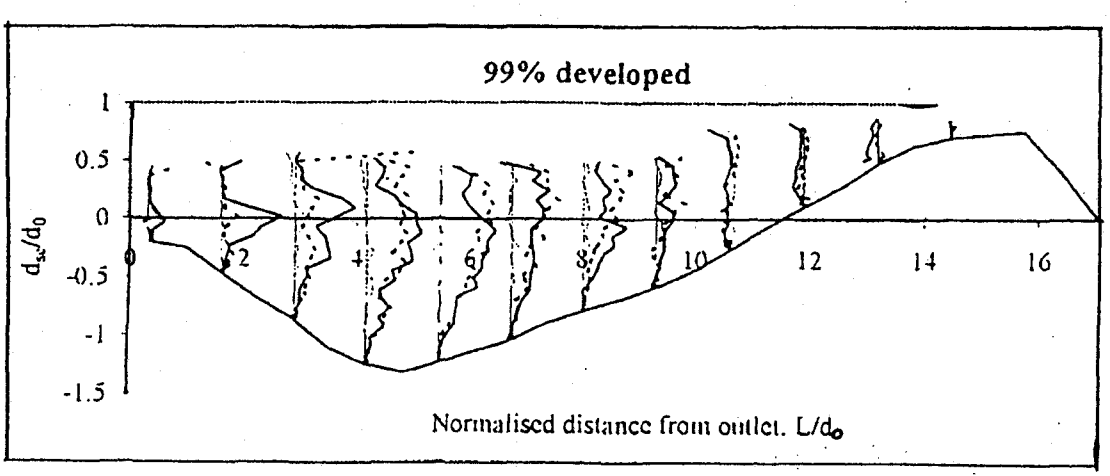

Figure 2.8 Turbulent intensities at 99% developed stage (Liriano et al. , 2002)

After analysing the mean velocities, Reynolds stresses, turbulence intensities and bursting structure in the scour hole, Liriano and co-workers proposed a model (Figure 2.9) for the near-bed turbulent flow structure downstream of pipe culvert outlet. The model suggested that the initial formation of the scour hole was a result of mean velocity exceeding the critical velocity. The subsequent growth in the scour was the result of sweeps in the area of maximum scour depth transporting sediment downstream.

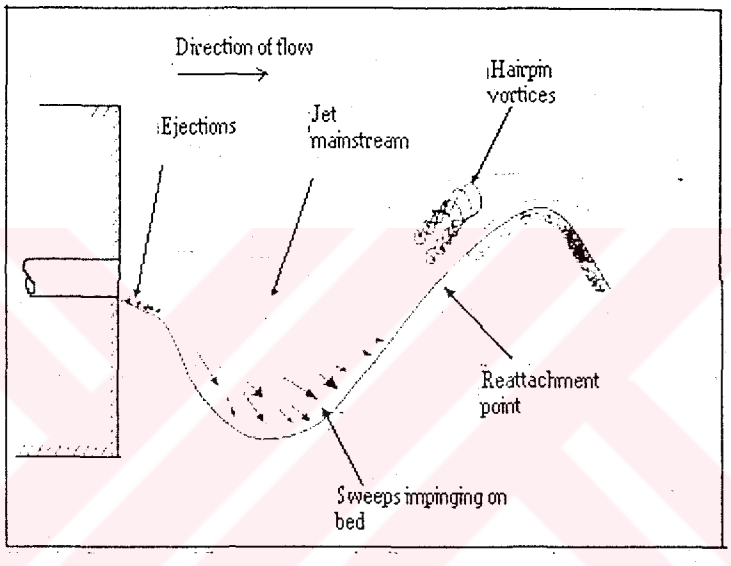

Figure 2.9 Diagram of flow structures leading to scour downstream of pipe culvert outlets (Liriano et al., 2002)

2.2 Turbulence Modelling

Turbulence modelling is one of three key elements in Computational Fluid Dynamics (CFD) (Gunal, 1996). Very precise mathematical theories have evolved the other two key elements, grid generation and algorithm development. By this nature-in creating a mathematical model that approximates the physical behaviour of turbulent flows-far less precision has been approximate an extremely complicated phenomenon.

The aim of a turbulence model is to express the Reynolds stress in the equations that result in the momentum, thermal energy and concentration due to replacing the velocities with a mean and fluctuating part by set of auxiliary equations (differential and/or algebraic) containing the time-mean quantities of the flow.

A turbulence model can be described as a set of relations and equations needed to determine the unknown turbulent correlations that have arisen from the averaging process. The task of turbulence modelling is to represent the turbulence correlations $\overline{u'^2}$ $\overline{u'v'}$, $\overline{v'^2}$ etc. in the mean-flow equations in a way which closes these equations by relating the correlations to the averaged dependent variables. Hypotheses must be introduced for the behaviour of these correlations which are based on empirical information; hence turbulence models always contain empirical constants and functions.

The basic concept of turbulence modelling is the parameterization of turbulence, which means that the local state of turbulence and hence the turbulence correlations is assumed to be characterized by only a few parameters. For quite, sometime the parameterization of turbulence and its effects has been achieved by the use of friction coefficients (Chow 1956) or mixing coefficients (Fischer et al. 1979).

2.2.1 Basic Formulations

Navier Stokes equation is known as the starting point for deriving a set of model equations, derivations of which can be found in many text books such as Chow (1959), Anderson (1995), and Versteeg and Malalasekera (1995). These equations describe the details of the turbulent fluctuating motion. The time averaged continuity and momentum equations in tensor notation can be obtained splitting instantenous values of velocity u_i and pressure p into its mean and fluctuating parts ($u_i = \overline{u_i} + u_i'$ and $p = \overline{p} + p'$) as (Hinze, 1959):

$$\frac{\partial u_i}{\partial x_i} = 0 \qquad \textbf{(2.11)}$$

$$\frac{\partial u_i}{\partial t} + u_j \frac{\partial u_i}{\partial x_j} = -\frac{1}{\rho}\frac{\partial p}{\partial x_i} + \frac{\partial}{\partial x_j}\left(\nu \frac{\partial u_i}{\partial x_j} - \overline{u_i' u_j'} \right) + g_i \qquad \textbf{(2.12)}$$

$$\overline{-u_i' u_j'} = \nu_t \left(\frac{\partial u_i}{\partial x_j} + \frac{\partial u_j}{\partial x_i} \right) - \frac{2}{3} k \delta_{ij} \qquad \textbf{(2.13)}$$

where; ν_t is the eddy viscosity , k is the turbulent kinetic energy and δ is the Kronecker delta.

Most turbulence models use the Equation 2.13 to determine the Reynolds stresses. The eddy viscosity, ν_t, is in contrast to the molecular viscosity ν, not a fluid property but depends strongly on the state of the turbulence and may vary considerably over the flow field. Hence a turbulence model has in general the task of determining the distribution of ν_t over the flow field.

For dimensional reasons ν_t is proportional to the velocity scale v_t and a length scale L_t characterising the turbulent motion:

$$\nu_t \propto u_t L_t \qquad \textbf{(2.14)}$$

Mc Guirk and Rodi (1978) developed a two-dimensional calculation method for open channel flows with recirculation zones which combines depth-averaged forms of the governing equations with an advanced turbulence model. The application of the method to the practically important heated side discharge problem showed that the velocity and temperature behaviour can be predicted correctly for this problem. In particular the method describes well the influence of the momentum flux ratio M, on the size and shape the recirculation zone and on the temperature distribution in the channel.

The success of the turbulence model based on the assumption of eddy viscosity concept depends on how well the distribution of u_t and L_t can be determined (Rodi,

1988). The assumptions of isotropic eddy viscosity may not be right for certain types of flows such as unconfined turbulent flows.

The dynamics of free-surface turbulence in an open channel flow should be well understood because it governs the mechanism of the transfer of mass, heat, momentum and vorticity accross a gas-liquid interface. Free-surfaces occur in numerous engineering and environmental situations such as hydraulic engineering, hydrodynamics, coastal engineering, acoustic and meteorology. Shi et al. (2000) carried out a large eddy simulation of flow with a deformable free-surface in which the surface is allowed to freely deform with the underlying turbulence. They used a moderately course resolution that allowed the simulation to be carried out on a workstation. The mean velocity profiles was fairly accurate but there was some variation in the second order turbulence statistics owing to the degree of resolution used. The two-point correlations showed that as the free-surface was approached the length scales of the vertical turbulence were reduced whilst that of the horizontal turbulence was increased.

Uijttewaal and Jirka (2001) studied the evolution of grid generated turbulence in shallow flows. An interesting view is obtained on the two dimensional characteristics of the turbulent motions in such flows. They observed that in a laterally homogeneous turbulent flow, large scale quasi two-dimensional eddies can emerge with dimensions much larger than the water depth. They pointed out that, in order to model such flows properly the differences in behaviour between the deep fully three-dimensional case and in the more shallow quasi two-dimensional case should be taken care of.

The grid generated turbulence in this study, served as an arche-type flow in which the dynamics of the large eddies was best revealed. In contrast to shallow flows with a mean shear like jets, wakes and mixing layers the only important property that influences the large eddy dynamics here was the 3D-turbulence generated in the bottom boundary layer.

Kutija and Hewett (2002) presented a hydrodynamic model for one-dimensional free-surface flows, named 'New C'. New C is a finite difference scheme which has a

major advantage over schemes used currently in engineering applications in that, while the algorithmic structure is of subcritical-flow–type, the model is capable of modelling subcritical, supercritical and transcritical flow conditions witout requiring any changes to the governing equations. Although the overall solution algorithm for the new scheme differs from the algorithms currently used, it can be easily incorporated into algorithms for the solution of flows in free-surface networks.

Li and Wang (2002) developed a three-dimensional numerical model , to achieve an accurate evaluation of the turbulent mixing and dispersion processes, incorporating the Large Eddy Simulation. The large scale turbulence was computed explicitly and subgrid scale turbulence was modelled. The model was applied to simulate a continous line source in free surface shear flow and the computed results showed the existence of the non-Fickian diffusion and dispersion region close to the source. They observed that , further downstream the transverse diffusion process obeyed Fick's Law and the transverse diffusion coefficient was in agreement with the empirical value measured in laboratory.

2.2.2 Classification Of Turbulence Models

The most common turbulence models are explained briefly in this section:

2.2.2.1 Zero-equation Models

2.2.2.2 One-equation Models

2.2.2.3 Two-equation Models

2.2.2.4 Reynolds Sress/Flux Models

2.2.2.5 Algebraic Stress/Flux Models

2.2.2.1 Zero Equation Models

Zero equation models uses only the partial differential equation for the mean flow field and no transport equations for turbulence quantities. The model uses the eddy viscosity concept and specifies eddy viscosity concept directly from empirical formula or relates it to the mean velocity distribution.

The model is based on the assumption of local equilibrium of turbulence which is dissipated at the same rate it is produced.The transport and history effects of turbulence are neglected. Thus, zero-equation models are not suitable when these effects are important.

Constant Eddy Viscosity Model

The velocity scale (Vs) and the length scale (Ls) are calculated directly from the local mean flow quantities.

All the simple turbulence models of this type employ the eddy viscosity concept and specify these parameters either directly from experiments by trial and error, through empirical formulas or by relating them to the mean-velocity distribution. It is often convenient to use this very simple model whilst the main features of the simulation are being put together. A more accurate turbulence model can be activated once you are satisfied that other aspects of the flow are well represented.

Mixing –Length Model

For near-field problems involving for example discharge jets, wakes, and the vicinity of banks and structures, the assumption of a constant eddy viscosity is not sufficient so that the distribution of ν_t over the flow field must be determined. The first model to describe this was suggested by Prandtl (1925) and is known as the Prandtl mixing-length hypothesis. Prandtl assumed that the eddy viscosity vt is proportional to a mean representation of the fluctuating velocity $\hat{V}$ and a "mixing-length l_m ", as :

$$\nu_t \alpha \hat{V} L \qquad \textbf{(2.15)}$$

Considering only shear layers with one significant velocity gradient dU/dZ, he postulated that the turbulent velocity scale $\hat{V}=l_m \partial U / \partial z$. With this , the following eddy-viscosity relation results:

$$\nu_t = l^2_m \left| \frac{\partial U}{\partial z} \right| \tag{2.16}$$

The model is

- Suitable for simple shear-layer dominated or pressure-driven flows
- Simple and computationally economical
- Unsuitable for complex flows because it is very difficult to estimate the distribution of the mixing length
- Cannot account for the transport effects of the turbulence

Lvel Turbulence Model :

The LVEL turbulence model is applicable only when walls are present, and it calculates ENUT via Spalding's law of the wall, which covers the entire laminar and turbulent regimes, thus:

$$\text{ENUT} = \frac{k}{E}\left[e^{x^+} - \sum_{i=0}^{4} \left(X^+\right)^{i/i!} \right] \tag{2.17}$$

where; k=0.41, E=8.6, and $X^+ = kU^+$.The local parameter X^+ is determined iteratively from a non-linear expression involving k, E and the local Reynolds number Re, which is based on a typical local velocity and the normal distance to the nearest wall WDIS.

- WDIS is calculated from an algebraic function of a scalar variable L and its gradient, while L itself is obtained by solving:

$$\frac{\partial}{\partial xi}\left(\frac{\partial L}{\partial xi}\right) = -1 \tag{2.18}$$

with L fixed to zero in solids.

- The model is useful for situations in which fluid flows through spaces cluttered with many solid objects (electronics cooling). In such cases the grid density between nearby solids is often too coarse for the k-e model to be meaningfully employed.

2.2.2.2 One-Equation Models:

To overcome the limitations occuring in the mixing-length hypothesis, turbulence models were developed which account for transport or history effects of turbulence quantities by solving differential transport equations for them. An important step in development was to give up the direct link between the fluctuating velocity scale and the mean velocity gradients to determine the scale from a transport equation. These are called one equation models. If the velocity fluctuations are to be characterized by one scale, it is natural to choose k where k is the kinetic energy of the turbulent motion per unit mass. According to this equation, k is a direct measure of the intensity of the turbulence fluctuations in the three directions.

When k is the velocity scale, there follows directly the relation:

$$\nu_t = c_\mu \sqrt{kL} \qquad (2.19)$$

where; c_μ is an empirical constant.This formula is known as the Kolmogorov-Prandtl expression.

Prandtl's K-L Model:

In 1945 Prandtl related the eddy viscosity to the turbulent kinetic energy which was obtained from a seperate modelled transport equation.This was the start of the k-l models(or one-equation models of turbulence) in which the turbulent length scale Ls , is specified empirically and the turbulent kinetic energy is obtained from the Reynolds-stress transport equation. However, as with all linear eddy viscosity models, these can not account for streamline curvature, body forces, and history effects on the individual Reynolds stress components.

In 1951, Rotta proposed a full Reynolds stress turbulent closure, now referred to as second-order or second-moment closure, based on the Reynolds stress transport equation and the statistical ideas of A. M. Kolmogrov. This closed Reynolds stress transport equation and had the advantage that it could account for both history and non-local effects on the evolution of the Reynolds stress tensor. But it also had the disadvantage that it required the solution of six additional transport equations for the individual components of the Reynolds stress tensor, which at the time was not computationally feasible.

- Prandtl's one-equation model can be summerised as follows:

$$\rho\frac{\partial k}{\partial t}+\rho\frac{\partial}{\partial x_i}\left(U_i k-\frac{C_\mu k^{1/2} l_m}{PRT(k)}\frac{\partial k}{\partial x_i}\right)=\rho(P_k+\Gamma_b-\varepsilon) \qquad \textbf{(2.20)}$$

where ;

$$\varepsilon=\frac{C_d k^{3/2}}{l_m};$$

$$P_k=C_\mu k^{1/2} l_m\times\frac{\partial U_i}{\partial x_j}\left(\frac{\partial U_i}{\partial x_j}+\frac{\partial U_j}{\partial x_i}\right)$$

$$\Gamma_b=\frac{-C_\mu k^{1/2} l_m\times g_i\dfrac{\partial\rho}{\partial x_i}}{\rho\times PRT(k)}$$

where; g_i is the gravity vector,l_m has to be prescribed, and the empirical constants are: C = 0.5478; C_d =0.1643; and PRT(k)=1.0.

- One-equation models account for V_s (velocity scale) transpoprt , which is important in developing and relaxing flows, and controlled by the free-stream turbulence.

- The main shortcomings concern L_s (length scale): its transport is not considered, which is important in seperated flows; and it must be prescribed, which is difficult for complex flows. The trend has been to use two-equation models.

2.2.2.3 Two-Equation Models:

The length scale L characterizing the size of those eddies which contribute most to the turbulent stress is subject to transport and history effects in a manner similar to the velocity scale k. Chou(1945) introduced a length–scale-determining equation, and models employing such an equation in addition to the k-equation have become increasingly popular. The length-scale-determining equation need to have L itself as a dependent variable ; any combination of the form $Z= k^m L^m$ will suffice because k is known already from solving the k-equation. A number of different combinations have been proposed by Rodi (1980), but the combination $k^{3/2}/L$, which physically represents the dissipation rate ε, has by far achieved the greatest popularity for the practical reason that ε-equation does not require a asecondary source term near walls while equations for other variables do.

The velocity scale Vs, is calculated from solution of a transport equation for k and the dependent variable of the second transport equation is not usually L_s itself, but rather $k^m L_s^m$.

Launder and Spalding (1984), and Rodi (1980) pointed out that k-ε equation became the most popular model because of the practical advantage of the ε-equation. The use of ε-equation was criticised by Mellor and Yamaha (1982) because of the process of dissipation is associated with the small scale turbulence while it is the length scale characterises the large scale turbulence. They proposed length scale relations for the various turbulence models.

The k-ε model has been applied succesfully to a number of two-dimensional flows. Jones and Launder (1972) applied to a strongly accelerated boundary layer flows. Stephenson (1976) modelled duct flows. Free shear flows were modelled by Launder et al.(1973) and recirculating flows modelled by Gosman et al. (1979). Mc Guirk

and Rodi (1978) determined the turbulent stresses and heat or concentration fluxes from a depth-avearged version of the k-ε turbulence model. They solved differential transport equations for k and ε to determine the relevant equations. Compared with the use of a constant turbulent viscosity as adopted in most existing calculation methods for open channel flow, McGuirk and Rodi (1980) found that the k-ε model offered much greater generality. Bernard (1991) applied k-ε models to the recirculating flows. Qingchao and Drewes (1994) calculated turbulence characteristics of free and force hydraulic jumps by means of k-ε model. Tominaga et al.(1995) developed an improved low Reynolds number k-ε turbulence model for predicting the turbulent flow over strip roughness in open channel. Gerolymos et al.(1995) modelled unsteady nozzle flows due to fluctuating back-pressure by three-dimensional compresible Navier Stokes equation using the Launder-Sharma near-wall k-ε turbulence model. Zeng et al.(1996) dealt with numerical and experimental modelling of tidal flow and heat transfer using the depth-averaged *k*- ε turbulence model. It has been shown that the modelling presented in this paper can be used to simulate the heat exchange and obtain practical results in coastal water.

Sarker and Rhodes (2001) used the low-Re number version of RNG k-ε turbulence model in combination with the Volume of Fluid (VOF) method for free surface modelling, during modelling physically a hydraulic jump downstream of a laboratory scale broad-crested weir. Good agreements was obtained between the 2-dimensional CFD solution and the physical measurements.

Because of the popularity and high efficiency of the k-ε model, several different and improved versions of this model have been proposed. The basic scope of the improvements was the remedying of defficiency of the standard model such as high costs that it is too dissipative and uses some overall criterias that don't correspont to the natural event. Here are the most important versions of k-ε turbulence model:

- Standard k-ε Model
- The Yap k-ε Model
- The RNG-derived k-ε Model
- The Chen-Kim k-ε Model

- Lam-Bremhorst k-ε Model
- Two Scale k-ε Model
- Low-Reynolds k-ε Model

The Standard k-ε Model:

The k-e turbulence model proposed by Harlow and Nakayama in 1968 is still the most widely-used two-equation eddy-viscosity turbulence, mainly because the ε was long believed to require no extra terms near walls. The popularity of the model, and its wide use and testing , has thrown light on both its capabilities and its short-comings, which are well-documented in the literature.

The basic assumption of this method is that the local state of turbulence is characterized by the two parameters k and ε , which are equivalent to the parameter pair k and L because ε is proportional to $k^{3/2}/L$. The model employs the eddy viscoity/diffusivity concept and the parameters k and ε is dictated by dimensional analyis:

$$Vt=c_\mu k^2/\varepsilon \qquad \textbf{(2.21)}$$

$$\Gamma=\nu_t/\sigma_t \qquad \textbf{(2.22)}$$

where; c_μ is an empirical constant and σ_t is again the turbulent Prandtl/Schmidt number.

The k-ε method has been applied to many different flow situations, perhaps not so much in the area of surface water problems but in mechanical and aeronautical engineering and has been found to work well with the standard constants in many cases. There are, however, a number of basic flow situations where the standard model performs rather poorly. Therefore corrections to the constants have been introduced for the round jet and for weak shear layers occuring mainly in far wakes (Rodi 1980).

Also, the model has a tendency to underpredict the size of seperation regions in unconfined flow(e.g. behind bluff bodies). Various modifications to the ε-equation have been suggested to improve the performance, for example, by making the production of ε more sensitive to normal stress than to shear stress (Hanjalic and

Launder 1982), but none of the proposals work entirely satisfactorily (Rodi 1984, Launder 1984).

The standard k- ε model uses the same eddy viscosity /diffusivity for all Reynolds stress and heat or mass flux components (isotropic eddy viscosity/diffusivity), but in certain flow situations the assumption of an isotropic eddy viscosity is too crude. For example, it does not produce the turbulence-driven secondary motions in straight open channels and it does not allow any directional influences on the stress and fluxes, for example, those due to buoyancy forces. The two-equation models presented are thus far valid only at high turbulent Reynolds numbers , and therefore they are not valid in the near-wall viscosity-affected region. The model requires the application of so-called 'wall functions' or alternatively, the introduction of a low-Reynolds-number extension.

The Yap k- ε Model:

For seperated and reattachment flows, the standard k- ε model encounters difficulties, e.g. as boundary layers develop towards seperation the predicted near-wall length scales become too large, and the length of seperation regions is underpredicted in flows past steps and obstacles.

Several variants of the k- ε model have been proposed for dealing with this defficiency, including the Yap (1987) modification to the ε-equation:

$$S_\varepsilon = \max\left(0.83\rho\frac{L}{L_e - 1}\left(\frac{L}{L_e}\right)^2\frac{\varepsilon^2}{k}, 0\right) \qquad \textbf{(2.23)}$$

where; $L = \frac{k^{3/2}}{\varepsilon}$ and $L_e = CL \times YN$, with $CL = \frac{(C_\mu C_d)^{3/4}}{K} (= 2.495)$, YN is the distance from the wall and K=0.41

The correction can produce substantial improvements, particularly in heat-transfer predictions in seperated flows.

The RNG k- ε Model:

Yakhot and Orszag (1986) derived a k-ε model based on Renormalization Group (RNG) methods. In this approach, RNG techniques are used to develop the theory for the large scales in which the effects of the small scales are represented by modified transport coefficients.

The standard k- ε turbulence model is known to be too dissipative, the turbulent viscosity in recirculations tends to be too high, thus damping out vorticises. RNG k-ε turbulence model is an attempt to correct this deficiency by using slightly different constants and by adding the following volumetric source term to the ε-equation:

$$S_\varepsilon = \frac{-\rho\alpha\varepsilon^2}{k}\ ; \qquad \textbf{(2.24)}$$

where; $\alpha = C_\mu C_d \eta^3 \frac{1-\frac{\eta}{\eta_0}}{1+\beta\eta^3}$; $\beta = 0.012$; $\eta_0 = 4.38$; and the dimensionless parameter $\eta = \frac{k}{\varepsilon}\left(\frac{\rho P k}{\mu_T}\right)^{1/2}$.

The changes to the mode constants are:

PRT(k)=0.7194, PRT(ε)=0.7194; C_{1E}= 1.42; C_{2E}= 1.68; C_μ =0.0845

Although the assumptions of this model is very good for seperation and reattachment, its predictions for jets and plumes are inferior to the standard model.

The Chen-Kim Modified k- ε Model:

The standard k-ε turbulence model employs a single time scale (k/ε) to characterize the various dynamic processes occuring in turbulent flows. Accordingly, the source , sink and transport terms contained in the closed set of model equations are held to proceed at rates proportional to ε/k. However, turbulence comprises fluctuating

motions with a spectrum of time scales, and a single –scale approach is unlikely to be adequate under all circumstances. In order to remedy this deficiency in the standard model, Chen and Kim (1987) proposed a modification which improves the dynamic response of the ε-equation by introducing an additional time scale (k/P) where P_k is the volumetric production rate of k.

The Chen-Kim turbulence model is a modified type of k- ε turbulence model which is another attempt to cure the over-dissipative nature of the k- ε model. This variant of the k- ε model uses slightly different constants and introduces an additional source term into the ε-equation:

$$S_{\varepsilon} = \frac{-\rho C_{4e} P_k}{k} \qquad (2.25)$$

where; C_{4e}=0.25

In addition, several standard-model coefficients are adjusted so that the model maintains good agreement with experimental data on classical turbulent shear layers. The changes to the model constants are:

PRT(k) = 0.75, Prt (ε) =1.15, C_{1e}=1.15 and C_{2e}= 1.19.

The model predicts reattachment points and vortices almost as well as the RNG version, but preserves the good behaviour for jets and flumes of the standard version.

Lam-Bremhorst k-ε Model

Lam and Bremhorst (1981) a low-Reynolds-number extension to the k-ε model that employs a transport equation for the total dissipation rate, with the advantage that the model requires no additional source terms. However, a disadvantage of the model is that one of the damping functions requires the calculation of the nearest wall. The Lam –Bremhorst low-Reynolds k-ε model differs from the standard form of model in that the empirical coefficients C_{μ}, C_{1E} and C_{2E} are multiplied by functions (see Lam and Bremhorst (1981) for further information of these functions).

Two-Scale k- ε Model :

This model splits the turbulence-energy spectrum into 2 regions, namely the 'production' (P) region and the 'transfer' (T) region. Spectral equilibrium is assumed between the T region and the region in which turbulence is dissipated, i.e. the dissipation (D) region. Two transport equations are solved for each of these regions. Namely, KP and EP for the P region; and KT and ET for the T region. EP is the energy transfer rate from the P to T range and ET is the dissipation rate.

The advantage of the 2-scale k-ε model lies in its capability to model the cascade process of turbulent kinetic energy; and to resolve the details of complex turbulent flows are better than the standard k-ε model. The disadvantage is that it requires 4 turbulence transport equations, as opposed to the 2 equations required for the standard k-ε model. It is recommended that the standard k-ε model or one of its variants be used in the first instance. However, in cases where these models are clearly giving poor predictions the 2-scale model should be used to see whether better predictions can be obtained.

Low Reynolds k-ε Model :

In the cases that the Reynolds number is low and the use of high Reynolds turbulence model is no valid, low Reynolds k-ε model can be used. The use of low Reynolds k-ε models are very expensive because they need many points inside the boundary layer (from 5 to 20 in both viscous sublayer and turbulent layer). This not only increases the computational cost, but it forces us to use very small time increments or high relaxation. The advantage of Reynolds Stress Model is that buoyancy, rotation and other effects are in principle introduced automatically.

The k-Omega Model

The first two-equation turbulence model was the k-omega model of Kolmogorov (1942). This model, which is also known as the k-f and k-w model, involves the solution of transport equations for the turbulent kinetic energy k and the turbulence

frequency f. It should be mentioned that other workers define f as the ratio ε to k, where ε is the dissipation rate of k.

Although the k-f model is not as popular as the k-ε model, it does have several advantages, namely that :

1. the model is reported to perform better in transitional flows and in flows with adverse pressure gradients;
2. the model is numerically very stable, especially the low-Re version, as it tends to produce converged solutions more rapidly than the k-ε models; and
3. the low-Re version is more economical and elegant than the low-Re k-ε models, in that it does not require the calculation of wall distances, additional source terms and/or damping functions based on the friction velocity.

The main weakness of the k-f model is that unlike the k-ε model, it is sensitive to the free-stream boundary condition for f in free-shear flows. Modified variants exist which claim to remove this sensitivity, but it is also pointed out that it is a desirable feature for transitional applications.

2.2.2.4 Reynolds Stress/Flux Transport Models:

These are models involving the solution of transport equations for the Reynolds stresses and fluxes, together with a transport equation for the length scale , usually ε. The advantage of the Reynolds stress model is that buoyancy, rotation and other effects are in principle introduced automatically.However, turbulent stress transport equations contain higher order correlations which need to be modelled.

2.2.2.5 Algebraic Stress/Flux Models:

To make a Reynolds stress model work with reasonable computational effort, Rodi (1976) proposed an algebraic relation for calculating the Reynolds stresses. These models simplify the stress/flux transport equations to provide algebraic expressions for the turbulent correlations , which are then solved together with a two-equation

model. The algebraic expressions together with the k and ε equations form an extended k-ε model (Nallasamy, 1987).

2.3 Conclusion

The studies on local scour due to horizontal jets from the pioneering study of Rouse et al. (1939) through most recent studies have been investigated in detail. Most of these studies have been empirical due to the complex structure of scouring process combined with turbulent flow. Particularly with the increasing performance of computers many researchers proposed numerical modelling of physical features of turbulent flow for different cases.

The genaral types of turbulence modelling have been investigated and are given in this chapter. The standard k-ε turbulence model that was proposed by Harlow and Nakayama in 1968 is still the most widely used and the most validated turbulence model in the literature. The other modified types of k-ε model are also mentioned in this chapter. The standard k-ε model is the simplest turbulence model for which only the boundary conditions are needed to be supplied and it is the most validated model in the literature. From tis knowledge, the writer decided to use standard k-ε model to simulate numerically the submerged horizontal jet occuring on frozen beds.

Chapter 3

Numerical Investigation of Submerged Horizontal Jets Occuring On Frozen Scoured Beds Using k-ε Model

3.1 Introduction

In the present study, the mean characteristics of the submerged horizontal jet occured on frozen bed profiles are investigated numerically using standard k-ε turbulence model. From an engineering point of view, understanding of the dynamics of free surface turbulence in an open channel is of great importance and very difficult because it governs the mechanism of the transfer of mass , heat, momentum and vorticity across a gas-liquid interface.

It is more realistic to implement the free surface conditions in Cartesian coordinates when we choose a very fine mesh. But it is computationally expensive and needs more computer memory and it is not practical. The boundary fitted coordinate system which is applied in this thesis, makes this problem far simpler. There are many examples of boundary-fitted coordinate system in the literature.

Boundary fitted coordinate system to extend the capabilities of finite difference methods was pioneered by Thompson et al. (1974) to deal with complex geometries. The basic idea was to transform the complex flow domain in the physical space to a simple rectangular flow domain in the computational space. Boundary conditions are then implemented naturally in the rectangular computational domain. This method makes the governing equations look complicated but they are easy to discretize in the rectangular computational domain. In this thesis, transformed governing equations

are solved with a finite volume method in the computational domain (ζ , η) to compute the mean flow and turbulence characteristics of submerged horizontal jet occuring on frozen scoured bed.

In the following section of this chapter, two-dimensional k-ε model using boundary fitted coordinates is explained. Some equations are repeated for the sake of completeness of the present analysis.

3.2 k- ε Turbulence Model

3.2.1 Governing Equations:

All fluids have viscosity, only their viscosity are different. Real fluid flow is generally described by the Navier –Stokes equations which reflect the relationship of the inertial force, pressure and viscous force. Therefore most of the CFD researchers start from the Navier-Stokes equations directly (Patankar, 1980).

The instantenous values of the velocities u and v in x and y directions and the pressure are seperated into mean and fluctuating quantities in tensor notation as:

$$u = \overline{u} + u', \quad v = \overline{v} + v', \quad p = \overline{p} + p' \tag{3.1}$$

where u', v' and p' are the fluctuating quantities of u, v and p. The mean quantities are defined as:

$$\overline{u} = \lim_{t_2 \to t_1} \left(\frac{1}{t_2 - t_1} \int_{t_1}^{t_2} u \, dt \right), \quad \overline{v} = \lim_{t_2 \to t_1} \left(\frac{1}{t_2 - t_1} \int_{t_1}^{t_2} v \, dt \right) \tag{3.2}$$

$$\overline{p} = \lim_{t_2 \to t_1} \left(\frac{1}{t_2 - t_1} \int_{t_1}^{t_2} p dt \right) \tag{3.3}$$

The overbars indicating averag values will be dropped from the equations describing mean flow quantities and the following continuity, momentum and transport

equations for the steady , incompressible and two-dimensional mean flow can be written as:

Continuity Equation:

$$\frac{\partial u}{\partial x}+\frac{\partial v}{\partial y}=0 \tag{3.4}$$

Momentum equations:

$$u\frac{\partial u}{\partial x}+v\frac{\partial u}{\partial y}=-\frac{1}{\rho}\frac{\partial \rho}{\partial x}+\frac{\partial(\overline{-u'^2})}{\partial x}+\frac{\partial(\overline{-u'v'})}{\partial y} \tag{3.5}$$

$$u\frac{\partial v}{\partial x}+v\frac{\partial v}{\partial y}=-\frac{1}{\rho}\frac{\partial \rho}{\partial y}+\frac{\partial(\overline{-v'^2})}{\partial y}+\frac{\partial(\overline{-u'v'})}{\partial x} \tag{3.6}$$

where; ρ is the density of water. The momentum equations (3.5) and (3.6) are also known as the Reynolds equations, and the fluctuating-velocity terms $-\rho\overline{u'^2}$,$-\rho\overline{v'^2}$ and $-\overline{u'v'}$ are the Reynolds (turbulent kinematic) stresses. As it is obviously seen, the continuity (3.4) and the momentum equations (3.5 and 3.6) form 3 equations with six unknown variables (u, v, p, $-\overline{u'^2}$,$-\overline{v'^2}$ and $-\overline{u'v'}$). Therefore these equations do not form a closed set. In order to solve these equations , additional relationships are needed to express Reynolds stress in terms of known or determinable quantities and these relationships are determined through the turbulence model.

The equations of the turbulent kinetic energy k and the dissipation of kinetic energy ε can be derived from the Navier-Stokes equations (Hinze,1975). However, these equations contain certain high order correlations which are approximated by k-ε model to achieve a closure of the momentum and transport equations. The modelled form of the turbulence energy k and the energy dissipation ε are as follows:

Transport equation of Turbulent Energy:

$$u\frac{\partial k}{\partial x}+v\frac{\partial k}{\partial y}=\frac{\partial}{\partial x}\left(\frac{\nu_t}{\sigma_k}\frac{\partial k}{\partial x}\right)+\frac{\partial}{\partial y}\left(\frac{\nu_t}{\sigma_k}\frac{\partial k}{\partial y}\right)+G-\varepsilon \tag{3.7}$$

Transport equation of Turbulence Energy Dissipation:

$$u\frac{\partial \varepsilon}{\partial x}+v\frac{\partial \varepsilon}{\partial y}=\frac{\partial}{\partial x}\left(\frac{\nu_t}{\sigma_\varepsilon}\frac{\partial \varepsilon}{\partial x}\right)+\frac{\partial}{\partial y}\left(\frac{\nu_t}{\sigma_\varepsilon}\frac{\partial \varepsilon}{\partial y}\right)+C_1\frac{\varepsilon}{k}G-C_2\frac{\varepsilon^2}{k} \tag{3.8}$$

where; G is the turbulence energy production term and defined as:

$$G=\nu_t\left[\left(\frac{\partial u}{\partial y}+\frac{\partial v}{\partial x}\right)^2+2\left(\frac{\partial u}{\partial x}\right)^2+2\left(\frac{\partial v}{\partial y}\right)^2\right] \tag{3.9}$$

The k- ε turbulence model is based on the assumption that the Reynolds stresses are related to the mean strain rate through the Boussinesq approximation:

$$-\overline{u'^2}=2\nu_t\frac{\partial u}{\partial x}-\frac{2}{3}k \tag{3.10}$$

$$-\overline{v'^2}=2\nu_t\frac{\partial v}{\partial y}-\frac{2}{3}k \tag{3.11}$$

$$-\overline{u'v'}=\nu_t\left(\frac{\partial u}{\partial y}+\frac{\partial v}{\partial x}\right) \tag{3.12}$$

In the above equations, ν_t is the turbulent or eddy viscosity which strongly depends on the state of turbulence and ν_t may vary from one point to another and also flow to flow (Rodi,1980). The turbulent viscosity ν_t is related to the turbulence energy k and turbulence dissipation ε by :

$$v_t = c_\mu \frac{k^2}{\varepsilon} \tag{3.13}$$

A number of model constants have been utilised in equations of (3.7), (3.8), (3.13) which are required because a number of simplification made to the models. They have been derived through rigorous investigation of experimental data and have been found to provide the most suitable solutions to the equations over a wide range of turbulent flows. Calculations based on k- ε model are most sensitive to the values of C_1 and C_2. According to Rodi (1980); for example a 5% change of either C_1 or C_2 resulted in a 20 % change of spreading of a jet. The values used in the standard k- ε model are provided in Table 3.1 below.

Table 3.1 Model constants used in standard k-ε method

Model Constant	**Value**
C_μ	0.09
C_1	1.44
C_2	1.92
σ_k	1.0
σ_ε	1.3

3.2.2 Governing Equations in Boundary-Fitted Coordinates:

The governing equations presented in this chapter are in Cartesian coordinates. However, owing to the curvature of the free and bed surfaces , a cartesian coordinate system is lesss effective as approximations have to be made at the surface for a rectangular grid. Such approximations make it necessary to use fine mesh in cartesian coordinates, but this is computationally expensive. In order to overcome this difficulty, the continuity and momentum equations with transport equations were transformed into the boundary fitted coordinate system.

Having already mentioned, the basic idea is that a curvilinear coordinate transformation is used to map the complex flow domain in the physical domain to a

simpler rectangular flow domain in the computational domain. The case of submerged horizontal jet requires only a simple transformation from the non-rectangular physical plane into a rectangular computational plane. Our particular case of submerged horizontal jet occuring on frozen scoured bed requires finer mesh in coordinate system and a different transformation logic owing to the differentiation in the coordinates of channel bed due to the scouring process. This modified transformation is:

$$\xi = x \tag{3.14}$$

$$\eta = \frac{y - y_o}{y_t - y_o} \tag{3.15}$$

where ; ξ and η are the coordinates of the transformed plane and y_o is the ordinate of the bed profile for the correspondent ordinate value, y, of any point in physical plane, and y_t is the tailwater depth.

Since during the present study two-dimensional steady flow is investigated, we will not consider the independent variable time (t) during the transformation process. So we will transform the independent variables in the physical plane (x ,y) to a new set of independent variables in transformed plane (ξ , η) as below:

$$\xi = \xi(x, y)$$

$$\eta = \eta(x, y) \tag{3.16}$$

The inverse tranformation is given by:

$$x = x(\xi, \eta)$$

$$y = y(\xi, \eta) \tag{3.17}$$

After performing the chain rule of differentiation, the following relations between the operators of two coordinate systems can be obtained.

$$\frac{\partial}{\partial x} = \frac{1}{J}\left(y_\eta \frac{\partial}{\partial \xi} - y\xi \frac{\partial}{\partial \eta} \right)$$

$$\frac{\partial}{\partial y} = \frac{1}{J}\left(x_\xi \frac{\partial}{\partial \eta} - x_\eta \frac{\partial}{\partial \xi} \right) \qquad \textbf{(3.18)}$$

where ;

$$J = x_\xi y_\eta - x_\eta y_\xi$$

$$x_\xi = \frac{\partial x}{\partial \xi} \quad , \quad y_\xi = \frac{\partial y}{\partial \xi} \qquad \textbf{(3.19)}$$

$$x_\eta = \frac{\partial x}{\partial \eta} \quad , \quad y_\eta = \frac{\partial y}{\partial \eta}$$

The continuity, momentum and transport equations (3.4), (3.5), (3.6), (3.7) and (3.8) can be rewritten in the (ξ ,η) coordinates using the above operators (equations (3.18) and (3.19)):

Continuity Equation:

$$\frac{\partial U}{\partial \xi} + \frac{\partial V}{\partial \eta} = 0 \qquad \textbf{(3.20)}$$

u-Momentum Equation:

$$U\frac{\partial u}{\partial \xi} + V\frac{\partial u}{\partial \eta} = \frac{\partial}{\partial \xi}\left[\frac{\nu_t}{J}(q_1 \frac{\partial u}{\partial \xi} + q_2 \frac{\partial u}{\partial \eta}) \right]$$

$$+ \frac{\partial}{\partial \eta}\left[\frac{\nu_t}{J}(q_2 \frac{\partial u}{\partial \xi} + q_3 \frac{\partial u}{\partial \eta}) \right] + JS_u(\xi, \eta) \qquad \textbf{(3.21)}$$

v-Momentum Equation :

$$U\frac{\partial v}{\partial \xi}+V\frac{\partial v}{\partial \eta}=\frac{\partial}{\partial \xi}\left[\frac{v_t}{J}(q_4\frac{\partial v}{\partial \xi}+q_5\frac{\partial v}{\partial \eta})\right]$$
$$+\frac{\partial}{\partial \eta}\left[\frac{v_t}{J}(q_5\frac{\partial v}{\partial \xi}+q_6\frac{\partial v}{\partial \eta})\right]+JS_v(\xi,\eta) \qquad \textbf{(3.22)}$$

Tranport Equation of Turbulent Energy k :

$$U\frac{\partial k}{\partial \xi}+V\frac{\partial k}{\partial \eta}=\frac{\partial}{\partial \xi}\left[\frac{v_t}{J\sigma_k}(q_7\frac{\partial k}{\partial \xi}+q_8\frac{\partial k}{\partial \eta})\right]$$
$$+\frac{\partial}{\partial \eta}\left[\frac{v_t}{J\sigma_k}(q_8\frac{\partial k}{\partial \xi}+q_9\frac{\partial k}{\partial \eta})\right]+JS_k(\xi,\eta) \qquad \textbf{(3.23)}$$

Transport of Turbulent Energy Dissipation ε :

$$U\frac{\partial \varepsilon}{\partial \xi}+V\frac{\partial \varepsilon}{\partial \eta}=\frac{\partial}{\partial \xi}\left[\frac{v_t}{J\sigma_\varepsilon}(q_7\frac{\partial \varepsilon}{\partial \xi}+q_8\frac{\partial \varepsilon}{\partial \eta})\right]$$
$$+\frac{\partial}{\partial \eta}\left[\frac{v_t}{J\sigma_\varepsilon}(q_8\frac{\partial \varepsilon}{\partial \xi}+q_9\frac{\partial \varepsilon}{\partial \eta})\right]+JS_\varepsilon(\xi,\eta) \qquad \textbf{(3.24)}$$

where;

$$U=uy_\eta-vx_\eta$$
$$V=vx_\xi-uy_\xi \qquad \textbf{(3.25)}$$

and ,

$$q_1=2y_\eta y_\eta+x_\eta x_\eta \qquad q_6=y_\xi y_\xi+2x_\xi x_\xi$$
$$q_2=-2y_\eta y_\xi+x_\eta x_\xi \qquad q_7=y_\eta y_\eta+x_\eta x_\eta \qquad \textbf{(3.26)}$$
$$q_3=2y_\xi y_\xi+x_\xi x_\xi \qquad q_8=-y_\xi y_\eta-x_\eta x_\xi$$
$$q_4=y_\eta y_\eta+2x_\eta x_\eta \qquad q_9=y_\xi y_\xi+x_\xi x_\xi$$
$$q_5=-y_\eta y_\xi-2x_\xi x_\eta$$

S (ξ , η) is the source term im transformed (ξ , η) coordinates and they can be written for each dependend variable (u, v, k and ε) as follows,

$$S_u = \frac{1}{J}\left[\frac{\partial}{\partial\xi}\left(-\frac{1}{\rho}y_\eta p - \frac{2}{3}y_\eta k\right) + \frac{\partial}{\partial\eta}\left(\frac{1}{\rho}y_\xi p + \frac{2}{3}y_\xi k\right)\right] + \tag{3.27}$$

$$\frac{1}{J}\left[\frac{\partial}{\partial\xi}\left[\frac{1}{J}v_t\left(x_\eta y_\xi \frac{\partial v}{\partial\eta} - y_\eta x_\eta \frac{\partial v}{\partial\xi}\right)\right] + \frac{\partial}{\partial\eta}\left[\frac{1}{J}v_t\left(y_\eta x_\xi \frac{\partial v}{\partial\xi} - y_\xi x_\xi \frac{\partial v}{\partial\eta}\right)\right]\right]$$

$$S_v = \frac{1}{J}\left[\frac{\partial}{\partial\xi}\left(\frac{1}{\rho}x_\eta p + \frac{2}{3}x_\eta k\right) + \frac{\partial}{\partial\eta}\left(-\frac{1}{\rho}x_\xi p - \frac{2}{3}x_\xi k\right)\right] + \tag{3.28}$$

$$\frac{1}{J}\left[\frac{\partial}{\partial\xi}\left[\frac{1}{J}v_t\left(x_\xi y_\eta \frac{\partial u}{\partial\eta} - x_\eta y_\eta \frac{\partial u}{\partial\xi}\right)\right] + \frac{\partial}{\partial\eta}\left[\frac{1}{J}v_t\left(y_\xi x_\eta \frac{\partial u}{\partial\xi} - y_\xi x_\xi \frac{\partial u}{\partial\eta}\right)\right]\right]$$

$$S_k = G(\xi,\eta) - \varepsilon \tag{3.29}$$

$$S_\varepsilon = C_1\frac{\varepsilon}{k}G(\xi,\eta) - C_2\frac{\varepsilon^2}{k} \tag{3.30}$$

It is seen from equations (3.29) and (3.30) that S_k and S_ε contain production of kinetic energy term G which is due to interactions of turbulent stresses with horizontal mean-velocity gradients (Rodi ,1980). G can be represented in the transformed plane by using the relations (Equation (3.19)) between the two coordinate systems and it is available in the Ph.D thesis submitted by Mustafa Günal, 1996, University of Manchester.

3.3 Boundary Conditions:

Since the finite difference form of governing equations are elliptic, they can be only solved for a given set of boundary conditions. The boundary conditions that were taken in this study are dicussed in the following sections.

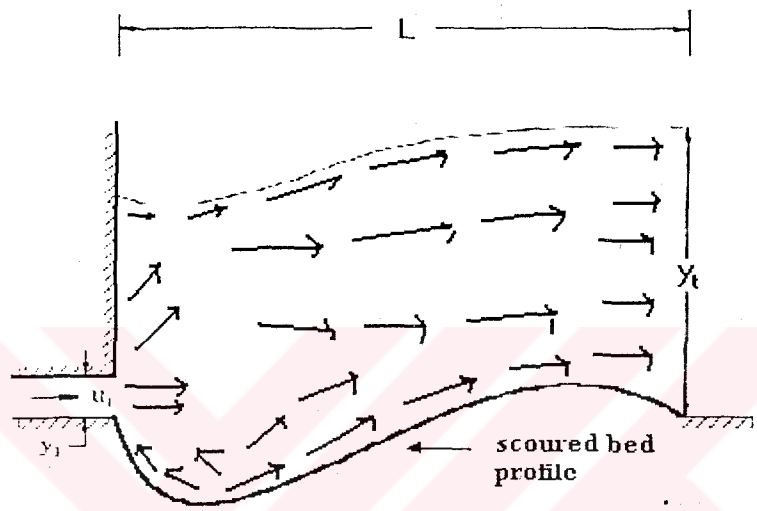

Figure 3.1 Definition sketch for a submerged horizontal jet

where ; u_1= initial velocity of jet, y_1 = width of sluice gate opening, L = total length of scour profile and y_t = downstream depth of water that is controlled by a gate (tailwater depth).

3.3.1 Inlet Conditions:

The velocity and turbulence quantities are specified at the inlet. At the inlet, the streamwise velocity u is assumed to be uniform and vertical velocity v is assumed as zero. The velocities U and V in the computational plane are calculated from equation (3.25). Zero pressure gradient is assumed in the streamwise direction next to the inlet. With the assumption of turbulence being locally isotropic and in equilibrium at the inlet, turbulence quantities k and ε are taken from the experimental measurements of Long et al.(1991) as,

$$k_{inlet}=1.4\,x\,10^{-3}\,u_1^2$$

$$\varepsilon_{inlet} = 2.2\,x\,10^{-5}\,\frac{u_1^3}{y_1} \tag{3.31}$$

3.3.2 Outlet Conditions:

At the outlet the downstream depth of water, y_t, is predefined in the present study by taking y_t values used in the studies that are compared with the present study. The tailwater depth can also be computed from the submergence formula and can be expressed as :

$$y_t = Sy_2 + y_2$$

where S is the submergence factor and y_2 is the downstream sequent depth of free jet. All other variables were constrained to have zero gradients in longitudinal direction i.e.,

$$\frac{\partial U}{\partial \xi} = \frac{\partial V}{\partial \xi} = \frac{\partial k}{\partial \xi} = \frac{\partial \varepsilon}{\partial \xi} = 0 \tag{3.32}$$

3.3.3 Free Surface Condition:

The free surface is assumed to be streamline. Therefore the velocity normal to the free surface and the pressure on the surface are taken zero. First derivatives of U, V, K and ε with respect to η are taken to vanish on the free surface . Thus the surface conditions are :

$$P_{surface} = 0$$

$$V_{surface} = 0 \tag{3.33}$$

$$\frac{\partial U}{\partial \eta} = \frac{\partial V}{\partial \eta} = \frac{\partial \varepsilon}{\partial \eta} = \frac{\partial k}{\partial \eta} = 0$$

3.3.4 Wall Condition:

At high Reynolds number, the viscous layer of a boundary layer is so thin it would require large computational resources to resolve flows at such small scale. In order to avoid this problem in CFD, wall functions are applied in the near wall region that rely on the existence of the logarithmic region in the velocity profile. Wall functions are commonly used to provide the boundary conditions for nodes nearest to the channel bed; they are proposed by Launder and Spalding (1974).

Implementation of wall boundary conditions for turbulence model is accessed by evaluating the scaled wall distance, y^+, between the wall surface and the computational node nearest the wall. For distances where $y^+ \geq 11.63$, the flow is turbulent and the wall function approach is used, for y^+ values les than 11.63 the near wall flow is taken as laminar.

From this assumption and the eddy viscosity formula, the following wall functions are developed.

$$u^+ = \frac{1}{\kappa}\ln(Ey^+)$$

$$k_{wall} = \frac{u_*^2}{\sqrt{C_\mu}} \qquad \textbf{(3.34)}$$

$$\varepsilon_{wall} = \frac{u_*^3}{\kappa y}$$

where; $\kappa = 0.41$ is the Von Karman constant (for smooth surfaces) but $\kappa = 0.43$ is taken in present study; and E is a wall roughness parameter = 9.0 (E value is taken smaller than 9.0 for rough surfaces (Versteeg and Malasekera, 1995). E value is taken as 8.5 in present study) ; $u^+ = u/u_*$; $y^+ = yu_*/\nu$ and u_* is the friction velocity defined by $u_* = (\tau_w/\rho)^{\frac{1}{2}}$ where τ_w is the wall shear stress.

The wall shear stress is the most important issue in wall functions. When the shear stress is estimated velocity in the fully developed outer region can be found easily through the wall functions (Gunal, 1996). Benim and Zinser proposed a wall model iteration technique for estimating the wall shear stress. Long et al. (1991) implemented this model and reported good results. So it is decided to use their model in this study. The logic of this model is that first two grid points in the solution domain are away from the viscous layer, but within the logarithmic layer. At the beginning, u_* is assumed and u_{n1}, v_{n1}, k_{n1}, ε_{n1} at node 1 can be determined. This will be used as wall conditions. After each iteration the information at node 2 is fed back to node 1 through the following relationship for the wall shear stress (Benim and Zinser, 1985).

$$\tau_w = \frac{\kappa_{n1} C_\mu^{1/4} \rho u_{n2} k_{n1}^{1/2}}{\ln\left(\frac{E C_\mu^{1/4} y_{n2} k_{n1}^{1/2}}{\nu}\right)}$$

3.4 Numerical Solution of The Partial Differential Equations

The transformed governing equations in (ξ,η) plane should be transformed into corresponding discrete forms in order to be solved. The finite volume method was chosen for the present study because it is easy to implement and conservation can always to be obtained in the coputational cells. In the Finite Volume Method the domain is first overlaid with cells which divide the whole domain into a number of control volumes. In the present formulation, a grid system is first generated numerically at the corner of each control volume. The velocities are calculated at a point half way between these grid nodes and the pressures are calculated at the center of each control volume. This staggered grid system as shown in Figure 3.2 is adopted for variable arrangement to avoid the well known chequerboard oscillations in the pressure and velocity. Since a staggered grid system has been employed for all velocity components (U,V) and scalar quantities (p, k, ε), a seperate control volume is to be considered for the integration of each governing equations. As an example of the procedure of the integration the tranformed governing equation (3.21) for a dependent variable, ϕ (given in Equatin 3.35) whose control volume is the same as

that of pressure, is described in the following section. The dimension of the control volume is $\Delta\xi$ to $\Delta\eta$.

Firstly the convection part (left side) of the equation (3.21) is taken and integrated over the control volume as shown in Figure 3.2.c:

$$\int_{e}^{w}\int_{s}^{n}\left[\frac{\partial}{\partial\xi}(U\Phi)+\frac{\partial}{\partial\eta}(V\Phi)\right]d\xi d\eta \qquad (3.35)$$

where ; Φ stands for any dependent variable (u , v, k or ε) and assume that Φ varies uniformly along the control volume faces. Using the linear interpolation between the control volume faces then the above expression (3.35) will look as follows:

$$\left[U_e\frac{(\Phi_p+\Phi_e)}{2}-U_w\frac{(\Phi_p+\Phi_w)}{2}\right]\Delta\eta+\left[V_n\frac{(\Phi_N+\Phi p)}{2}-V_s\frac{(\Phi_s+\Phi_p)}{2}\right]\Delta\xi \qquad (3.36)$$

The right hand side (the diffusion part) of the equation 3.21 can be integrated and described as:

$$\int_{e}^{w}\int_{s}^{n}\frac{\partial}{\partial\xi}\left[\frac{\nu_t}{J\sigma_\Phi}(q_1\frac{\partial\Phi}{\partial\xi}+q_2\frac{\partial\Phi}{\partial\eta})\right]d\xi d\eta$$

$$+\int_{e}^{w}\int_{s}^{n}\frac{\partial}{\partial\xi}\left[\frac{\nu_t}{J\sigma_\Phi}(q_1\frac{\partial\Phi}{\partial\xi}+q_2\frac{\partial\Phi}{\partial\eta})\right]d\xi d\eta \qquad (3.37)$$

making the same assumption that is made in equation 3.35 , it can be written as follows:

$$\left[\frac{\nu_t}{J\sigma_\Phi}\left(q_1(\frac{\Phi_E-\Phi_P}{\Delta\xi_e})+q_2(\frac{\Phi_{NE}-\Phi_{SE}}{\Delta\eta})\right)\right]_w\Delta\eta$$

$$-\left[\frac{\nu_t}{J\sigma_\Phi}\left(q_1\left(\frac{\Phi_p-\Phi_w}{\Delta\xi_w}\right)+q_2\left(\frac{\Phi_{Nw}-\Phi_{Sw}}{\Delta\eta}\right)\right)\right]_w\Delta\eta$$

$$+\left[\frac{\nu_t}{J\sigma_\Phi}\left(q_3\left(\frac{\Phi_N-\Phi_P}{\Delta\eta_n}\right)+q_2\left(\frac{\Phi_{NE}-\Phi_{NW}}{\Delta\xi}\right)\right)\right]_n\Delta\eta \qquad \textbf{(3.38)}$$

$$-\left[\frac{\nu_t}{J\sigma_\Phi}\left(q_3\left(\frac{\Phi_P-\Phi S}{\Delta\eta s}\right)+q_2\left(\frac{\Phi_{sE}-\Phi_{sW}}{\Delta\xi}\right)\right)\right]_n\Delta\eta$$

In the same way, source term can be integrated and the terms which cannot be written in terms of five nodes (P, E, W, S and N as shown in Figure 3.2) are moved into the source term. After rearrangement, the following discretization equation for Φ_P and neighbouring variables can be written as follows (Patankar, 1980).

$$A_p\Phi_p = A_E\Phi_E + A_W\Phi_W + A_N\Phi_N + A_S\Phi_S + S_\Phi \qquad \textbf{(3.39)}$$

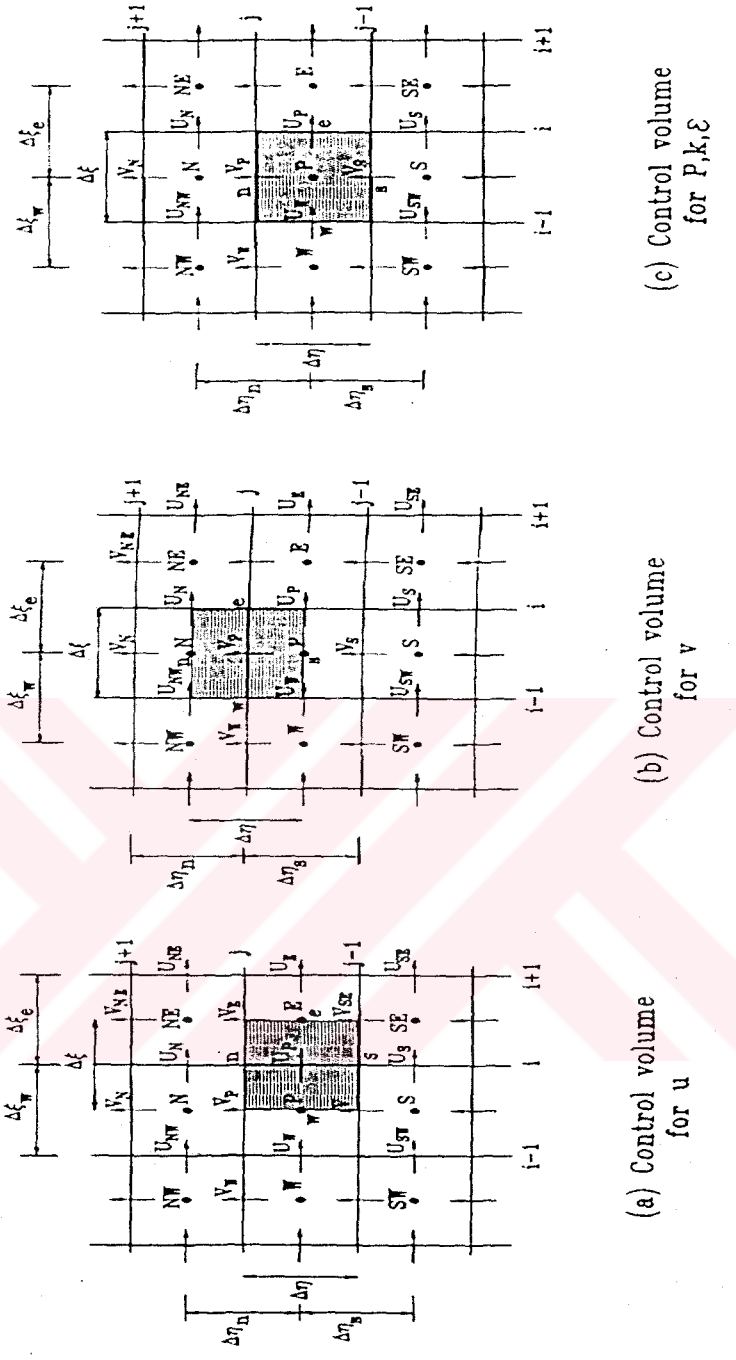

Figure 3.2 Arrangement of different control volumes

3.4.1 Pressure Correction Equation

The momentum equations can be solved only when the pressure field is given or estimated. Unless the correct pressure field is employed the resulting velocity field will not satisfy the continuity equation. Thus, the aim here is to find a way of improving the guessed pressure such that the resulting velocity field satisfies the continuity equation.

The continuity equation (3.21) in the computational plane can be written in a discretisized form over each control volume as follows (see Figure 3.2 c).

$$(U_e - U_W)\Delta\eta + (V_n - V_S)\Delta\xi = 0 \tag{3.40}$$

If we assume that u^* and v^* will satisfy the momentum equations in the physical plane with a given distribution of p^*. Since the pressure will not satisfy the continuity equation, the pressure p^* must be corrected. The correct pressure p is obtained from:

$$p = p^* + p_c \tag{3.41}$$

where ; p_c is called the pressure correction. The corresponding velocity corrections u_c, v_c can be introduced as

$$u = u^* + u_c \qquad v = v^* + v_c \tag{3.42}$$

Shy et al (1985) have derived the pressure correction assuming that u^* and v^* can be obtained from

$$u_p^* = \sum_{i=E,W,S,N} A_i^u u_i^* + D^u + (B^u p_\xi^* + C^u p_\eta^*)$$

$$v_p^* = \sum_{i=E,W,S,N} A_i^v v_i^* + D^v + (B^v p_\xi^* + Cv p_\eta^*) \tag{3.43}$$

where; D^u *and* D^v are the derivative viscous terms in the u and v momentum equations, and

$$B^u = -\frac{y_\eta}{A_p^u}\Delta\xi\Delta\eta \qquad C^u = \frac{y_\xi}{A_p^u}\Delta\xi\Delta\eta$$

$$B^v = -\frac{x_\eta}{A_p^v}\Delta\xi\Delta\eta \qquad C^v = -\frac{x_\xi}{A_p^v}\Delta\xi\Delta\eta \tag{3.44}$$

Shy et al. (1985) assumed that the velocity components can be corrected by the following formulas:

$$u = u^* + (B^u p_{c\xi} + C^u p_{c\eta})$$
$$v = v^* + (B^v p_{c\xi} + C^v p_{c\eta}) \tag{3.45}$$

The above equation is derived to correct the velocities in Cartesian coordinates. The velocity corrections for U and V in the computational plane can be obtained by substituting equation 3.45 to 3.26 as follows :

$$U = U^* + (B^u y_\eta - B^v x_\eta)p_{c\xi}$$
$$V = V^* + (C^v x_\xi - C^u y_\xi)p_{c\eta} \tag{3.46}$$

By substituting Equation 3.46 into discretized continuity equation 3.40, the pressure correction equation can be written as folows :

$$A_p p_p = A_E p_E + A_W p_w + A_S p_s + A_N p_N + S_p \tag{3.47}$$

3.4.2 Hybrid Numerical Scheme

In the literature, various types of interpolation practice can be found in order to avoid the faults while discretization of governing equations. In the model of the present study the most widely-used interpolation practice known as the Hybrid Differencing Scheme that was proposed by Spalding in 1972 has been used. It is the combination

of central and upwind differencing scheme. The hybrid differencing scheme basicly switches from upwind to central differencing or vice versa in evaluating the convection term according to the cell peclet number. For example , the flux accross the east face of the control volume (see Figure 3.2 c) is evaluated by

$$\left[U_P\left(\frac{\Phi_P+\Phi_E}{2}\right)-\left(\frac{\nu_t q_1}{J\sigma_\Phi}\right)\left(\frac{\Phi_E-\Phi_P}{\Delta\xi_e}\right)\right]\Delta\eta, \qquad \text{when } -2 > p_e < 2$$

$$\begin{aligned} &U_p\Phi_p\Delta_\eta, \text{ when } \quad p_e \geq 2 \\ &U_p\Phi_E\Delta_\eta, \text{ when } \quad p_e \leq -2 \end{aligned} \tag{3.48}$$

where; Φ is the dependent variable , J is the Jacobian and ν_t is the turbulent viscosity and σ_Φ is the model constant and p_e is the cell Peclet number and defined as :

$$p_e = \frac{U_E\Delta\xi_e}{\left(\frac{\nu_t q_1}{J\sigma_\Phi}\right)} \tag{3.49}$$

In the present study, the Equations 3.39 and 3.47 are formulated using the hybrid finite difference formulation proposed by Runchal (1972). The detailed derivation of the all transformed governing equations in the computational plane are given in Appendix 1 of the Ph.D. Thesis submitted by Mustafa Günal, 1996, University of Manchester, in detail.

3.5 Solution Technique

The algebraic equations (3.39) and (3.47) exist for every computational node in the computational domain. There are (M x N) equations with (M x N) unknowns. These equations can be solved by a direct or iterative method. The direct solution by matrix inversion would consume more time and demands more computer storage than the iterative method. The linearized algebraic equations (3.39) and (3.47) are themselves

approximations of the partial differential equations and it would be inappropriate to adopt a direct solution method.

The system equations are solved by Tri-diagonal Matrix Algorithm (TDMA) , a line iterative method, with alternating sweep directions. In an iterative scheme it is often desirable to speed up or slow down the changes of dependent variables from iteration to iteration, which is known as over relaxation or under relaxation. Because the Navier Stokes equations are non-linear, the process of convergence needs to be slowed down. In the present study, in order to avoid divergence, under relaxation factor with changable values in each run of program was used for velocities and pressures. The under relaxation factors are mainly problem dependent and have no influence on the converged solution.

3.6 Solution Algorithm and Calculation Flow chart

The pressure gradients which are present in the momentum equations must be known in order to solve the momentum equations by the pre-mentioned iterative method. Thus, the derived pressure correction equation (3.47) is solved after solving discretized governing equation (3.39) for new velocity field based on a guessed pressure. The pressure and velocity fields are then corrected respectively before starting to the next iteration. This algorithm is known as SIMPLE, which stands for Semi-Implicit Method for Pressure-Linked Equations. The SIMPLE algorithm has been described by Patankar and Spalding (1972) and Patankar (1980). The procedure of SIMPLE algorithm for the governing equations can be summarized as follows:

1. Initialize all dependent variables in the domain including pressure,
2. Solve the discretized governing equation (3.39) to obtain new velocities based on a guessed pressure field.
3. Solve the discretized pressure correction equation (3.47).
4. Correct the pressure field (equation 3.41).
5. Calculate a new velocity field using the velocity correction equations (equation 3.38)
6. Solve the transport equations and update the turbulent viscosity ν_t.

7. Return the step 2 and repeat the whole procedure until a converged solution is obtained.

The convergence is monitored by the absolute residual sum for the continuity equation. The program stopped when the residual sum is 0.0001. The computer program is written in Fortran 77 which is presented in Appendix. The calculation flow chart is given in Figure 3.3.

3.7 Conclusion

Standard k-ε model using boundary fitted coordinates is developed to predict the internal mean and turbulent structure of flow in submerged horizontal jet occuring on erodible beds. The two-dimensional continuity, momentum and transport equations for steady state and imcompressible flows are solved numerically by the finite volume method in boundary fitted coordinates. The non-rectangular domain of the submerged horizontal jet with the free surface is transformed into a rectangular computational domain. The governing equations with the boundary are transformed into the computational plane using the relations between the operators of the two coordinate systems. The transformed equations are then solved initially assuming that the free surface is flat.

However, the free surface is modified after each iteration in order to satisfy the free surface condition. After each iteration, the mesh is regenerated according to the new surface profile and next iteration takes place with the new surface profile.

The numerical results are presented in terms of mean velocity field, mean horizontal and vertical velocity distribution, turbulence intensity, Reynolds stresses, surface profile and bed shear stress. In the present thesis no detailed experiments were carried out. The author's numerical results are compared with the experimental results of Ali and Lim (1986), and the numerical results of Karim and Ali (2000).

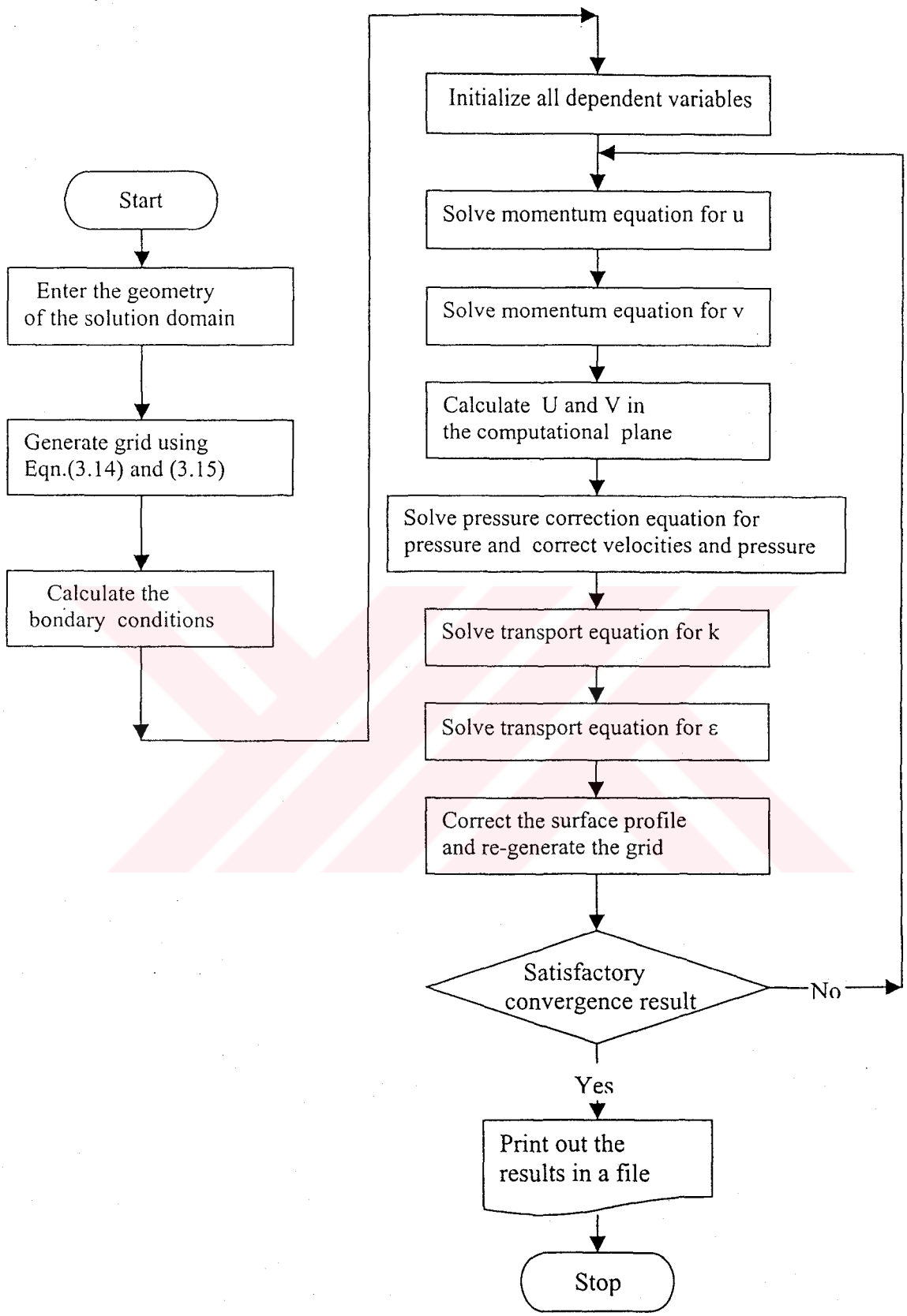

Figure 3.3 Calculation flow chart

Chapter 4

Presentation and Discussion of Results

4.1 Introduction

It was decided to study on submerged hydraulic jump at the beginning of this study but it has been experienced by the author that some serious singularity problems occur while dealing with hydraulic jump. The problem was noticed to be due to Froude number value larger than 1. Hydraulic jump has a complex dynamic structure. Moreover, it is very difficult to study hydraulic jump together with a moving (erodible) bed due to the fact that the coupling between the shape of the eroded bed profile and the hydrodynamic characteristics of the jet flow increase the complexity.

The significant experiment of Rajaratnam is that the mean motion within the hydraulic jump behaves in a manner that is typical of a plane turbulent wall jets. Narayanan (1975). From this knowledge the author decided that study on horizontal turbulent jet can also give opinion about the flow pattern of hydraulic jump on scoured beds.

Laboratory studies of two-dimensional scour downstream of a sluice gate are well documented, however, a comprehensive understanding of the scour mechanism remains elusive because of the complex nature of the process. (Hogg et al., 1997). Therefore many scientists decided to study on frozen (rigid) scoured beds in order to eliminate the hydrodynamic difficulties of sediment motion. This objective is reached by allowing the water to flow on erodible bed until asymptotic (equilibrium) state is reached and binding the scoured bed by chemicals (e.g. glue, cement) after dewatering the flume. By this way the mean characteristics of the jet can be

measured on rigid scoured bed. A lot of studies can be seen in the literature that studied with the same procedure that is explained above.

The writer decided to study with the same procedure and some experimental studies from the literature have been chosen to make comparisons. For this purpose, the experimental results of Ali and Lim (1986) and the numerical results of Karim and Ali (2000) have been taken as reference to check the numerical results of the present study.

The computer program is written and run for data obtained from aforementioned studies.The data that is needed to run the program are: (see Figure 3.1)

- tailwater depth (y_t)
- scour profile of bed (at equilibrium state)
- initial jet velocity (u_1)
- sluice gate opening (y_1)

By running the program for several data groups, it was observed that the program diverged. The divergence problem occured at pressure increments and vertical velocity. By decreasing the under-relaxation numbers, the problem was relatively solved but at this time the convergence problem arised. Therefore it was decided to study with the articles including shallow tailwater condition. This was only an assumption but later trials contributed this assumption.

The experimental results of Ali and Lim (1986) and Liriano et al. (2002) and the numerical results of Karim and Ali (2000) were used. Eventually, the program was observed to run well with shallow tailwater depth. The outputs of the computer program for different scour profiles, inlet and outlet conditions are presented in this chapter. The comparisons of results of present study with the reference studies were also presented in this chapter.

The k-ε turbulence model suffers from some limitations when applied to reattaching flows enclosing zones of recirculation as pointed out by Bernard (1991), Launder (1991) and Boyson (1993). This two-dimensional study is restrictive because the

flow in recirculating region of the jet is three-dimensional. Moreover, the k-ε model for three-dimensional flow assumes the normal components of the Reynolds stress tensor to be isotropic and such an assumption precludes the prediction of secondary mean currents in recirculating region.

The standard k-ε model is also deficient when the turbulence quantities are affected by streamline curvature (Bernard, 1991) and in the case of hydraulic jump, the free surface (Rodi, 1980). In the jump analogous to wall jet , since the shear stress is not zero at the position of maximum velocity (Gartshore and Newman, 1969), the gradient diffusion model is not strictly appropriate there. The aforementioned limitations of standard k-ε model was reduced to a degree by other modified versions, RNG k-ε, Chen-Kim k-ε and Yap k-ε models. The advantages of these modified models are explained in literature survey chapter.

The computed results for the submerged horizontal jet presented in this thesis must be tempered in view of the deficiencies of the k-ε model. Despite the deficiencies of k-ε model, the agreements between the predicted and experimental results are quite satisfactory. Especially very good agreements were observed with Ali and Lim (1986)'s and experimental results and Fluent package program's predicted results in Karim and Ali (2000). The reasons of some distinctions between the present study and the experimental and predicted results can be due to the initial boundary condition assumptions.

4.2 Presentation and Comparison of Numerical Results

Figure 4.1 shows the actual grid mesh in the physical and computational domain for F_1= 0.78 and S = 0.86. In finite difference solution, the absolute size of cells within the grid is an important issue, since if the cells are too large the solution obtained can be dependent on the cell size rather than purely on the physical constraints of the solution domain and the input conditions (Karim and Ali, 2000). Fluent package program was run by Karim and Ali (2000) for different number of grids and they observed that the program gave better agreement with experimental results with a 71x11 grid arrangement. But the writer used 71x21 grid arrangment to avoid some serious numerical diffusion problems due to large grid size and observed

that the results of 71x21 grid arrangement were much better than those of 71x11 grid arrangement. It can easily be seen from the figures that the computational domain is always rectangular. Thus it is easy to discretize the governing equations and more important, the boundary conditions are applied much more easily without any interpolation on the boundary cells.

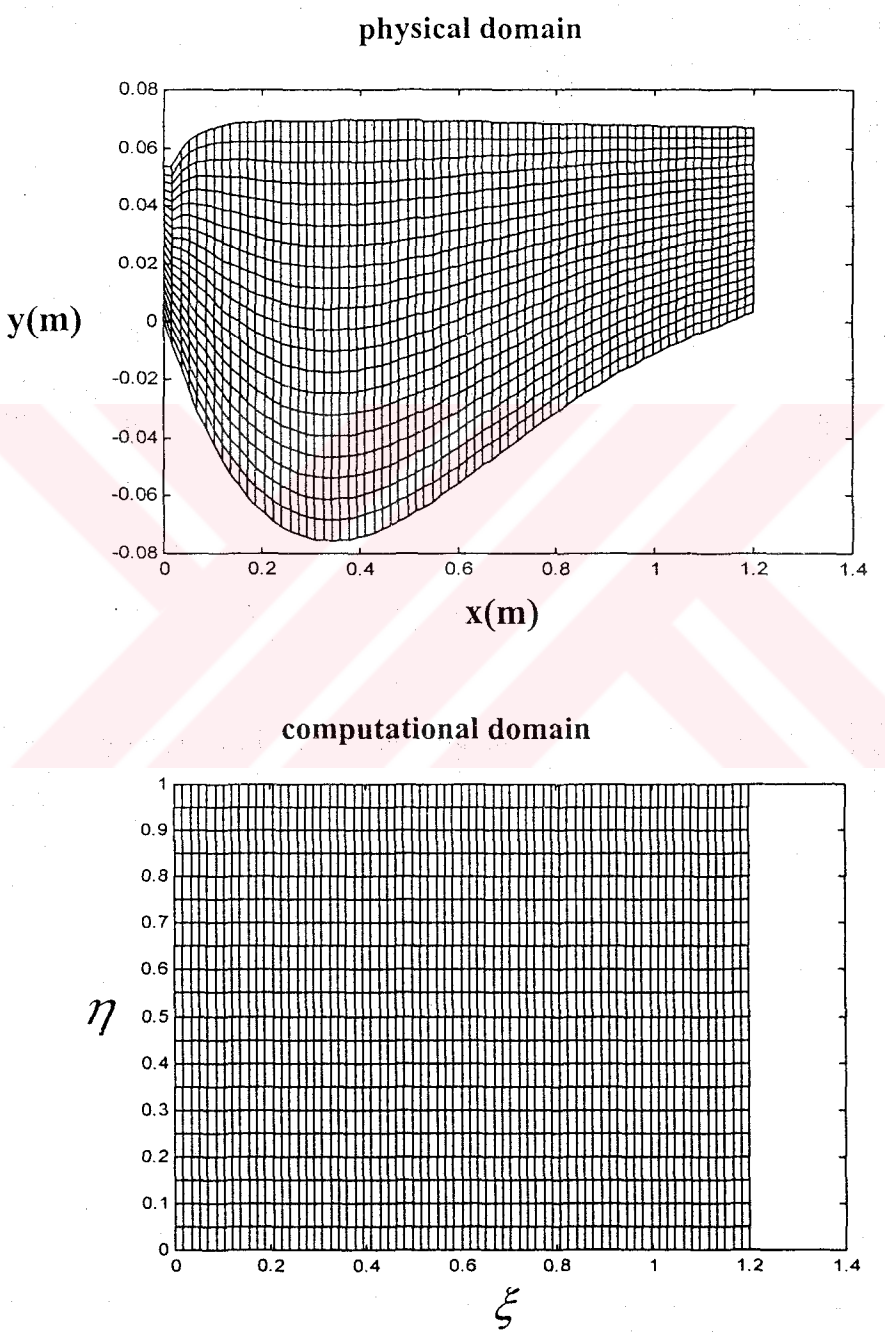

Figure 4.1 Grid transformation for F_1=0.78 and S = 0.86.

The final velocity vector field for F_1= 0.78 and submergence factor = 0.86 is plotted in Figure 4.2. The formation of a jump at just downstream of the sluice gate can clearly be seen. This figure was observed to be in a strict agreement with the numerical prediction of Fluent package program that is presented in Karim and Ali (2000).

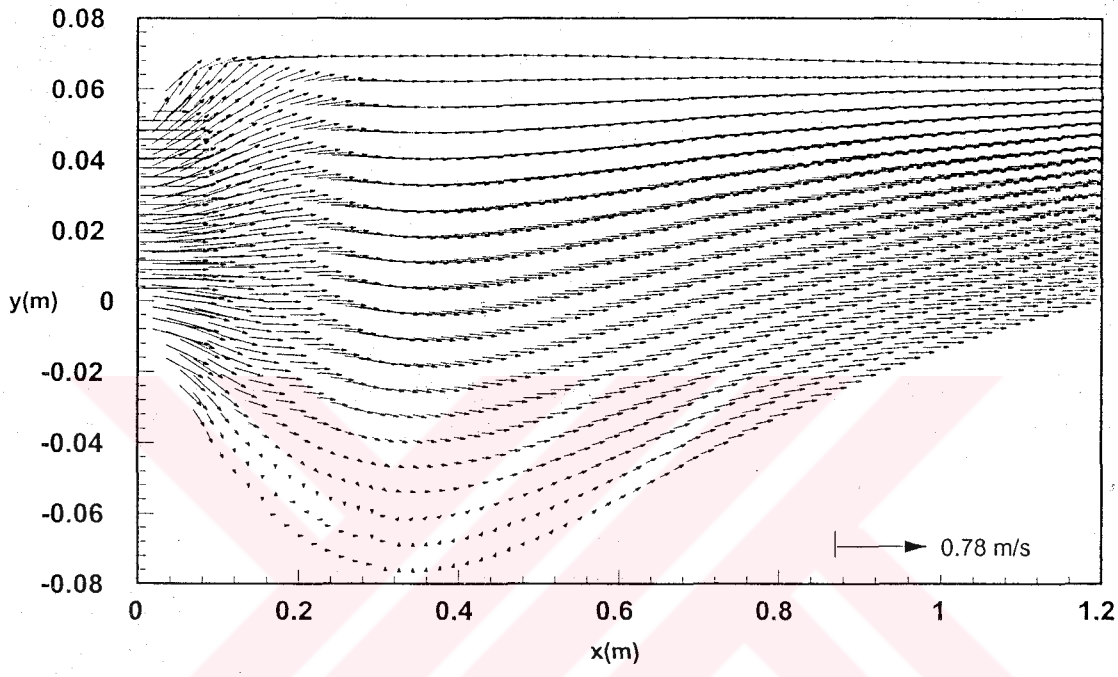

Figure 4.2 Velocity vector field from numerical calculation for F_1 =0.78 and S = 0.86.

Figure 4.3, 4.4, 4.5 and 4.6 present the results of the present k-ε model for the mean velocities u and v, turbulence kinetic energy k and turbulence energy dissipation rate ε for F_1 = 0.78 and submergence factor S = 0.86. All the quantities are made non-dimensional using velocity and length scales respectively as u_1 and y_1.

Figure 4.3 shows a good agreement between the mean velocity distribution of horizontal jet occured on rigid scoured bed and wall jet analogy but no similarity with typical plane jet distribution is seen. At each profile in the figure, the mean horizontal velocity values are observed to approach zero close to the bed and reach a peak value over the original bed level. Although it can not clearly been observed from the figure, reverse velocities take place in the region between downstream of sluice gate and maximum scour depth.

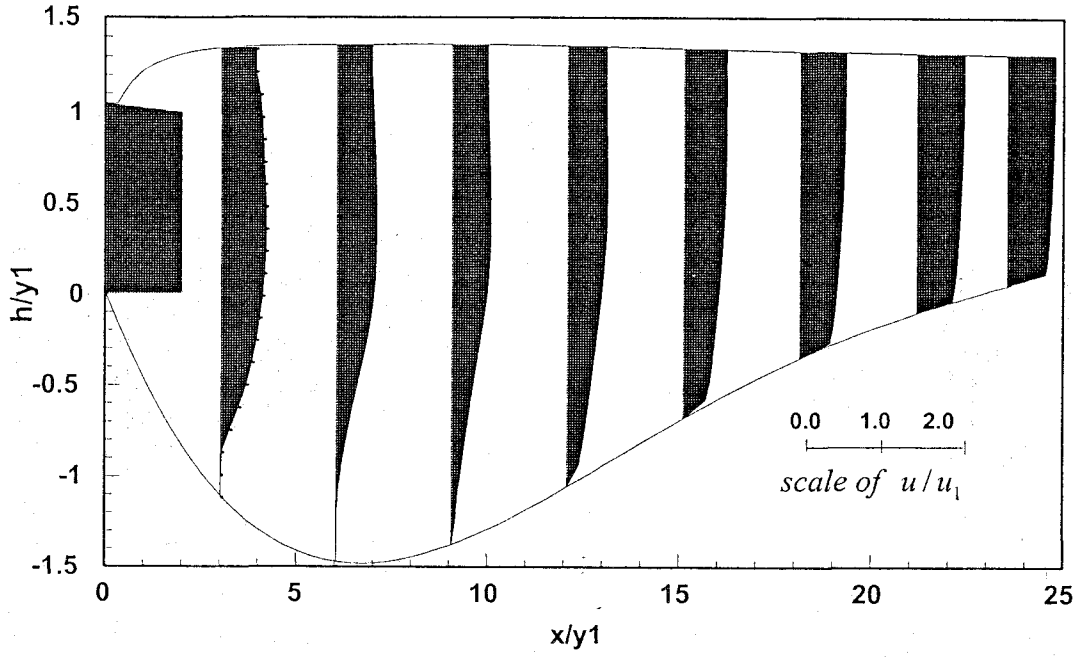

Figure 4.3 Distribution of longitudinal velocity of u/u_1 scour from the numerical prediction for $F_1 = 0.78$ and $S = 0.86$.

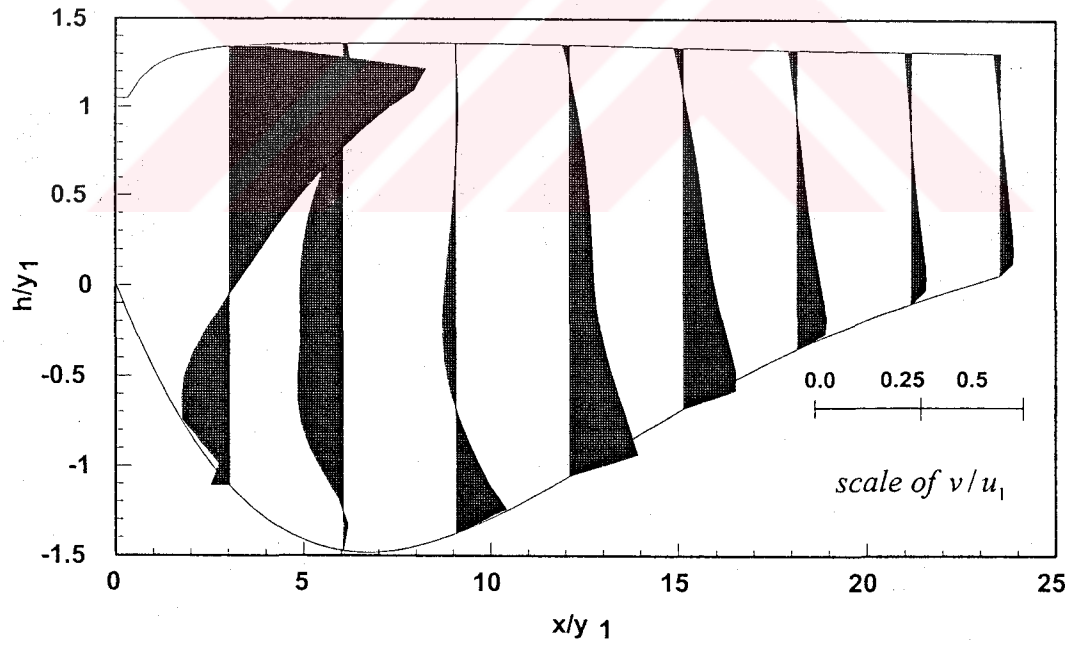

Figure 4.4 Distribution of vertical velocity of v/u_1 along scour from the numerical prediction for $F_1 = 0.78$ and $S = 0.86$.

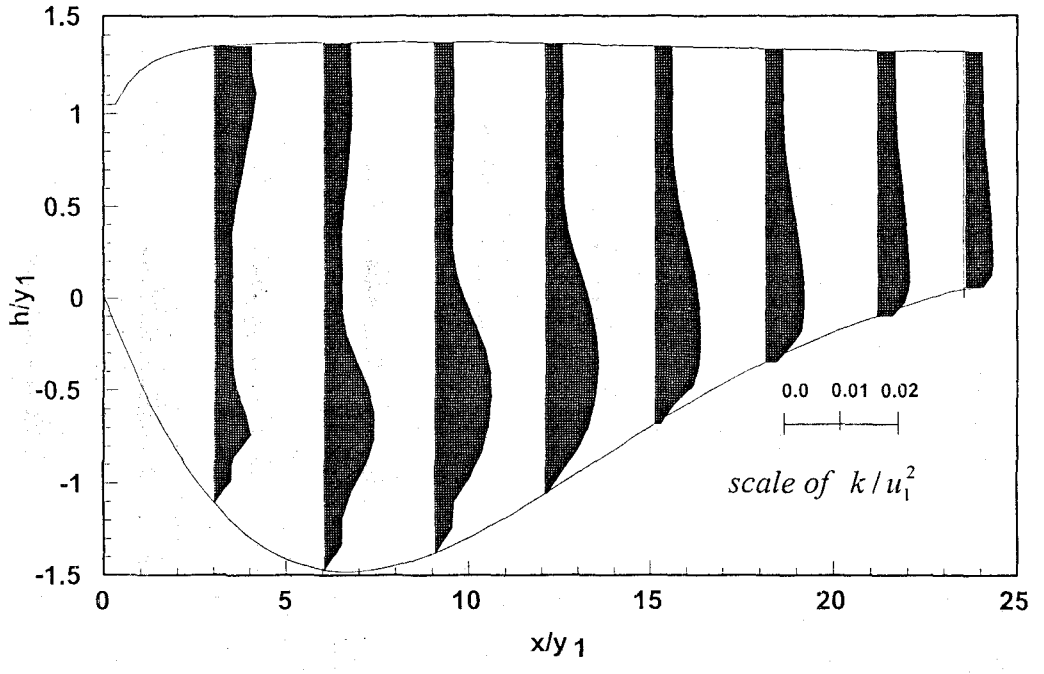

Figure 4.5 Distribution of k/u_1^2 along the scour from the numerical prediction for $F_1 = 0.78$ and $S = 0.86$.

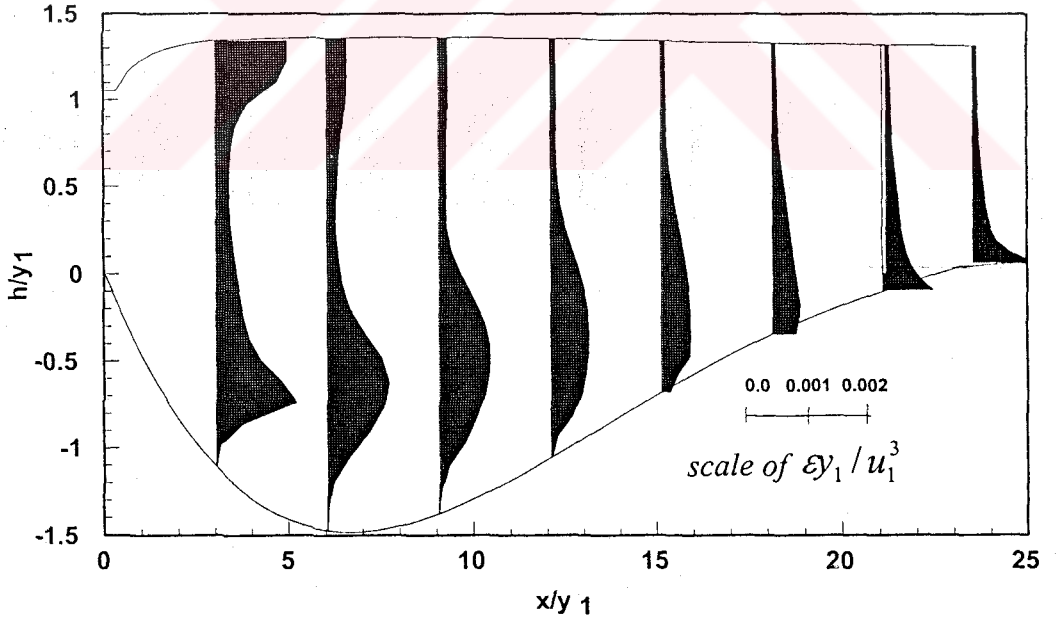

Figure 4.6 Distribution of $\varepsilon y_1/u_1^3$ along the scour from the numerical prediction for $F_1 = 0.78$ and $S = 0.86$.

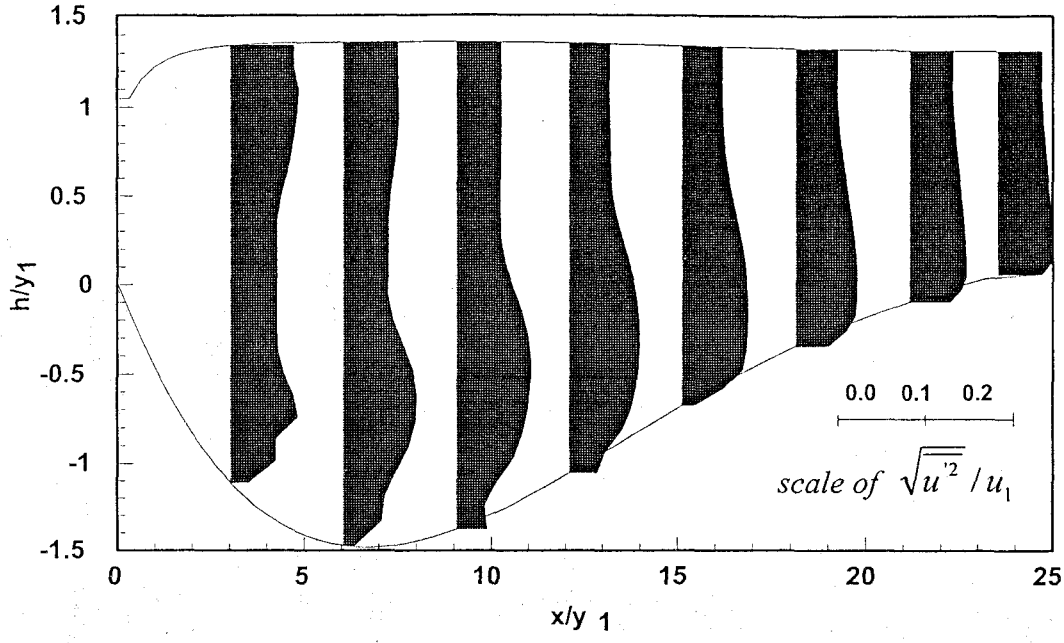

Figure 4.7 Distribution of $\sqrt{u'^2}/u_1$ along the scour from the numerical prediction for $F_1 = 0.78$ and $S = 0.86$.

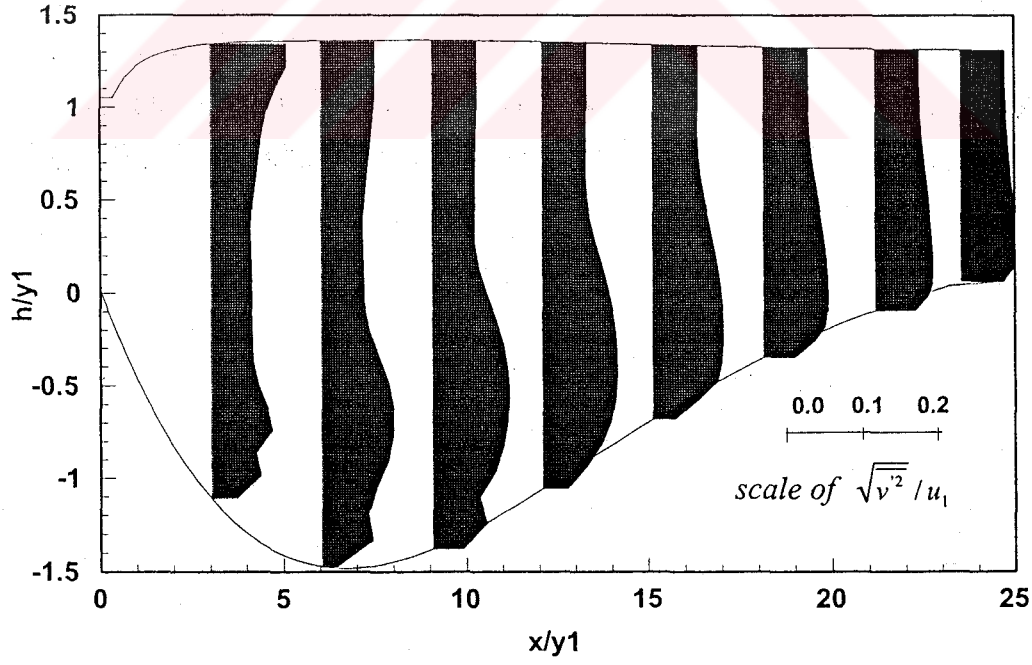

Figure 4.8 Distribution of $\sqrt{v'^2}/u_1$ along the scour from the numerical prediction for $F_1 = 0.78$ and $S = 0.86$.

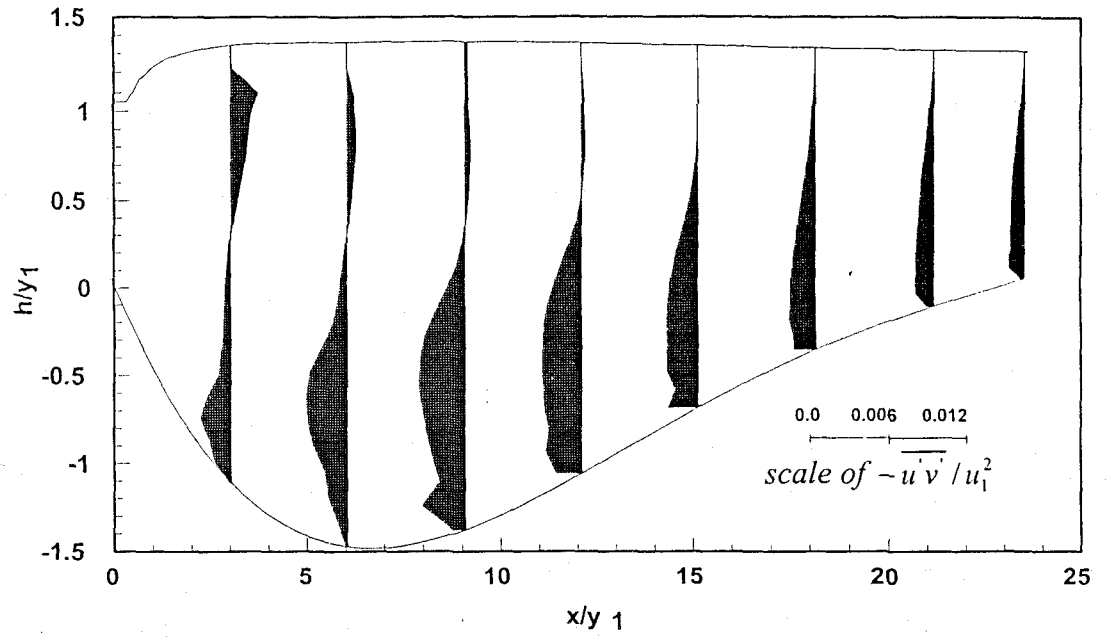

Figure 4.9 Distribution of $-\overline{u'v'}/u_1^2$ along the scour from the numerical prediction for $F_1 = 0.78$ and $S = 0.86$.

Figure 4.4 represents the vertical velocity distribution along the scour profile. Particularly at upstream of sluice gate and maximum scour depth region negative vertical velocities are observed under the original bed level. At just downstream of sluice gate maximum positive vertical velocity is observed. From the maximum scour depth region through the outlet the vertical velocities are observed to be positive and become nearly zero at outlet. All these observations illustrate the manners of different jet formations that are aforementioned.

Figures 4.5 and 4.6 represent the turbulent kinetic energy and diffusion of turbulent kinetic energy respectively. The peak value at just downstream of sluice gate nearby the free surface is due to high amount of vertical velocity. Generally the peak values occur just below the original bed level and steady decrease at kinetic energy and at diffusion of kinetic energy is observed from the upstream of scour profile through the outlet. Also the values of both kinetic enrgy and diffusion of kinetic enrgy decrease steadily through the free surface and approach zero.

Figure 4.7 and 4.8 represent the turbulent intensities for longitudinal and vertical directions along the scoured bed. All the quantities are non-dimensionalised with respect to u_1 and y_1. In both figures, it is seen that the turbulent intensity profiles

show a peak value in the region of maximum scour depth. At each profile the intensities approach to zero close to the bed and get maximum value below the original bed level and from the maximum intensity to the free surface the values of intensity get smaller until the original bed level, then shows a steady value through the free surface. At downstream of sluice gate it can be clearly seen that the turbulence intensity get a second peak value near free surface and get smaller through the dune. This event was also pointed out by Liriano et al. (2000) . The turbulence intensity in longitudinal direction shows larger values than those of vertical direction. ($\sqrt{u'} = 1.3\sqrt{v'}$). Measurements of turbulent intensity in different directions show the turbulent flow to be non-isotropic with $u' \cong 1.6v'$ for the fully developed bed. (Liriano et al., 2000). Liriano et al. (2000) observed that $\sqrt{u'^2}$ along the jet centreline increased at a decreasing rate as the distance from the outlet increased and this is also seen in the numerical predictions of this study.

Figure 4.9 represents the Reynolds stress profiles along the scoured bed. All the quantities are non-dimensionalised with rescpect to u_1^2 and y_1. The figure shows that the maximum Reynolds stress occures at maximum scour depth. At each profile the Reynolds stress gain larger values from the downstream of sluice gate through the maximum scour depth but starts to get smaller from the maximum scour depth to the downstream of the jet. The Reynolds stresses are observed to approach zero close to the bed. The magnitude of Reynolds stress is observed to be generally negative but at just downstream of sluice gate and close to free surface the maximum positive value of Reynolds stress is observed. Then the positive value of Reynolds stress aproach to zero through downstream of the jet. The positive values are observed in the region $x/y_1 \geq 12$. All the negative peak values are observed to be below the original bed level.

The deviation of pressure from hydrostatic distribution (p_d) can be defined in an nondimensional form following Long et al. (1991) as :

$$p_d = \frac{\rho g(h-y) - p}{\rho u_1^2 / 2} \qquad \textbf{(4.1)}$$

where h is the total depth of flow, y is the vertical distance from the bed and p is the pressure. Equation 4.1 is non-dimensionalised with respect to dynamic pressure ($\rho u_1^2/2$). Figures 4.10 shows non-dimensionalised pressure departure from the hydrostatic for F_1= 0.78 and S = 0.86. The figure shows that the presure field beneath the recirculating region deviates more from the hydrostatic. The pressure distribution is observed to be nearly hydrostatic for x/y_1>20. The deviation is more apparent particularly in the region immediately downstream of sluice.

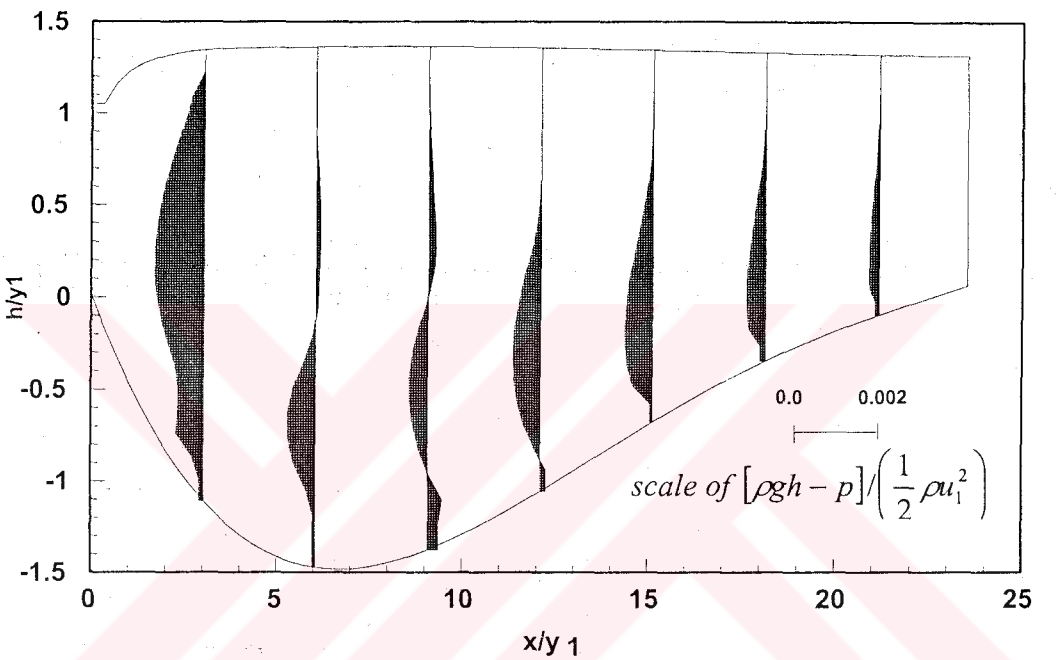

Figure 4.10 Deviation of pressure from hydrostatic distribution along the rigid scoured bed for F_1= 0.78 and S = 0.86.

Figure 4.11 shows the decay of maximum mean velocity u_m along the streamwise direction x for F_1= 0.78 and S = 0.86. u_m and x are non-dimensionalised respectively dividing by u_1 and y_1. From the figure it is observed that there is a rapid decrease in the maximum velocity until the maximum scour depth and then a steady increase occurs just after the region of maximum scour depth. The present results are also compared with the numerical predictions of Karim and Ali (2000) in Figure 4.12. It can certainly be said that there is a strict agreement between the numerical results of present study and those of Fluent package program's that is presented in Karim and Ali (2000). At $0<x/y_1<4$ it can be said that a 100% agreement between the two numerical results have been achieved and 2% distinction is observed along region $4<x/y_1<24$.

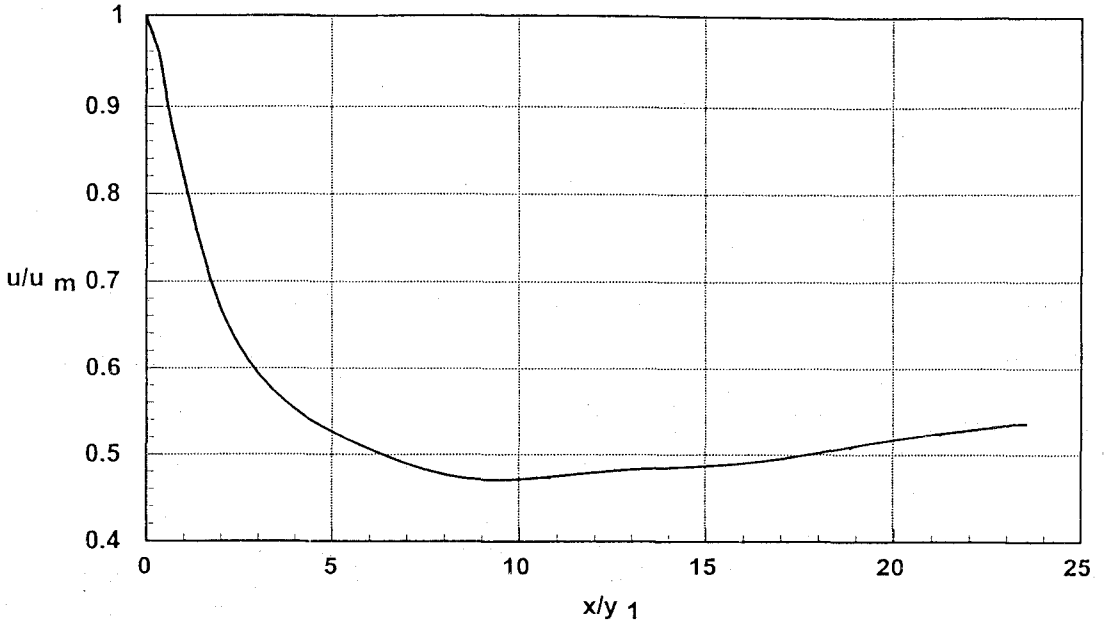

Figure 4.11 Predicted decay of maximum horizontal velocity along the rigid scoured bed for F_1=0.78 and S = 0.86.

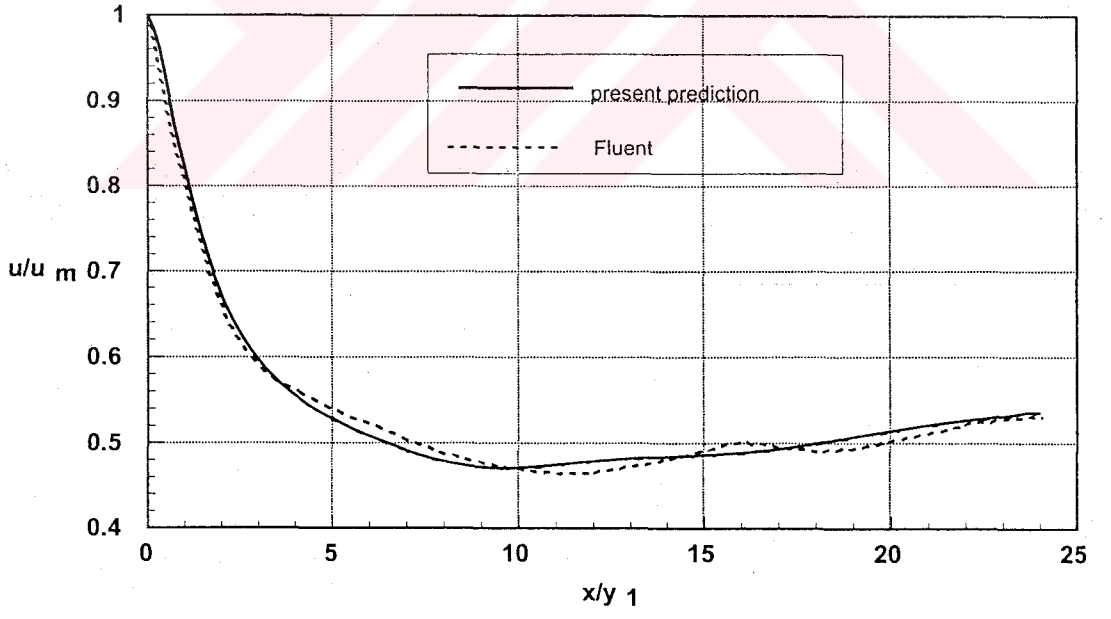

Figure 4.12 Comparison between the present study's predicted decay of maximum horizontal velocity and the predicted results of Karim and Ali (2000) for F_1=0.78 and S = 0.86.

Figure 4.13 shows the comparison between the predicted bed shear stress results of present study and the numerical results of Fluent package program (Karim and Ali, 2000) and the experimental results of Ali and Lim (1986). A good agreement can easily be noticed between the three results except for the maximum scour depth region. And also it is obviously seen that the experimental results of Ali and Lim (1986) falls just in the middle of two numerical predictions. The reason of the distinction is the fact that Fluent package program predicts much rougher bed surface than the prediction of present study. Although it cannot be easily observed from the figure, the results of present study also show reverse horizontal velocities in the vicinity of maximum scour depth. But these values are much smaller that those of Fluent. At $0<x/y_1<2$ almost 100% agreement is observed and 15 % distinction is observed between the two numerical results along $2<x/y_1< 8$ region. 6 % distinction is observed at $8<x/y_1<24$ region between the two numerical results. The distinction between present numerical results and the experimental results of Ali and Lim (1986) is almost half of the above distinction values because the experimental results fall just between the two numerical results.

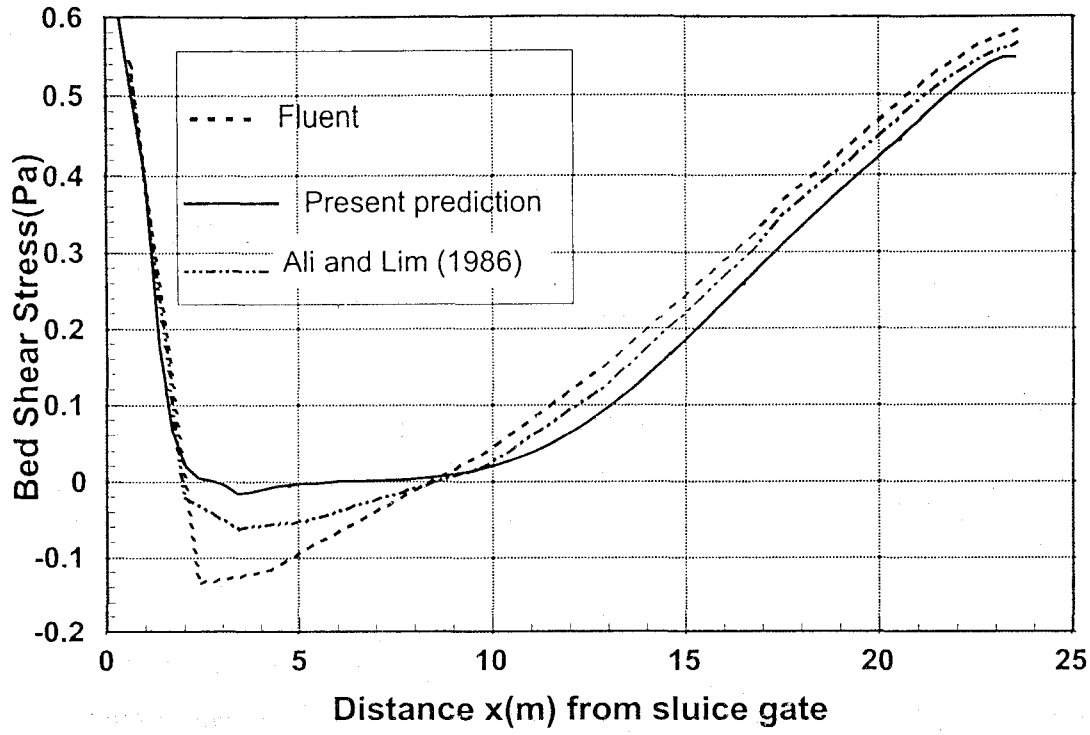

Figure 4.13 Comparison between present study's predicted bed shear-stress distribution and the numerical results of Karim and Ali (2000) and the experimental results of Ali and Lim (1986) for $F_1 = 0.78$ and $S = 0.86$.

In Figure 4.14, the numerical prediction of surface profile with bed profile and its comparison with the predicted surface profile of Fluent package program presented in Karim and Ali (2000) is shown for $F_1 = 0.78$ and $S = 0.86$. A sudden jump can be easily observed just downstream of the sluice. After reaching a peak value just in the region of the maximum scour depth, the surface is observed to fall in a very small amount through the start of dune. It can be seen in the Figure 4.14 that the upstream region for the present study's predictions are relatively smaller than those of Fluent's that 1 % distinction is observed at $0<x/y_1<7$ region. And almost 100 % agreement is achieved along the rest of surface profile. From a general view, it can be said that there is a good agreement between the two numerical predictions.

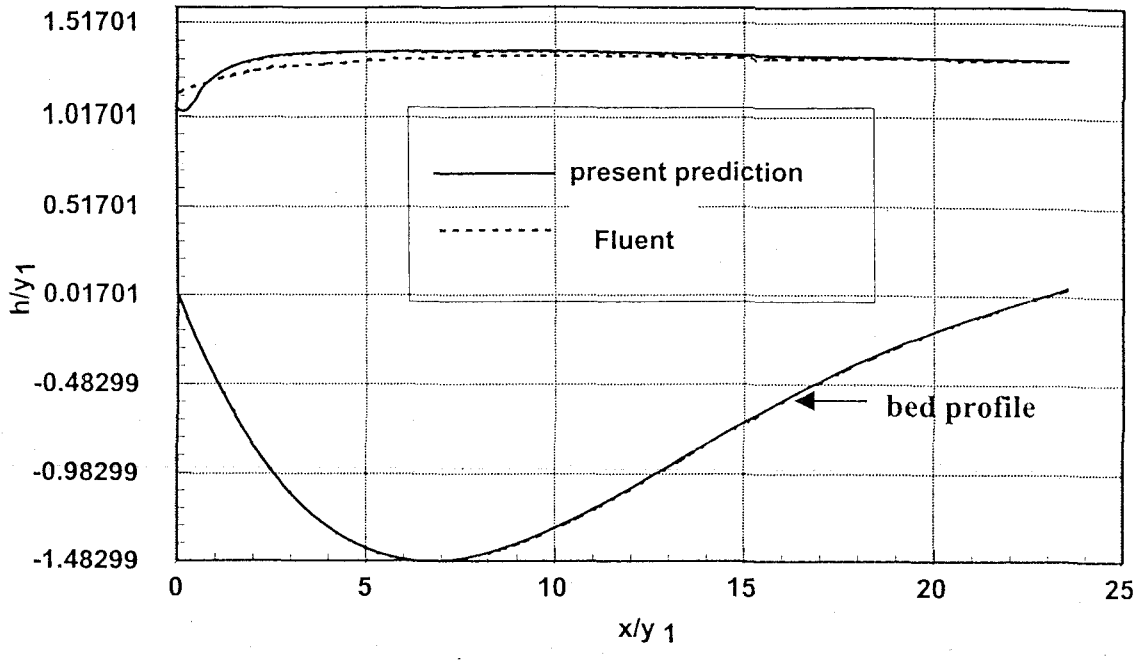

Figure 4.14 Comparison between present study's and Fluent's numerical prediction of surface profile for $F_1 = 0.78$ and $S = 0.86$.

Figure 4.15, 4.16 and 4.17 represent the maximum turbulent quantities $(\sqrt{\overline{u'^2}})_m$, $(\sqrt{\overline{v'^2}})_m$ and $(\overline{-u'v'})_m$ in the streamwise direction with bed profile. Figure 4.15 shows the maximum logitudinal turbulent intensity $(\sqrt{\overline{u'^2}})_m$ that is non-dimensionalised with respect to u_1 for F_1=0.78 and S =0.86. It is seen from figure (for $x/y_1 \leq 2$) that there is a rapid fall in the decay of maximum longitudinal intensity at just downstream of sluice gate but after that a steay decrease after a small peak is observed. For $4 \leq x/y_1 \leq 25$, the longitudinal turbulence intensity is observed to steadily increase upto maximum scour depth region and then steadily decrease through the downstream of scoure profile. The reason of this pattern of longitudinal turbulent intensity is the dominant effect of turbulence and reverse flows in maximum scour depth region.

Figure 4.16 shows the maximum vertical turbulence intensity $\left(\sqrt{v'^2}\right)_m$ that is non-dimensionalised with respect to u_1 for F_1=0.78 and S = 0.86. A fluctuating decrease in the decay of maximum vertical intensity is observed after a rapid increase at just downstream of sluice (for $x/y_1 \leq 4$) after that a maximum value is seen in the

maximum scour depth region and then a steady decrease follows from maximum scour depth region through the downstream of the jump. This pattern of vertical turbulent intensity is due to occurance of vertical velocity component of flow through free surface at higher rates, at maximum scour depth region rather than upstream and downstream of this region.

Figure 4.17 represents the maximum Reynolds stress quantity $(\overline{-u'v'})_m$ that is non-dimensionalised with respect to u_1 for F_1= 0.78 and S = 0.86. The figure shows a sharp fluctuating in the decay of Reynolds stress quantity for $x/y_1 \leq 3$ with a peak value at $x/y_1 = 1$. After that, a steady increase is observed until a maximum value at maximum scour depth region. A steady decrease in the decay take place from the maximum scour depth region through downstream of the jump. This can be explained by occurance of turbulence at high rate at maximum scour depth region.

The large and unrealistic turbulent production would cause large Reynolds stresses and lead to the undulated shape of $(\overline{-u'v'})_m$ *distribution.The reason is the difficulty of predicting the production and dissipation of the turbulence particularly in the region upstream of the jump where the velocity gradients are very steep.* (Gunal, 1996).

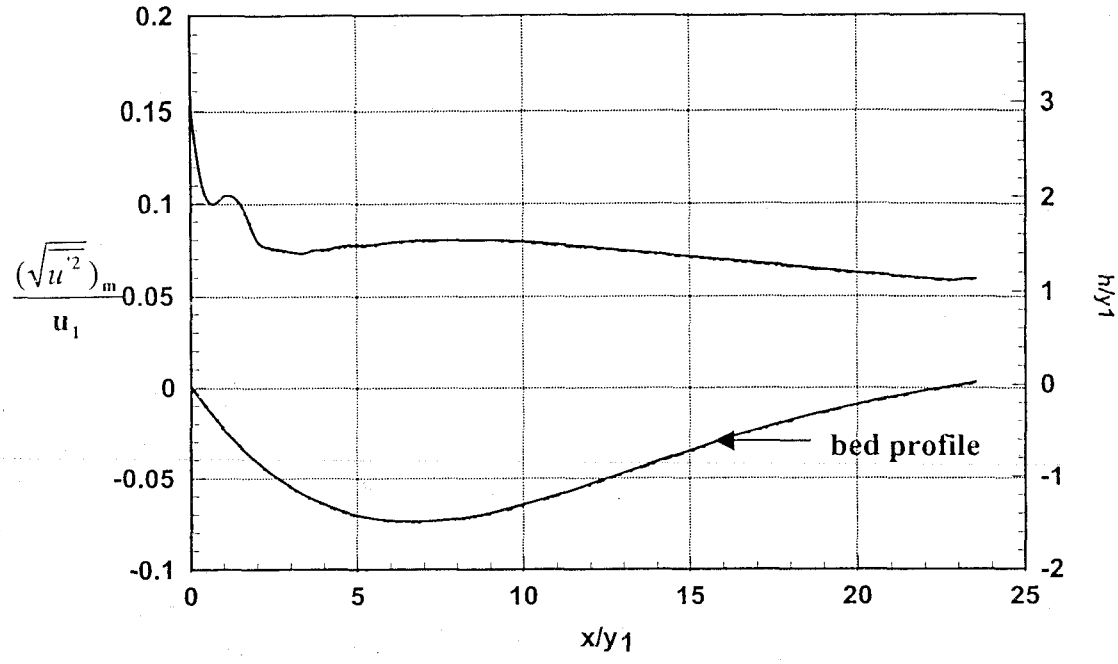

Figure 4.15 Decay of maximum longitudinal turbulence intensity along the scour from the prediction of $F_1 = 0.78$ and $S = 0.86$.

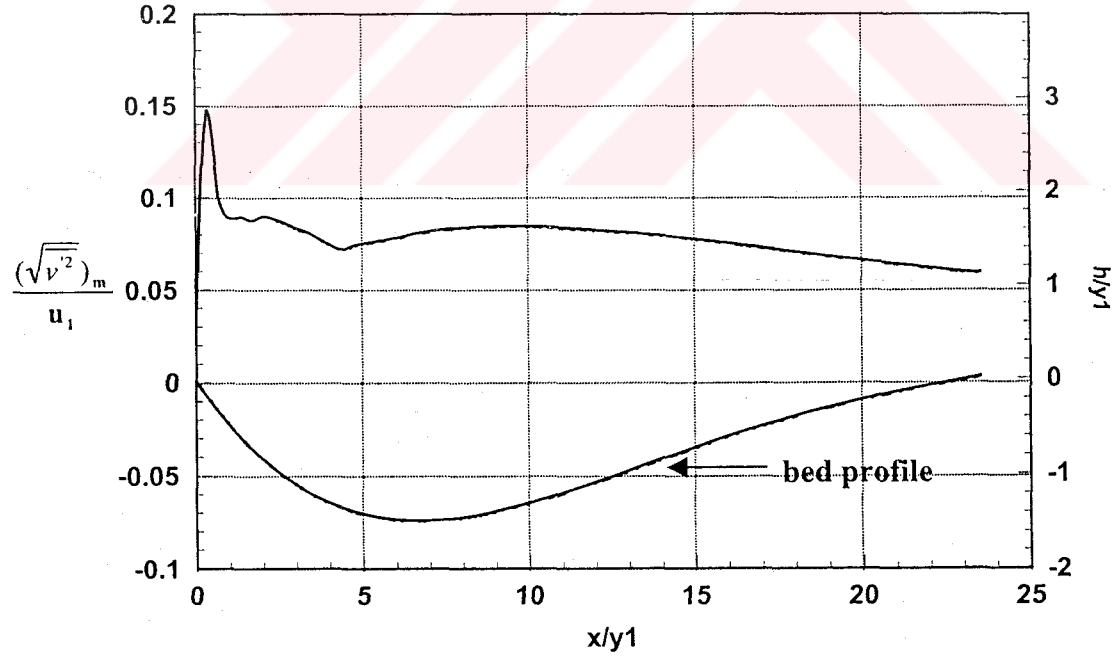

Figure 4.16 Decay of maximum vertical turbulence intensity along the scour from the prediction of $F_1 = 0.78$ and $S = 0.86$.

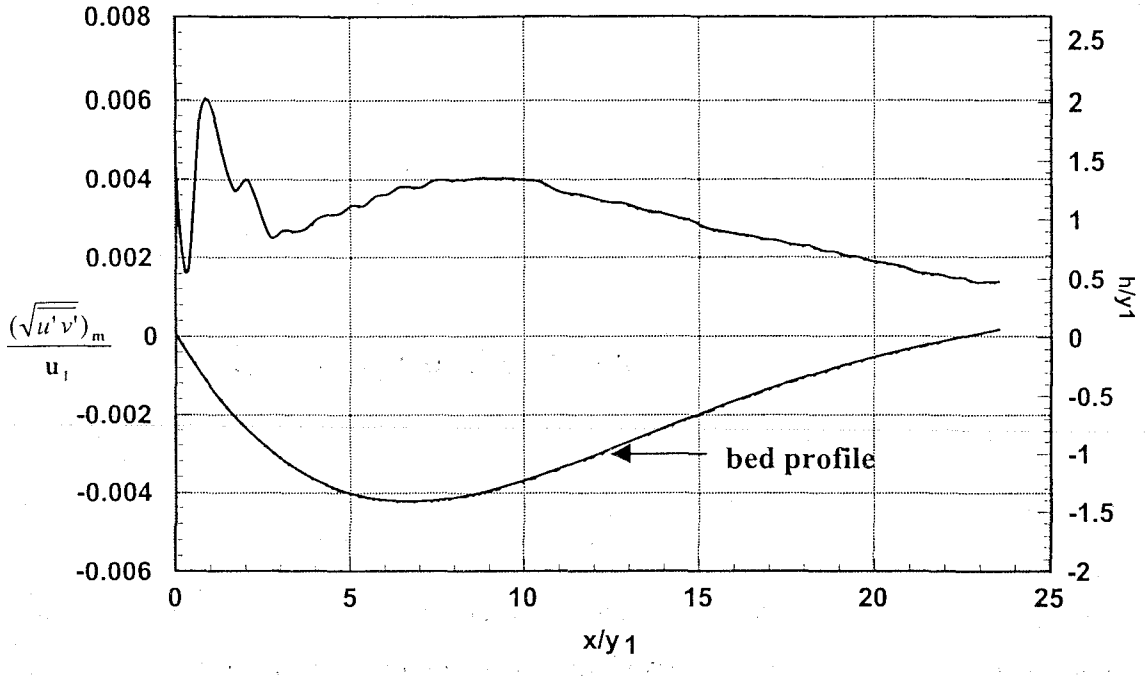

Figure 4.17 Decay of maximum Reynolds stress along the scour from the prediction of $F_1 = 0.78$ and $S = 0.86$.

Chapter 5

Conclusions and Further work

5.1 Conclusions

The studies in this thesis have been carried out to investigate the three aspects of horizontal jets. The first is a detailed literature survey of horizontal jets and the important effects of local scour induced by horizontal jets to hydraulic structures. The second is the hydrodynamic and mean characteristics of horizontal jets issuing on rigid scoured beds. The third is the k-ε turbulence modelling of the submerged horizontal jet using the boundary fitted coordinates. Some basic conclusions are as follows :

5.1.1 Mean and Hydrodynamic Characteristics of Local Scour Due to Horizontal Jets Occuring on Rigid Scoured Beds

In the present study the validity of k-ε turbulence modelling of the scour process due to horizontal jets is presented. Based on the application of the numerical work, it is found that the flow pattern and the shear stress at the bed , which is the main factor influencing the scouring process, is predicted with a good agreement with the experimental and numerical results in the literature.

From the numerical results of this study it can be understood that the turbulence intensity and Reynolds stresses are the most dominant in maximum scour depth region. The water jet is also observed to impinge on downtream and upstream of maximum scour depth region. This may lead extreme undermining of soil and failure of the hydraulic structures.

The numerical results of vectoral velocity distribution of horizontal jet show three types of jet formation. A free jet formation at just downstream of sluice gate; a wall jet formation with reverse velocity formation in maximum scour depth region and a typical wall jet formation at downstream of scoure profile. This prediction of present study present strict agreements with the experimental results of Ali and Lim (1986) and the numerical results of Karim and Ali (2000).

The turbulent intensity and stress distribution along the scour profile may help the designers to prevent undesired conditions by constructing protective structures in the vicinity of high turbulence-intensity regions. Using apron at upstream of the scoured region can decrease the depth of maximum scour and the impinging effect of water jet on the soil (Nik Hassan and Narayanan, 1985).

5.1.2 k-ε Turbulence Modelling of Submerged Horizontal Jet Using Boundary Fitted Coordinates

In present study, two-dimensional k-ε turbulence modelling using boundary fitted coordinates to predict the internal mean and turbulence structure of flow in submerged horizontal jet is presented. The present numerical predictions are compared with experimental results of Ali and Lim (1986) and Liriano et al. (2002) and the numerical results of Karim and Ali (2000). The boundary fitted coordinate system is found to be more appropriate for modelling submerged horizontal jets because the free surface boundary conditions can be easily applied without making any assumptions.

It is found that the numerical results of present study are in a strictly good agreement with the numerical results of Karim and Ali (2000) and the experimental results of Ali and Lim (1986) and Liriano et al. (20002). But some distinctions occur especially in numerical results of mean velocity distribution in maximum scour region between present study and Karim and Ali (2000). This distinction is assumed to be due to assumptions of initial boundary conditions. The experimental results of Ali and Lim (1986) fall just in the middle of the the two numerical results when the presenting the results non-dimensionally with respect to appropriate scales.

In present study, the turbulence intensity in longitudinal direction shows larger values than those of vertical direction. This condition is also pointed out by Liriano et al. (2002). The present numerical results show the relation between the longitudinal and vertical turbulence intensities as $u' \cong 1.7v'$ and Liriano et al. (2002) as $u' \cong 1.6v'$ for the fully developed bed. It can be said that there is a good agreement between the numerical results of present study and the experimental results of Liriano et al. (2002) .

The predicted surface profile of of present study and that of Karim and Ali (2000) show a good agreement except that the upstream formation of surface profile in present study is a bit higher that those of Karim and Ali (2000).

It is well known that the standard k-ε turbulence model show deficiencies in modelling near-wall viscosity-affected flows. Also the standard k- ε turbulence model is known to be too dissipative, the turbulent viscosity in recirculations tends to be too high, thus damping out vorticises. All the deficiencies are suggested to be solved by modifying the model results to more realistic values.

5.2 Suggestions for Further Work

In this thesis, internal and turbulence charateristics of submerged horizontal jet occuring on frozen scoured beds were investigated. Although the measured mean characteristics of horizontal jet along scour profile in equilibrium state can be related to the whole scouring process, a question may arise whether the kinematics of flow that exist in a steady case of a rigid model will be representative of those in a time dependent case of scour that normally occurs (Nik Hassan and Narayanan, 1985). To represent the real characteristics of normal scouring process, it is suggested to extend the present study to a time-dependent k-ε turbulence modelling. Thus there will be no need to predict the scour profile.

It is known that the turbulence quantites in turbulent jets are three-dimensional. To cover all the characteristics of the turbulent jets, three-dimensional k-ε turbulence modelling is suggested.

REFERENCES

1. Ade, F. and Rajaratnam, N., (1998). Generalised study of erosion by circular horizontal turbulent jets. *Journal of Hydr. Res.*, 36(4), 613-635.

2. Ali, U., (1988). Scour downstream of vertical gate. *Journal of Hydr. Engng*, 114(7), 811-817

3. Ali, K.H.M. and Lim, S.Y. , (1985). *Local scour caused by two-dimensional reattached jets*. Civil Engineering Department, University of Liverpool, Technical Report.

4. Ali, K.H.M. and Lim, S.Y., (1986). Local scour caused by submerged vertical gates. *Proc. Instn Civ. Engrs*, Part 2, 607-645

5. Ali, K. H. M. and Lim, S.Y., (1987). Local scour caused by submerged wall jets. *Proc. Instn Civ. Engrs*, Part 2, 875-886.

6. Ali, K.H.M. and Neyshaboury, A.A., (1991). Localised scour downstream of a deeply submerged horizontal jet. *Proc. Instn Civ. Engrs*, Part 2, 1-18.

7. Altnbilek, H.D. and Basmac, Y., (1980). Localised scour below submerged vertical gates. *Proc. Speciality Conf. Computerd Physical Modelling in Hydr. Engng*, Chicago, 39-50.

8. Anderson, J.D.A. , (1995). *Computational Fluid Dynamics*. McGraw-Hill Inrenational Editions.

9. ASCE Task Committee on Turbulence Models in Hydraulic Computations, (1988). Turbulence Modelling of surface water flow and transport. Part I to V., *ASCE, J. of Hydraulic Engineering*, Vol.114(9), 970-1073.

10. Balachandar, R., Kells, J. A., Thiessen, R.J. , (2000). The effect of tailwater depth on the dynamics of local scour. *Canadian Journal of Civ. Engrs*, 27, 138-150.

11. Balachandar, R., Kells, J.A., (1997). Local channel scour in uniformly graded sediments: the time-scale problem. *Canadian Journ. of Civ.Engrs*, 24, 799-807.

12. Balachandar, R., Kells, J.A. , (1998). Instantenous water surface and bed profiles using video image analysis. *Canadian Journal of Civ. Engrs*, 25(4), 662-667.

13. Balachandar, R., Kells, L.M. , (1999). *Counter-measures for clear-water local scour in channels*. Dep. of Civ. Engng, Uni. of Saskatchevan, Techical Paper.

14. Bernard, R.S., (1991). A turbulence model recirculating flow. *USAE Waterways Experiment Station*, Hydraulics Laboratory, Vicksburg, Technical Report HL-91-14- 30 pages.

15. Breusers, H.N.C., (1975). Computation of velocity profiles in scour holes. *Proc. 16th Congr. Int. Assoc. for Hydr. Res.*, Sau Paolo, 2, 300-306.

16. Chatterjee, S.S. and Ghosh, S.H. , (1980). Submerged horizontal jet over erodible bed. *ASCE Journal of Hydr. Div.*, 106(11), 1765-1782.

17. Chow, V.T. , (1959). *Open-Channel Hydraulics*. McGraw-Hill International Editions.

18. Ead, S.A., and Rajaratnam, N.(2002). Hydraulic Jumps on Corrugated Beds. *Journal of Hydraulic Engineering*, 128(7), 656-663.

19. El Hadidi, B.M.N, (1998). *A computational study of flow in mechanically ventilated space*. Ms.C.Thesis submitted to the Faculty of Engineering at Cairo University, Giza, Egypt.

20. Farhoudi, J. and Smith, K.V.H. , (1982). Time scale for scour downstream of hydraulic jump. *Journal of Hydr. Div., ASCE*, 108(HY10), 1147-1162.

21. Gunal, M., (1996). *Numerical and Experimental Investigations of Hydraulic Jumps*. A Ph.D. Thesis submitted to University of Manchester, Institute of Science and Technology.

22. Gunal,M., and Narayanan, R., (1998). k-ε turbulence modelling of submerged hydraulic jump using boundary-fitted coordinates. Proc. Instn Civ. Engrs Wat., Marit. & Energy, pp104-114, 1998.

23. Hoffmans, G.J.C.M. , (1998). Jet scour in equilibrium phase. *Journal of Hydr. Engng*, 124(4), 430-437.

24. Hoffmans, G. J.C.M. and Pilrczyk, K.W. , (1995). Local scour downstream of hydraulic Structures. *Journal of Hydraulic Engineering*, 121(4), 326-340.

25. Hoffmans, G. J.C.M. and Booij, R. , (1993). The influence of upstream turbulence on local scour holes. *Proc., 25th IAHR Congr.*, 1, A14, 471-478.

26. Hogg, A.J., Huppert, H.E. and Dade, W.B. , (1997). Erosion by planar turbulent jets. *Journal of Fluid Mechanics,* 338, 317-340.

27. Johnston, A.J., (1990). Scourhole developments in shallow tailwater. *Journal of Hydraulic Research*, 28(3), 341-354.

28. Johnston, A.J. and Halliwell, A.R. , (1986). Jet behaviour in shallow receiving waters. *Proc . Instn Civ. Engrs*, Part 2, 549-568.

29. Karim, O.A. and Ali, K.H.M. , (2001). Predicition of flow patterns in loacl scour caused by turbulent water jets. *Journal of Hydr. Res.*, 38(4), 279-287.

30. Kutija, V., and Hewett, J.M.C. , (2002). Modelling of supercritical flow condition revisited; New C Scheme.*Journal of Hydr. Res.*, 40(2), 145-152.

31. Leutheusser, H.J., and Fan, J.J., (2001). Backward Flow Velocities of Submerged Hydraulic Jumps. *Journal of Hydraulic Engineering*, 127(6), 514-517.

32. Li, C.W. and Wang, J.H., (2002). Large eddy simulation of dispersion in free surface shear flow. *Journal of Hydr. Res.*, 40(3), 351-358.

33. Li, C.W. and Wang, J.H. , (2000). Large eddy simulation of free surface shallow water flow. *International Journal for Numerical Methods in Fluids*, 34(1), 31-46.

34. Liriano, S.L., Day, R.A., White, W.R. , (2002). Scour at culvert outlets as influenced by the turbulent flow structure. *Journal of Hydr. Res.*, 40(3), 367-376.

35. Long, D., Steffler, P.M. and Rajaratnam, N., (1991). A numerical study of submerged hydraulic jumps. *IAHR, J. Hydraulic Research* Vol.29(3), pp 293-308.

36. Ma, F., Hou, Y. And Prinos, P., (2001). Numerical calculation of submerged hydraulic jumps. *Journal of Hyr.Res.*,39(5), 289-298.

37. Mason, P.J. , (1989). Effects of air entrainment on plunge pool scour.*Journal of Hydr. Engng*, 115(3), 385-399.

38. Mohamed, M.S. and McCorquodale, J.A. , (1992). Short-term local scour. *Journal of Hydr.Res.*, 30(5), 685-699.

39. Mc Guirk, J.J., and Rodi, W. , (1978). A depth averaged mathematical model for the near field of side discharges into open-channel flow. *Journal of Fluid Mechanics*, 86(4), 761-781

40. Nik-Hassan., (1985). Erosion of alluvial bed downstream of sluice gate. *PhD. thesis submitted to University of Manchester Insttute of Science and Technology.*

41. Nik Hassan, N.M.K. and Narayan, R. , (1985). Local scour downstream of apron. *Journal of Hydr. Engineering*, 111(11), 1371-1385.

42. Patankar, S.V., (1980). *Numerical Heat Transfer and Fluid Flow.* McGrawhill Book Company.

43. Rajaratnam, N. , (1980). Erosion by circular wall jets in cross flow. *Journal Hydr. Div. Proc. of American Society of Civ. Engrs*, 106(HY11), 1867-1883.

44. Rajaratnam, N. , (1981). Erosion by plane turbulent jets. *Journal of Hydr. Res.*, 19(4), 339-357.

45. Rajaratnam, N., (1982). Erosion by submerged circular jets. *Journal of Hydr. Div. ASCE*, 108(2), 262-266.

46. Rodi, W., (1980). Turbulence models and their applications in hydraulics-A state of the art review. *IAHR*, 104 page.

47. Sarker, M.A., and Rhodes, D.G., (2001). Physical modelling of CFD to hydraulic jump. *ASCE*, Technical Report.

48. Shi, J., Thomas, T.G., and Williams, J.J.R., (2000). Free-surface in open channel flow at moderate froude and Reynold's numbers. *Journal of Hydr. Res.*, 38(6), 465-474.

49. Straw,M.P., (2000). Computation and Measurement of Wind Induced Ventilation. *Ph. D. Thesis submitted to the University of Nottingham.*

50. Thomas, T.G., and Williams, J.J.R. , (1995). Large eddy simulation of turbulent flow in an asymmetric compound open channel. *Journal of Hydr. Res.*,33, 27-42.

51. Tominaga, A., Liu, J., Nezu, I. And Nagao, M. , (1995). A modified k-e turbulence model for turbulent flow over strip roughness in open channel. *Proc. of Int. Symp. on Mathematical Modelling of Turbulent Flows*, Tokyo, 339-344, Dec., 1995.

52. Uyumaz, A. , (1988). Scour downstream of vertical gate. *Journal of Hydr. Engng., ASCE*, 114(7), 811-816.

53. Versteeg, H. and Malalasekera, W. , (1995). *An Introduction to Computational Fluid Dynamics: The Finite Volume Method*, Longman Scientific and Technical, New York.

APPENDIX

Computer Program of k-ε Model

```
C.... Program Submerged Horizontal Jet
C*********************************************************************

*
*               K-EPSILON  TURBULENCE MODEL
*                          USING
*               BOUNDARY FITTED COORDINATES
*
*               BY :  A GUVEN & M GUNAL
*
*               DEPARTMENT OF CIVIL ENGINEERING
*
*              UNIVERSITY OF GAZIANTEP
*
C*********************************************************************

Parameter (m=71, n=21)
Implicit double precision (a-h,o-z)
Real u(m,n),v(m,n),p(m,n),tk(m,n),td(m,n),pp(m,n)
* ,x(m,n),y(m,n),h(m,n),z(m,n),xz(m,n),xe(m,n),yz(m,n),ye(m,n),
* a(m,n),b(m,n),c(m,n),jac(m,n),gen(m,n),temp(m,n),
* bu(m,n),cu(m,n),ubar(m,n),vbar(m,n),bv(m,n),cv(m,n),
* udsq(m,n),vdsq(m,n),udvd(m,n),L,tvis(m,n),TW2(m,n),K,Umax(m)

open (unit=4,file='c:/aytac/dresult.res')
open (unit=8,file='c:/Matlab/bin/dcomph.dat')
open (unit=9,file='c:/Matlab/bin/dcompz.dat')
open (unit=10,file='C:/MATLAB/bin/dmeshx.dat')
open (unit=11,file='C:/MATLAB/bin/dmeshy.dat')
open (unit=12,file='C:/MATLAB/bin/dpolx.dat')
open (unit=13,file='C:/MATLAB/bin/dpoly.dat')
open (unit=77,file='c:/aytac/dvelocity.dat')
open (unit=78,file='c:/aytac/dvelcon.res')
open (unit=79,file='c:/aytac/ddimless.res')
open (unit=80,file='c:/aytac/dwallshear.dat')
open (unit=90,file='c:/aytac/ddecay.dat')
open (unit=91,file='c:/aytac/dsurface.dat')
open (unit=92,file='c:/aytac/dbed.dat')

data c1,c2,cmu,deltak,deltad/1.43d0,1.92d0,0.09d0,1.0d0,1.3d0/
data in/4/
u1=0.9d0
y1=0.051d0
Fr=u1/sqrt(9.81*y1)
L=1.2d0
yt=0.067do

x(1,1)=0.0d0
x(M,1)=L
y(M,1)=0.0d0
x(1,N)=0.0d0
y(1,N)=yt
x(M,N)=L
y(M,N)=yt

tol=0.0001d0
write(*,*)'u1=',u1
write(*,*)'yt=',yt
write(*,*)'Fr=',Fr

vis=1.d-6
rynm=u1*y1/vis
```

```
write(*,*)'rey.num.=',rynm
ckk=0.41d0
cee=9.0d0
call grid (1,m,n,x,y,h,z,xz,xe,yz,ye,jac,a,b,c,tol,y1,y2,Fr,Subm,
* L,yt)

call inlet (m,n,u,v,z,h,u1,vis,tk,td,tvis,cmu,ye,yz,xe,xz,y,
* ubar,vbar,y1,jac)

call wal l (M,N,U1,CMU,VIS,U,V,TK,TD,TVIS,x,z,Y,h,ckk,cee,
*  ye,yz,xe,xz,y1,ubar,vbar,jac)
call GUESS (M,N,U,V,TK,TD,TVIS,P,PP,U1,VIS,CMU,h,y,ubar,vbar)

omegau=0.3d0
omegav=0.3d0
omegap=0.3d0
omegah=0.3d0
omegas=0.3d0
omegad=0.3d0
omegak=0.3d0

do ii=1,500
write (*,*)'iter.no',ii
call solveu (m,n,u,v,tvis,xz,yz,xe,ye,jac,z,h,p,tk,u1,du,
*   vis,cmu,omegau,ubar,vbar,temp,x,y,bu,cu)
call solvev (m,n,u,v,tvis,xz,yz,xe,ye,jac,z,h,p,
*        tk,u1,dv,vis,cmu,omegav,ubar,vbar,temp,x,y,bv,cv)
call uvbar (m,n,u,v,ubar,vbar,ye,yz,xe,xz,jac,x,y)
call solvep (m,n,u,v,tvis,xz,yz,xe,ye,jac,z,h,p,pp
*   ,tk,u1,dp,vis,cmu,y,omegap,omegah,ubar,vbar,x,bu,bv,cu,cv)
call surf (m,n,p,y,y1,u,v,x,u1,omegas,dh)
call grid (2,m,n,x,y,h,z,xz,xe,yz,ye,jac,a,b,c,tol,y1,y2,Fr,Subm,
*L,yt)
call inlet (m,n,u,v,z,h,u1,vis,tk,td,tvis,cmu,ye,yz,xe,xz,y,
* ubar,vbar,y1,jac)
enddo

do ii=1,500
call genterm (m,n,u,v,xe,xz,ye,yz,jac,gen,tvis,h,z,udsq,tk,
*    vdsq,udvd)
call tdre (m,n,td,tk,tvis,xz,yz,xe,ye,jac,z,h,gen,
*   c1,c2,dd,cmu,omegad,ubar,vbar,deltad,temp,u,v,p,u1,y1,y)
call tkee (m,n,td,tk,tvis,xz,yz,xe,ye,jac,z,h,gen,
*   dk,cmu,omegak,ubar,vbar,deltak,temp,u,v,p,u1)
call turvis (m,n,td,tk,tvis,vis,cmu)
enddo
omegau=0.3d0
omegav=0.3d0
omegap=0.2d0
omegah=0.2d0
omegas=0.2d0
omegad=0.1d0
omegak=0.1d0

do 46 ii=1,5000
write (*,*)'iter.no',ii
call solveu (m,n,u,v,tvis,xz,yz,xe,ye,jac,z,h,p,tk,u1,du,
*  vis,cmu,omegau,ubar,vbar,temp,x,y,bu,cu)
call solvev (m,n,u,v,tvis,xz,yz,xe,ye,jac,z,h,p,
*  tk,u1,dv,vis,cmu,omegav,ubar,vbar,temp,x,y,bv,cv)
call uvbar (m,n,u,v,ubar,vbar,ye,yz,xe,xz,jac,x,y)
call solvep (m,n,u,v,tvis,xz,yz,xe,ye,jac,z,h,p,pp
*   ,tk,u1,dp,vis,cmu,y,omegap,omegah,ubar,vbar,x,bu,bv,cu,cv)
call converg (m,n,ubar,vbar,h,z,err)
call genterm (m,n,u,v,xe,xz,ye,yz,jac,gen,tvis,h,z,udsq,tk,
*    vdsq,udvd)
call tdre (m,n,td,tk,tvis,xz,yz,xe,ye,jac,z,h,gen,
*   c1,c2,dd,cmu,omegad,ubar,vbar,deltad,temp,u,v,p,u1,y1,y)
call tkee (m,n,td,tk,tvis,xz,yz,xe,ye,jac,z,h,gen,
*   dk,cmu,omegak,ubar,vbar,deltak,temp,u,v,p,u1)
call turvis (m,n,td,tk,tvis,vis,cmu)
call surf (m,n,p,y,y1,u,v,x,u1,omegas,dh)
call grid (2,m,n,x,y,h,z,xz,xe,yz,ye,jac,a,b,c,tol,y1,y2,Fr,Subm,L, yt)
call inlet (m,n,u,v,z,h,u1,vis,tk,td,tvis,cmu,ye,yz,xe,xz,y,
*   ubar,vbar,y1,jac)
call WALSHR (M,N,U,V,TK,TD,TW2,Cee,Ckk,VIS,CMU,DW,x,y)
```

```
if (err.lt.tol) goto 113
46 continue
113 write (IN,*)'M=',M,'N=',N
 write (IN,*) 'yin=',y1,'yout=',y2
 write (IN,*) 'yt=',yt
 write (IN,*)'Froude Num.=',Fr
 write (IN,*) 'Submergence factor=',Subm
 write (IN,*) 'Inlet Velocity=',U1
 write (IN,*) 'Reynolds No=',Rynm
 write (IN,*) '     x          y       u          v        p
 *   tk      td      tvis'
 write(77,*) '     x          y       u          v       tk'

do 40 i=1,m
write (91,51) x(i,1)/y1,y(i,n)/y1
write (92,51) x(i,1)/y1,y(i,1)/y1
write (80,51) x(i,1),TW2(i,1)
do 40 j=1,n
write (IN,50) x(i,j),y(i,j),u(i,j),v(i,j),p(i,j),tk(i,j),td(i,j)
* ,tvis(i,j)
write (79,50) x(i,j)/y1,y(i,j)/y1,u(i,j)/u1,v(i,j)/u1,
*(p(i,j)-p(i,n))/(500.0d0*u1**2),tk(i,j)/u1**2,y1*td(i,j)/u1**3

write(78,50) x(i,j),y(i,j),u(i,j),v(i,j),p(i,j),tk(i,j),td(i,j),
*  tvis(i,j)
 40 continue
close(78)
50 format(8f12.5)
51 format(2f12.5)

do j=1,N
Write(8,100)(h(i,j),i=1,M)
Write(9,100)(z(i,j),i=1,M)
Write(10,100)(x(i,j),i=1,M)
write(11,100)(y(i,j),i=1,M)
End do
100 format (x,71(f12.6,x))

Do i=1,M
Um=u(i,1)
Do j=2,N
If(u(i,j)>Um) Um=U(i,j)
Enddo
Umax(i)=Um
Enddo

Do i=1,m
do j=1,n
If(u(i,j)=Umax(i)*0.5d0) uh=u(i,j)
b=y(i,j)-y(i,1)
enddo
uhalf(i)=uh
bb(i)=b
enddo

do i=1,m
do j=1,n)
write(90,51) x(i,1)/y1,Umax(i)/u1,u(i,j)/Umax(i),y(i,j)/bb(i)
Enddo
Enddo
stop
end
*****************************************************************
SUBROUTINE CONVERG (m,n,ubar,vbar,h,z,err)
implicit double precision (a-h,o-z)
real ubar(m,n),vbar(m,n),h(m,n),z(m,n)

err=0.0d0
do i=2,m
qin=0.0d0
qout=0.0d0
do j=1,n
if(j.eq.1)dh=h(i,1)
if(j.gt.1)dh=h(i,j)-h(i,j-1)
qin=ubar(i-1,j)*dh+qin
qout=ubar(i,j)*dh+qout
```

```
enddo
err1=abs(qin-qout)
err=err1+err
enddo
err=err/(m-1)
print*,'err=',err
return
end
*****************************************************************
SUBROUTINE INLET (m,n,u,v,z,h,u1,vis,tk,td,tvis,cmu,ye,yz,xe,xz,y,
* ubar,vbar,y1,jac)
implicit double precision (a-h,o-z)
real U(M,N),V(M,N),TK(M,N),TD(M,N),TVIS(M,N),h(M,N),z(m,n)
* ,ye(m,n),yz(m,n),xe(m,n),xz(m,n),y(m,n),ubar(m,n),vbar(m,n),
*  jac(m,n)

tko=0.0014d0*u1**2
tdo=2.2d-5*u1**3/y1
tnuo=cmu*tko**2/tdo

DO 10 J=1,N
if(y(1,j).GT.0.0d0.and.y(1,J).LT.y1)then
u(1,j)=u1
v(1,j)=0.0d0
tk(1,j)=tko
td(1,j)=tdo
tvis(1,j)=tnuo
if(j.eq.1)then
ubar(1,1)=u(1,1)*ye(1,1)-v(1,1)*xe(1,1)
vbar(1,1)=v(1,1)*xz(1,1)-u(1,1)*yz(1,1)
else
if(j.ne.n)then
v(1,j)=0.
yee=(ye(1,j)+ye(1,j-1))/2.0d0
xee=(xe(1,j)+xe(1,j-1))/2.0d0
vv=(v(1,j)+v(1,j-1))/2.0d0
ubar(1,j)=u(1,j)*yee-vv*xee
uu=(u(1,j)+u(1,j+1))/2.0d0
vbar(1,j)=v(1,j)*xz(1,j)-uu*yz(1,j)
else
ubar(1,n)=u(1,n)*ye(1,n)-v(1,n)*xe(1,n)
vbar(1,n)=0.0d0
endif
endif
else
u(1,j)=0.0d0
v(1,j)=0.0d0
ubar(1,j)=0.0d0
vbar(1,j)=0.0d0
tk(1,j)=0.0d0
td(1,j)=0.0d0
tvis(1,j)=0.0d0
endif
10 CONTINUE
RETURN
END
*****************************************
SUBROUTINE WALL (M,N,U1,CMU,VIS,U,V,TK,TD,TVIS,x,z,y,h,CK,CE,
*  ye,yz,xe,xz,y1,ubar,vbar,jac)
 implicit double precision (a-h,o-z)
real U(M,N),V(M,N),TK(M,N),TD(M,N),TVIS(M,N),y(M,N),
* h(m,n),X(M,n),z(m,n),ye(m,n),yz(m,n),xe(m,n),xz(m,n),vbar(m,n),
* jac(m,n),ubar(m,n)

DO 30 I=2,M
IF(x(I,1)/y1.GT.50.)GOTO 11
CF=0.0059d0*(0.0001d0/0.0059d0)**(x(I,1)/y1/50.0d0)
GOTO 12
11 CF=0.0001
12 USTAR=SQRT(CF/2.0d0)*U1
TK(I,1)=USTAR**2/SQRT(CMU)
TD(I,1)=USTAR**3/CK/abs(y(i,1))
 u(i,1)=USTAR/CK*LOG(CE*abs(y(i,1)-y(i,2))*USTAR/VIS)
v(i,1)=0.0d0
TVIS(I,1)=CMU*TK(I,1)**2/TD(I,1)+VIS
ubar(i,1)=u(i,1)*ye(i,1)
```

```
vbar(i,1)=-u(i,1)*(yz(i,1)+yz(i-1,1))/2.0d0
30 CONTINUE
RETURN
END
****************************************
SUBROUTINE GUESS (M,N,U,V,TK,TD,TVIS,P,PP,U1,VIS,CMU,h,y,ubar,vbar)
Implicit double precision (a-h,o-z)
real U(M,N),V(M,N),TK(M,N),TD(M,N),TVIS(M,N),ubar(m,n)
* ,P(M,N),PP(M,N),h(m,n),y(m,n),vbar(m,n)

DO 10 I=2,M
DO 10 J=2,n
u(i,j)=u1/2.0d0
v(i,j)=0.0d0
TK(I,J)=0.0014d0*u1**2
TD(I,J)=2.2d-5*u1**3/y(1,n)
10 CONTINUE
DO 60 I=1,M
DO 60 J=1,N
PP(I,J)=0.0d0
P(I,J)=9810.0d0*y(i,n)
IF(TK(I,J).lt.0.000000000001d0)THEN
TVIS(I,J)=VIS
ELSE
if(td(i,j).lt.0.00000001d0)then
tvis(i,j)=0.0d0
else
TVIS(I,J)=cmu*tk(i,j)**2/td(i,j)+vis
endif
ENDIF
60 CONTINUE
RETURN
END
****************************************************************
SUBROUTINE UVBAR (m,n,u,v,ubar,vbar,ye,yz,xe,xz,jac,x,y)
implicit double precision (a-h,o-z)
real u(m,n),v(m,n),jac(m,n),xz(m,n),xe(m,n),yz(m,n),
* ubar(m,n),vbar(m,n),x(m,n),y(m,n),ye(m,n)

do 11 i=2,m
do 10 j=1,n
if(j.eq.1)then
vee=(v(i,1)+v(i+1,1))/2.0d0
ubar(i,1)=u(i,1)*ye(i,1)-vee*xe(i,1)
else
yee=(ye(i,j)+ye(i,j-1))/2.0d0
if(i.ne.m)vee=(v(i,j)+v(i,j-1)+v(i+1,j)+v(i+1,j-1))/4.0d0
if(i.eq.m)vee=(v(i,j)+v(i,j-1))/2.0d0
xee=(xe(i,j)+xe(i,j-1))/2.0d0
ubar(i,j)=u(i,j)*yee-vee*xee
endif
10  continue
11  continue
do 20 i=2,m
do 21 j=1,n
if(j.eq.1)then
xzz=(xz(i,1)+xz(i-1,1))/2.0d0
yzz=(yz(i,1)+yz(i-1,1))/2.0d0
uu=(u(i,1)+u(i-1,1))/2.0d0
vbar(i,1)=v(i,1)*xzz-uu*yzz
else if(j.eq.n)then
vbar(i,n)=0.0d0
else
xzz=(xz(i,j)+xz(i-1,j))/2.0d0
uu=(u(i,j)+u(i-1,j)+u(i,j+1)+u(i-1,j+1))/4.0d0
yzz=(yz(i,j)+yz(i-1,j))/2.0d0
vbar(i,j)=v(i,j)*xzz-uu*yzz
endif
21 continue
20  continue
return
end
```

```
SUBROUTINE TURVS (m,n,td,tk,tvis,vis,cmu)
implicit double precision (a-h,o-z)
```

```
real tvis(m,n),tk(m,n),td(m,n)

do 10 i=2,m
do 10 j=2,n
vis(i,j)=cmu*tk(i,j)**2/td(i,j)
if(tvis(i,j).gt.0.999d0)tvis(i,j)=1.0d0
10 continue
return
end
*****************************************************************
SUBROUTNE UMOM (i,j,m,n,u,v,tvis,xz,yz,xe,ye,jac,z,h,p,
*  tk,u1,du,vis,cmu,omegau,ubar,vbar,ae,aw,an,as,su,bu,cu)
implicit double precision (a-h,o-z)
real jac(m,n),h(m,n),z(m,n),tvis(m,n),tk(m,n),u(m,n),
* xz(m,n),xe(m,n),yz(m,n),ye(m,n),p(m,n),bu(m,n),cu(m,n),
* ubar(m,n),vbar(m,n),v(m,n)
real jacn,jacs,jace,jacw

dz=(z(i+1,j)-z(i-1,j))/2.0d0
dh=h(i,j)-h(i,j-1)
C.....CONVECTIONS..
ce=(ubar(i+1,j)+ubar(i,j))/4.0d0*dh
cw=(ubar(i-1,j)+ubar(i,j))/4.0d0*dh
cn=(vbar(i+1,j)+vbar(i,j))/4.0d0*dz
cs=(vbar(i+1,j-1)+vbar(i,j-1))/4.0d0*dz
C.....DIFFUSIONS..
yee=(ye(i,j)+ye(i+1,j)+ye(i,j-1)+ye(i+1,j-1))/4.0d0
xee=(xe(i,j)+xe(i+1,j)+xe(i,j-1)+xe(i+1,j-1))/4.0d0
tvise=tvis(i+1,j)
q1e=2.0d0*yee**2+xee**2
jace=(jac(i,j)+jac(i+1,j)+jac(i,j-1)+jac(i+1,j-1))/4.0d0
dze=z(i+1,j)-z(i,j)
de=tvise*q1e/jace/dze*dh
tvisw=tvis(i,j)
yew=(ye(i,j)+ye(i-1,j)+ye(i,j-1)+ye(i-1,j-1))/4.0d0
xew=(xe(i,j)+xe(i-1,j)+xe(i,j-1)+xe(i-1,j-1))/4.0d0
jacw=(jac(i,j)+jac(i-1,j)+jac(i,j-1)+jac(i-1,j-1))/4.0d0
q1w=2.0d0*yew**2+xew**2
dzw=z(i,j)-z(i-1,j)
dw=tvisw*q1w/jacw/dzw*dh

tvisn=(tvis(i,j)+tvis(i+1,j)+tvis(i,j+1)+tvis(i+1,j+1))/4.0d0
yzn=yz(i,j)
xzn=xz(i,j)
jacn=jac(i,j)
q3n=2.0d0*yzn**2+xzn**2
dhn=(h(i,j+1)-h(i,j-1))/2.0d0
dn=tvisn*q3n/jacn/dhn*dz

tviss=(tvis(i,j)+tvis(i+1,j)+tvis(i,j-1)+tvis(i+1,j-1))/4.0d0
jacs=jac(i,j-1)
xzs=xz(i,j-1)
yzs=yz(i,j-1)
q3s=2.0d0*yzs**2+xzs**2
if(j.ne.2)dhs=(h(i,j)-h(i,j-2))/2.0d0
if(j.eq.2)dhs=h(i,2)/2.0d0
ds=tviss*q3s/jacs/dhs*dz

C.....SOURCE TERM..
yes=ye(i,j-1)
yen=ye(i,j)
xen=xe(i,j)
xes=xe(i,j-1)
yze=(yz(i,j)+yz(i,j-1)+yz(i+1,j)+yz(i+1,j-1))/4.0d0
xze=(xz(i,j)+xz(i,j-1)+xz(i+1,j)+xz(i+1,j-1))/4.0d0
yzw=(yz(i,j)+yz(i,j-1)+yz(i-1,j)+yz(i-1,j-1))/4.0d0
xzw=(xz(i,j)+xz(i,j-1)+xz(i-1,j)+xz(i-1,j-1))/4.0d0

q2w=-(2.0d0*yew*yzw+xew*xzw)
q2e=-(2.0d0*yee*yze+xee*xze)
q2n=-(2.0d0*yen*yzn+xen*xzn)
q2s=-(2.0d0*yes*yzs+xes*xzs)

une=(u(i,j+1)+u(i+1,j+1)+u(i,j)+u(i+1,j))/4.0d0
unw=(u(i,j+1)+u(i-1,j+1)+u(i,j)+u(i-1,j))/4.0d0
usec=(u(i,j)+u(i+1,j)+u(i,j-1)+u(i+1,j-1))/4.0d0
```

```
usw=(u(i,j)+u(i-1,j)+u(i,j-1)+u(i-1,j-1))/4.0d0

su1=tvise*q2e*(une-usee)/dh/jace*dh
*   -tvisw*q2w*(unw-usw)/dh/jacw*dh
*   +tvisn*q2n*(une-unw)/dz/jacn*dz
*   -tviss*q2s*(usee-usw)/dz/jacs*dz

tke=tk(i+1,j)
tkw=tk(i,j)
tkn=(tk(i+1,j)+tk(i,j)+tk(i+1,j+1)+tk(i,j+1))/4.0d0
tks=(tk(i+1,j)+tk(i,j)+tk(i+1,j-1)+tk(i,j-1))/4.0d0
pe=p(i+1,j)
pw=p(i,j)
pn=(p(i+1,j)+p(i,j)+p(i+1,j+1)+p(i,j+1))/4.0d0
ps=(p(i+1,j)+p(i,j)+p(i+1,j-1)+p(i,j-1))/4.0d0
dpdz=(pe-pw)
dpde=(pn-ps)
dkdz=(tke-tkw)
dkde=(tkn-tks)
yep=(ye(i,j)+ye(i,j-1))/2.0d0
yzp=(yz(i,j)+yz(i,j-1))/2.0d0

su2=-2.0d0/3.0d0*((tke*yee-tkw*yew)*dh-(tkn*yzn-tks*yzs)*dz)
if(i.eq.2)su2=0.0d0
su3=-1.0d0/1000.0d0*((pe*yee-pw*yew)*dh-(pn*yzn-ps*yzs)*dz)

C>>>>>**** term d/dy(nu dv/dx) .....
if(i.lt.m-1)ve=(v(i+1,j)+v(i+2,j)+v(i+1,j-1)+v(i+2,j-1))/4.0d0
if(i.eq.m-1)ve=(v(i+1,j)+v(i+1,j-1))/2.0d0
vw=(v(i-1,j)+v(i,j)+v(i-1,j-1)+v(i,j-1))/4.0d0
if(j.gt.2)vs=(v(i,j-1)+v(i+1,j-1)+v(i,j-2)+v(i+1,j-2))/4.0d0
if(j.eq.2)vs=(v(i,j-1)+v(i+1,j-1))/2.0d0
vn=(v(i,j+1)+v(i+1,j+1)+v(i,j)+v(i+1,j))/4.0d0
vp=(v(i,j)+v(i+1,j)+v(i,j-1)+v(i+1,j-1))/4.0d0

dvdzn=(v(i+1,j)-v(i,j))/dz
dvden=(vn-vp)/((h(i,j+1)-h(i,j-1))/2.0d0)

dvdzs=(v(i+1,j-1)-v(i,j-1))/dz
if(j.gt.2)dvdes=(vp-vs)/((h(i,j)-h(i,j-2))/2.0d0)
if(j.eq.2)dvdes=(vp-vs)/((h(i,j)-h(i,j-1))/2.0d0)

dvdee=(v(i+1,j)-v(i+1,j-1))/dh
dvdze=(ve-vp)/(z(i+1,j)-z(i,j))

dvdew=(v(i,j)-v(i,j-1))/dh
dvdzw=(vp-vw)/(z(i,j)-z(i-1,j))

su4n=tvisn/jac(i,j)*
*   (ye(i,j)*xz(i,j)*dvdzn-yz(i,j)*xz(i,j)*dvden)*dz
su4s=tviss/jac(i,j-1)*
*   (ye(i,j-1)*xz(i,j-1)*dvdzs-yz(i,j-1)*xz(i,j-1)*dvdes)*dz
su4e=tvis(i+1,j)/jace*
*   (xee*yze*dvdee-yee*xee*dvdze)*dh
su4w=tvis(i,j)/jacw*
*   (xew*yzw*dvdew-yew*xew*dvdzw)*dh
su4=su4n-su4s+su4e-su4w

*>>>>>>>>>>>>>>>>>>>>>>>>>>>>>>>>
su=(su1+su2+su3+su4)
c....hybrid scheme
AE=(DE+ABS(CE)+ABS(DE-ABS(CE)))/2.0d0-CE
AW=(DW+ABS(CW)+ABS(DW-ABS(CW)))/2.0d0+CW
AS=(DS+ABS(CS)+ABS(DS-ABS(CS)))/2.0d0+CS
AN=(DN+ABS(CN)+ABS(DN-ABS(CN)))/2.0d0-CN
AP=AE+AW+AS+AN
bu(i,j)=-yep*dh/ap/1000.0d0
cu(i,j)=yzp*dz/ap/1000.0d0
C.....FORMING TDMA
AE=AE/AP
AW=AW/AP
AS=AS/AP
AN=AN/AP
SU=Su/AP
return
end
```

```
****************************************************************
*%%%%%%%%%%%%%%%%%%%% SUBROUTINE FOR SOLVING  %%%%%%%%%%%%%%%%*
*%%%%%%%%%%%%%%%%%%%%%     U-MOMENTUM       %%%%%%%%%%%%%%%%%*
*%%%%%%%%%%%%%%%%%%%%%%     EQUATION       %%%%%%%%%%%%%%%%%%*
****************************************************************
SUBROUTNE SOLVEU (m,n,u,v,tvis,xz,yz,xe,ye,jac,z,h,p,tk,u1,du,
*  vis,cmu,omegau,ubar,vbar,temp,x,y,bu,cu)
implicit double precision (a-h,o-z)
real jac(m,n),h(m,n),z(m,n),tvis(m,n),tk(m,n),u(m,n),
* xz(m,n),xe(m,n),yz(m,n),ye(m,n),p(m,n),temp(m,n),
* a(250),b(250),c(250),t(250),f(250),ubar(m,n),vbar(m,n),x(m,n),
* y(m,n),bu(m,n),cu(m,n),v(m,n)

DO 1 I=1,M
DO 1 J=1,n
temp(i,j)=u(i,j)
1 CONTINUE

C==============================
C.....SWEEP IN X-DIRECTION..
C==============================
DO 10 J=2,N-1
DO 20 I=2,M-1
call umom (i,j,m,n,u,v,tvis,xz,yz,xe,ye,jac,z,h,p,
*  tk,u1,du,vis,cmu,omegau,ubar,vbar,ae,aw,an,as,su,bu,cu)

IF(I.GT.2)GOTO 50
A(I-1)=0.0d0
B(I-1)=1.0d0
C(I-1)=-AE
F(I-1)=AW*u(I-1,J)+AS*u(I,J-1)+AN*u(I,J+1)+SU
GOTO 20
50 IF(I.EQ.M-1)GOTO 60
A(I-1)=-AW
B(I-1)=1.0d0
C(I-1)=-AE
F(I-1)=AS*u(I,J-1)+AN*u(I,J+1)+SU
GOTO 20
60 A(I-1)=-AW
B(I-1)=1.0d0
C(I-1)=0.0d0
F(I-1)=AS*u(I,J-1)+AN*u(I,J+1)+SU+ae*u(i+1,j)
20 CONTINUE
C.....CALCULATE FINITE DIFF. EQU...
CALL TRIDAG(A,B,C,F,M-2,T)
C.....UNDERRELAXATION OF U
DO 70 I=2,M-1
u(I,J)=(1.0d0-OMEGAU)*u(I,J)+OMEGAU*T(I-1)
70 CONTINUE
u(m,j)=u(m-1,j)
if(j.ne.n-1)goto 10
do 80 i=2,m
u(i,n)=u(i,n-1)
80 continue
10 continue

c....Sweep in y-direction
do 110 i=2,m-1
do 120 j=2,n-1
call umom(i,j,m,n,u,v,tvis,xz,yz,xe,ye,jac,z,h,p,
*  tk,u1,du,vis,cmu,omegau,ubar,vbar,ae,aw,an,as,su,bu,cu)

IF(J.GT.2)GOTO 150
A(J-1)=0.0d0
B(J-1)=1.0d0
C(J-1)=-AN
F(J-1)=AW*u(I-1,J)+AS*u(I,J-1)+AE*u(I+1,J)+SU
GOTO 120
150 IF(J.EQ.N-1)GOTO 160
A(J-1)=-AS
B(J-1)=1.0d0
C(J-1)=-AN
F(J-1)=AE*u(I+1,J)+AW*u(I-1,J)+SU
GOTO 120
160 A(J-1)=-AS
B(J-1)=1.0d0
```

```
C(J-1)=0.0d0
F(J-1)=AE*u(I+1,J)+AW*u(I-1,J)+Su+an*u(i,j+1)
120 CONTINUE

C.....CALCULATE FINITE DIFF. EQU...
CALL TRIDAG(A,B,C,F,N-2,T)
C.....UNDERRELAXATION OF U
DO 170 J=2,N-1
IF(I.EQ.2.AND.J.EQ.2) DU=0.0d0
UO=u(I,J)
u(I,J)=(1.0d0-OMEGAU)*u(I,J)+OMEGAU*T(J-1)
DU=ABS(u(I,J)-UO)+DU
170 CONTINUE
u(i,n)=u(i,n-1)
if(i.ne.m-1)goto 110
do 180 j=2,n
u(m,j)=u(m-1,j)
180 continue
110 CONTINUE

do 171 i=2,m
do 171 j=2,n
u(I,J)=(1.0d0-0.50d0)*temp(I,J)+0.5d0*u(i,j)
171 CONTINUE

DU=du/(n-2)/(m-2)/u1
print*,'du=',du
return
end
*****************************************************************
SUBROUTNE VMOM (i,j,m,n,u,v,tvis,xz,yz,xe,ye,jac,z,h,p,
*  tk,u1,dv,vis,cmu,omegav,ubar,vbar,ae,aw,an,as,sv,bv,cv)
implicit double precision (a-h,o-z)
real jac(m,n),h(m,n),z(m,n),tvis(m,n),tk(m,n),u(m,n),
* xz(m,n),xe(m,n),yz(m,n),ye(m,n),p(m,n),v(m,n),
* ubar(m,n),vbar(m,n),bv(m,n),cv(m,n)
real jacn,jacs,jace,jacw
dz=z(i,j)-z(i-1,j)
dh=(h(i,j+1)-h(i,j-1))/2.0d0
C.....CONVECTIONS..
ce=(ubar(i,j+1)+ubar(i,j))/4.0d0*dh
cw=(ubar(i-1,j+1)+ubar(i-1,j))/4.0d0*dh
cn=(vbar(i,j+1)+vbar(i,j))/4.0d0*dz
cs=(vbar(i,j-1)+vbar(i,j))/4.0d0*dz
C.....DIFFUSIONS..
yee=ye(i,j)
xee=xe(i,j)
q4e=2.0d0*xee**2+yee**2
tvise=(tvis(i,j)+tvis(i+1,j)+tvis(i,j+1)+tvis(i+1,j+1))/4.0d0
jace=jac(i,j)
dze=(z(i+1,j)-z(i-1,j))/2.0d0
de=tvise*q4e/jace/dze*dh

yew=ye(i-1,j)
xew=xe(i-1,j)
q4w=2.0d0*xew**2+yew**2
if(i.ne.2)then
dzw=(z(i,j)-z(i-2,j))/2.0d0
tvisw=(tvis(i,j)+tvis(i-1,j)+tvis(i,j+1)+tvis(i-1,j+1))/4.0d0
else
dzw=z(2,j)/2.0d0
tvisw=(tvis(1,j+1)+tvis(1,j))/2.0d0
endif
jacw=jac(i-1,j)
dw=tvisw*q4w/jacw/dzw*dh

yzn=(yz(i,j)+yz(i-1,j)+yz(i,j+1)+yz(i-1,j+1))/4.0d0
xzn=(xz(i,j)+xz(i-1,j)+xz(i,j+1)+xz(i-1,j+1))/4.0d0
jacn=(jac(i,j)+jac(i-1,j)+jac(i,j+1)+jac(i-1,j+1))/4.0d0
q6n=2.0d0*xzn**2+yzn**2
tvisn=tvis(i,j+1)
dhn=h(i,j+1)-h(i,j)
dn=tvisn*q6n/jacn/dhn*dz
yzs=(yz(i,j)+yz(i-1,j)+yz(i,j-1)+yz(i-1,j-1))/4.0d0
xzs=(xz(i,j)+xz(i-1,j)+xz(i,j-1)+xz(i-1,j-1))/4.0d0
jacs=(jac(i,j)+jac(i-1,j)+jac(i,j-1)+jac(i-1,j-1))/4.0d0
```

```
q6s=2.0d0*xzs**2+yzs**2
tviss=tvis(i,j)
dhs=h(i,j)-h(i,j-1)
ds=tviss*q6s/jacs/dhs*dz

C.....SOURCE TERM..
yes=(ye(i,j)+ye(i-1,j)+ye(i,j-1)+ye(i-1,j-1))/4.0d0
xes=(xe(i,j)+xe(i-1,j)+xe(i,j-1)+xe(i-1,j-1))/4.0d0
yen=(ye(i,j)+ye(i-1,j)+ye(i,j+1)+ye(i-1,j+1))/4.0d0
xen=(xe(i,j)+xe(i-1,j)+xe(i,j+1)+xe(i-1,j+1))/4.0d0
yze=yz(i,j)
xze=xz(i,j)
yzw=yz(i-1,j)
xzw=xz(i-1,j)

q5w=-(yew*yzw+2.0d0*xew*xzw)
q5e=-(yee*yze+2.0d0*xee*xze)
q5n=-(yen*yzn+2.0d0*xen*xzn)
q5s=-(yes*yzs+2.0d0*xes*xzs)
vne=(v(i,j+1)+v(i+1,j+1)+v(i,j)+v(i+1,j))/4.0d0
vnw=(v(i,j+1)+v(i-1,j+1)+v(i,j)+v(i-1,j))/4.0d0
vse=(v(i,j)+v(i+1,j)+v(i,j-1)+v(i+1,j-1))/4.0d0
vsw=(v(i,j)+v(i-1,j)+v(i,j-1)+v(i-1,j-1))/4.0d0

sv1=tvise*q5e*(vne-vse)/dh/jace*dh
*   -tvisw*q5w*(vnw-vsw)/dh/jacw*dh
*   +tvisn*q5n*(vne-vnw)/dz/jacn*dz
*   -tviss*q5s*(vse-vsw)/dz/jacs*dz

tke=(tk(i,j)+tk(i+1,j)+tk(i,j+1)+tk(i+1,j+1))/4.0d0
tkw=(tk(i,j)+tk(i-1,j)+tk(i,j+1)+tk(i-1,j+1))/4.0d0
tkn=tk(i,j+1)
tks=tk(i,j)
dkde=(tkn-tks)
dkdz=(tke-tkw)
pe=(p(i,j)+p(i+1,j)+p(i,j+1)+p(i+1,j+1))/4.0d0
pw=(p(i,j)+p(i-1,j)+p(i,j+1)+p(i-1,j+1))/4.0d0
pn=p(i,j+1)
ps=p(i,j)
dpde=(pn-ps)
dpdz=(pe-pw)
xzp=(xz(i,j)+xz(i-1,j))/2.0d0
xep=(xe(i,j)+xe(i-1,j))/2.0d0

sv2=-2.0d0/3.0d0*((tkn*xzn-tks*xzs)*dz-(tke*xee-tkw*xew)*dh)
if(i.eq.2)sv2=0.0d0
sv3=-1.0d0/1000.0d0*((pn*xzn-ps*xzs)*dz-(pe*xee-pw*xew)*dh)

C>>>>>**** term d/dx(nu du/dy) .....
ue=(u(i,j+1)+u(i,j)+u(i+1,j+1)+u(i+1,j))/4.0d0
if(i.gt.2)uw=(u(i-1,j+1)+u(i-1,j)+u(i-2,j+1)+u(i-2,j))/4.0d0
if(i.eq.2)uw=(u(i-1,j+1)+u(i-1,j))/2.0d0
us=(u(i,j)+u(i,j-1)+u(i-1,j)+u(i-1,j-1))/4.0d0
if(j.lt.n-1)un=(u(i,j+2)+u(i,j+1)+u(i-1,j+2)+u(i-1,j+1))/4.0d0
if(j.eq.n-1)un=(u(i,j+1)+u(i-1,j+1))/2.0d0
up=(u(i,j+1)+u(i,j)+u(i-1,j+1)+u(i-1,j))/4.0d0

dudzn=(u(i,j+1)-u(i-1,j+1))/dz
duden=(un-up)/(h(i,j+1)-h(i,j))

dudzs=(u(i,j)-u(i-1,j))/dz
dudes=(up-us)/(h(i,j)-h(i,j-1))

dudee=(u(i,j+1)-u(i,j))/dh
dudze=(ue-up)/((z(i+1,j)-z(i-1,j))/2.0d0)
dudew=(u(i-1,j+1)-u(i-1,j))/dh
if(i.gt.2)dudzw=(up-uw)/((z(i,j)-z(i-2,j))/2.0d0)
if(i.eq.2)dudzw=(up-uw)/((z(i,j)-z(i-1,j))/2.0d0)

sv4n=tvis(i,j+1)/jacn*
*    (yzn*xen*dudzn-yzn*xzn*duden)*dz
sv4s=tvis(i,j)/jacs*
*    (yzs*xes*dudzs-yzs*xzs*dudes)*dz
sv4e=tvise/jac(i,j)*
*    (xz(i,j)*ye(i,j)*dudee-ye(i,j)*xe(i,j)*dudze)*dh
sv4w=tvisw/jac(i-1,j)*
```

```
*    (xz(i-1,j)*ye(i-1,j)*dudew-ye(i-1,j)*xe(i-1,j)*dudzw)*dh
     sv4=sv4n-sv4s+sv4e-sv4w
C>>>>>>>>>>>>>>>>>>>>>>>>>>>>>
sv=(sv1+sv2+sv3+sv4)

c....hybrid scheme
AE=(DE+ABS(CE)+ABS(DE-ABS(CE)))/2.0d0-CE
AW=(DW+ABS(CW)+ABS(DW-ABS(CW)))/2.0d0+CW
IF(I.EQ.2)AW=2.0d0*CW+DW
AS=(DS+ABS(CS)+ABS(DS-ABS(CS)))/2.0d0+CS
AN=(DN+ABS(CN)+ABS(DN-ABS(CN)))/2.0d0-CN
AP=AE+AW+AS+AN

 bv(i,j)=xep*dh/ap/1000.0d0
cv(i,j)=-xzp*dz/ap/1000.0d0

C.....FORMING TDMA
AE=AE/AP
AW=AW/AP
AS=AS/AP
AN=AN/AP
Sv=Sv/AP
return
end
*****************************************************************
*%%%%%%%%%%%%%%%%%%%% SUBROUTINE FOR SOLVING  %%%%%%%%%%%%%%%%*
*%%%%%%%%%%%%%%%%%%%%%%    V-MOMENTUM      %%%%%%%%%%%%%%%%%%*
*%%%%%%%%%%%%%%%%%%%%%%%      EQUATION      %%%%%%%%%%%%%%%%%%%*
*****************************************************************
SUBROUTINE SOLVEV (m,n,u,v,tvis,xz,yz,xe,ye,jac,z,h,p,
*      tk,u1,dv,vis,cmu,omegav,ubar,vbar,temp,x,y,bv,cv)
implicit double precision (a-h,o-z)
real jac(m,n),h(m,n),z(m,n),tvis(m,n),tk(m,n),u(m,n),
* xz(m,n),xe(m,n),yz(m,n),ye(m,n),p(m,n),temp(m,n),v(m,n),
* a(250),b(250),c(250),t(250),f(250),ubar(m,n),vbar(m,n),x(m,n),
* y(m,n),bv(m,n),cv(m,n)

DO 1 I=1,M
DO 1 J=1,n
temp(i,j)=v(i,j)
1 CONTINUE
do 2 i=2,m
uc=(u(i,n)+u(i-1,n))/2.0d0
yzn=(yz(i,n)+yz(i-1,n))/2.0d0
xzn=(xz(i,n)+xz(i-1,n))/2.0d0
v(i,n)=uc*yzn/xzn
2 continue
do 1000 ii=1,1

C==============================
C.....SWEEP IN X-DIRECTION..
C==============================
DO 10 J=2,N-1
DO 20 I=2,M-1
call vmom(i,j,m,n,u,v,tvis,xz,yz,xe,ye,jac,z,h,p,
*  tk,u1,dv,vis,cmu,omegav,ubar,vbar,ae,aw,an,as,sv,bv,cv)
c....forming TDMA
IF(I.GT.2)GOTO 50
A(I-1)=0.0d0
B(I-1)=1.0d0
C(I-1)=-AE
F(I-1)=AW*v(I-1,J)+AS*v(I,J-1)+AN*v(I,J+1)+Sv
GOTO 20
50 IF(I.EQ.M-1)GOTO 60
A(I-1)=-AW
B(I-1)=1.0d0
C(I-1)=-AE
F(I-1)=AS*v(I,J-1)+AN*v(I,J+1)+Sv
GOTO 20
60 A(I-1)=-AW
B(I-1)=1.0d0
C(I-1)=0.0d0
F(I-1)=AS*v(I,J-1)+AN*v(I,J+1)+Sv+ae*v(i+1,j)
20 CONTINUE
C.....CALCULATE FINITE DIFF. EQU...
CALL TRIDAG(A,B,C,F,M-2,T)
```

```
C.....UNDERRELAXATION OF v
DO 70 I=2,M-1
v(I,J)=(1.-OMEGAv)*v(I,J)+OMEGAv*T(I-1)
!    if(v(i,j).gt.u1/5.0d0)v(i,j)=u1/5.0d0
70 CONTINUE
v(m,j)=v(m-1,j)
10 continue

c....sweep in y-direction
DO 110 i=2,m-1
DO 120 j=2,n-1
call vmom(i,j,m,n,u,v,tvis,xz,yz,xe,ye,jac,z,h,p,
*  tk,u1,dv,vis,cmu,omegav,ubar,vbar,ae,aw,an,as,sv,bv,cv)

IF(J.GT.2)GOTO 150
A(J-1)=0.0d0
B(J-1)=1.0d0
C(J-1)=-AN
F(J-1)=AW*v(I-1,J)+AS*v(I,J-1)+AE*v(I+1,J)+Sv
GOTO 120
150 IF(J.EQ.N-1)GOTO 160

A(J-1)=-AS
B(J-1)=1.0d0
C(J-1)=-AN
F(J-1)=AE*v(I+1,J)+AW*v(I-1,J)+Sv
GOTO 120
160 A(J-1)=-AS
B(J-1)=1.0d0
C(J-1)=0.0d0
F(J-1)=AE*v(I+1,J)+AW*v(I-1,J)+Sv+an*v(i,j+1)
120 CONTINUE
C.....CALCULATE FINITE DIFF. EQU...
CALL TRIDAG(A,B,C,F,N-2,T)
C.....UNDERRELAXATION OF v
DO 170 J=2,N-1
IF(I.EQ.2.AND.J.EQ.2) Dv=0.0d0
vO=v(I,J)
v(I,J)=(1.-OMEGAv)*v(I,J)+OMEGAv*T(J-1)
Dv=ABS(v(I,J)-vO)+Dv
170 CONTINUE
if(i.ne.m-1)goto 110
do 180 j=2,n
v(m,j)=v(m-1,j)
180 continue
110 CONTINUE
1000 continue

Dv=Dv/(N-2)/(M-2)
Dv=Dv/(U1/30.0d0)
print*,'dv=',dv

do 171 i=2,m
do 171 j=2,n
v(I,J)=(1.0d0-0.5d0)*temp(I,J)+0.5d0*v(i,j)
171 CONTINUE
return
end
*********************************************************************
SUBROUTNE PCOR (i,j,m,n,u,v,tvis,xz,yz,xe,ye,jac,z,h,p,pp
*   ,tk,u1,dp,vis,ubar,vbar,ae,aw,an,as,sp,ap,bu,bv,cu,cv)
implicit double precision (a-h,o-z)
real jac(m,n),h(m,n),z(m,n),tvis(m,n),tk(m,n),bv(m,n),
* xz(m,n),xe(m,n),yz(m,n),ye(m,n),p(m,n),pp(m,n),cv(m,n),
* bu(m,n),cu(m,n),ubar(m,n),vbar(m,n),u(m,n),v(m,n)
dz=z(i,j)-z(i-1,j)
dh=h(i,j)-h(i,j-1)

yee=(ye(i,j)+ye(i,j-1))/2.0d0
xee=(xe(i,j)+xe(i,j-1))/2.0d0
bvc=(bv(i+1,j)+bv(i+1,j-1)+bv(i,j)+bv(i,j-1))/4.0d0
dze=(z(i+1,j)-z(i-1,j))/2.0d0
ae=(bu(i,j)*yee-bvc*xee)*dh/dze

yew=(ye(i-1,j)+ye(i-1,j-1))/2.0d0
xew=(xe(i-1,j)+xe(i-1,j-1))/2.0d0
```

```
bvc=(bv(i,j)+bv(i,j-1)+bv(i-1,j)+bv(i-1,j-1))/4.0d0
if(i.ne.2)dzw=(z(i,j)-z(i-2,j))/2.0d0
if(i.eq.2)dzw=z(2,j)/2.0d0
aw=(bu(i-1,j)*yew-bvc*xew)*dh/dzw

yzs=(yz(i,j-1)+yz(i-1,j-1))/2.0d0
xzs=(xz(i,j-1)+xz(i-1,j-1))/2.0d0
cuc=(cu(i,j)+cu(i,j-1)+cu(i-1,j)+cu(i-1,j-1))/4.0d0
if(j.ne.2)dhs=(h(i,j)-h(i,j-2))/2.0d0
if(j.eq.2)dhs=h(i,2)/2.0d0
as=(cv(i,j-1)*xzs+cuc*yzs)*dz/dhs

yzn=(yz(i,j)+yz(i-1,j))/2.0d0
xzn=(xz(i,j)+xz(i-1,j))/2.0d0
cuc=(cu(i,j)+cu(i-1,j)+cu(i,j+1)+cu(i-1,j+1))/4.0d0
dhn=(h(i,j+1)-h(i,j-1))/2.0d0
an=(cv(i,j)*xzn+cuc*yzn)*dz/dhs
sp=(ubar(i,j)-ubar(i-1,j))*dh+(vbar(i,j)-vbar(i,j-1))*dz
AP=AW+AE+AS+AN
 return
 end
*****************************************************************
*%%%%%%%%%%%%%%%    SUBROUTINE FOR SOLVING   %%%%%%%%%%%%%%%%%%*
*%%%%%%%%%%%%%%%     CONTINUITY EQUAION     %%%%%%%%%%%%%%%%%%*
*%%%%%%%%%%%%%%%%%          AND          %%%%%%%%%%%%%%%%%%*
*%%%%%%%%%%%%%%%%    CORRECTION FOR U AND V   %%%%%%%%%%%%%%%%%%*
*****************************************************************
SUBROUTNE SOLVEP (m,n,u,v,tvis,xz,yz,xe,ye,jac,z,h,p,pp
*   ,tk,u1,dp,vis,cmu,y,omegap,omegah,ubar,vbar,x,bu,bv,cu,cv)
implicit double precision (a-h,o-z)
real jac(m,n),h(m,n),z(m,n),tvis(m,n),tk(m,n),x(m,n),
* xz(m,n),xe(m,n),yz(m,n),ye(m,n),p(m,n),pp(m,n),cu(m,n),cv(m,n),
* y(m,n),ubar(m,n),vbar(m,n),u(m,n),v(m,n),bu(m,n),bv(m,n),
* a(250),b(250),c(250),f(250),t(250)
real(kind=8) jace,jacn

do 101 i=2,m-1
do 101 j=2,n-1
call umom(i,j,m,n,u,v,tvis,xz,yz,xe,ye,jac,z,h,p,
*  tk,u1,du,vis,cmu,omegau,ubar,vbar,ae,aw,an,as,su,bu,cu)
call vmom(i,j,m,n,u,v,tvis,xz,yz,xe,ye,jac,z,h,p,
*  tk,u1,dv,vis,cmu,omegav,ubar,vbar,ae,aw,an,as,sv,bv,cv)
101 continue
c=============================================================
C.....SOLVE CONTINUITY EQN. FOR PRECOR. THREE TIMES DOUBLE SWEEP
C=============================================================
DO 1000 K=1,3
C=========================
C.....SWEEP IN X-DIRECTION
C=========================

DO 30 J=2,N-1
do 40 i=2,m-1
call pcor(i,j,m,n,u,v,tvis,xz,yz,xe,ye,jac,z,h,p,pp
*   ,tk,u1,dp,vis,ubar,vbar,ae,aw,an,as,sp,ap,bu,bv,cu,cv)

IF(I.GT.2)GOTO 45
A(I-1)=0.0d0
B(I-1)=ap
C(I-1)=-ae
if(j.ne.2)F(I-1)=AN*PP(I,J+1)+AS*PP(I,J-1)+SP
if(j.eq.2)F(I-1)=AN*PP(I,J+1)+SP
GOTO 40
45 IF(I.EQ.M-1)GOTO 50
A(I-1)=-AW
B(I-1)=ap
C(I-1)=-AE
if(j.ne.2)F(I-1)=AN*PP(I,J+1)+AS*PP(I,J-1)+SP
if(j.eq.2)F(I-1)=AN*PP(I,J+1)+SP
GOTO 40
50 A(I-1)=-AW
B(I-1)=ap-ae
C(I-1)=0.0d0
if(j.ne.2)F(I-1)=AN*PP(I,J+1)+AS*PP(I,J-1)+SP
if(j.eq.2)F(I-1)=AN*PP(I,J+1)+SP
40 CONTINUE
```

```
C.....CALCULATE FINITE DIFF. EQN.
CALL TRIDAG(A,B,C,F,M-2,T)
DO 60 I=2,M-1
PP(I,J)=(1.0d0-OMEGAP)*PP(I,J)+OMEGAP*T(I-1)
60 CONTINUE
pp(m,j)=0.0d0
pp(1,j)=pp(2,j)
if(j.ne.n-1)goto 30
do 390 i=2,m
pp(i,n)=pp(i,n-1)
pp(i,1)=pp(i,2)
390 continue
30 CONTINUE
C============================
C.....SWEEP IN Y-DIRECTION
C============================
DO 130 I=2,M-1
do 140 j=2,n-1
call pcor(i,j,m,n,u,v,tvis,xz,yz,xe,ye,jac,z,h,p,pp
*   ,tk,u1,dp,vis,ubar,vbar,ae,aw,an,as,sp,ap,bu,bv,cu,cv)

IF(j.GT.2)GOTO 145
A(j-1)=0.0d0
B(j-1)=ap
C(j-1)=-an
if(i.ne.2)F(j-1)=AW*PP(I-1,J)+AE*PP(I+1,J)+SP
if(i.eq.2)F(j-1)=AE*PP(I+1,J)+SP
GOTO 140
145 IF(j.EQ.n-1)GOTO 150
A(j-1)=-As
B(j-1)=ap
C(j-1)=-An
if(i.ne.2)F(j-1)=AW*PP(I-1,J)+AE*PP(I+1,J)+SP
if(i.eq.2)F(j-1)=AE*PP(I+1,J)+SP
GOTO 140
150 A(J-1)=-AS
B(J-1)=ap-an
C(J-1)=0.0d0
if(i.ne.2)F(j-1)=AW*PP(I-1,J)+AE*PP(I+1,J)+SP
if(i.eq.2)F(j-1)=AE*PP(I+1,J)+SP
140 CONTINUE
C.....CALCULATE FINITE DIFF. EQN.
CALL TRIDAG(A,B,C,F,N-2,T)
DO 164 J=2,N-1
PP(I,J)=(1.0d0-OMEGAP)*PP(I,J)+OMEGAP*T(J-1)
164 CONTINUE
pp(i,n)=pp(i,n-1)
pp(i,1)=pp(i,2)
if(i.ne.m-1)goto 130
do 222 j=1,n
pp(m,j)=0.0d0
pp(1,j)=pp(2,j)
222 continue
130 CONTINUE
1000 CONTINUE
C=============================================================
C  RELAX THE PRESSURE CORRECTION
C  FIND NEW VELOCITY FIELD AND RE-SOLVE THE MOM.EQN.
C=============================================================
DO 500 I=1,M-1
DO 500 J=1,N
P(I,J)=P(I,J)+OMEGAH*PP(I,J)
500 CONTINUE


DO 700 I=2,M-1
DO 701 J=2,N-1
dz=z(i,j)-z(i-1,j)
dh=h(i,j)-h(i,j-1)
yee=(ye(i,j)+ye(i,j-1))/2.0d0
yze=(yz(i,j)+yz(i,j-1))/2.0d0
xee=(xe(i,j)+xe(i,j-1))/2.0d0
xze=(xz(i,j)+xz(i,j-1))/2.0d0
jace=(jac(i,j)+jac(i,j-1))/2.0d0
jacn=(jac(i,j)+jac(i-1,j))/2.0d0
yzn=(yz(i,j)+yz(i-1,j))/2.0d0
```

```
xzn=(xz(i,j)+xz(i-1,j))/2.0d0
xen=(xe(i,j)+xe(i-1,j))/2.0d0
yen=(ye(i,j)+ye(i-1,j))/2.0d0
dze=(z(i+1,j)-z(i-1,j))/2.0d0
dpdz=(pp(i+1,j)-pp(i,j))/dze
dhn=(h(i,j+1)-h(i,j-1))/2.0d0
dpde=(pp(i,j+1)-pp(i,j))/dhn

U(I,J)=U(I,J)+(bu(i,j)*dpdz+cu(i,j)*dpde)*omegah
v(I,J)=v(I,J)+(bv(i,j)*dpdz+cv(i,j)*dpde)*omegah

701 continue
uc=(u(i,n)+u(i-1,n))/2.0d0
yzn=(yz(i,n)+yz(i-1,n))/2.0d0
xzn=(xz(i,n)+xz(i-1,n))/2.0d0
v(i,n)=uc*yzn/xzn
700 continue

do 180 j=2,n
v(m,j)=v(m-1,j)
u(m,j)=u(m-1,j)
180 continue
DP=0.od0
DO 850 I=2,M-1
DO 850 J=2,N-1
DP=ABS(PP(I,J))+DP
850 CONTINUE
DP=DP/(M-2)/(N-2)/9810.0d0/y(m,n)
print*,'dp=',dp

DO 1 I=1,M
DO 1 J=1,N
PP(I,J)=0.0d0
1 CONTINUE
RETURN
END
*****************************************************************
SUBROUTINE SURF (m,n,p,y,y1,u,v,x,u1,omegas,dh)
implicit double precision (a-h,o-z)
real P(M,N),Y(M,N),U(M,N),V(M,N),X(M,n)
RFS=omegas
DH=0.0d0
DO 10 I=1,M-1
IF(I.EQ.1)THEN
DY1=y(1,n)-Y(1,N-2)
DY2=Y(1,N-2)-Y(1,N-3)
ELSE
H=(Y(I,N)+Y(I-1,N))/2.0d0
DY1=H-(Y(I,N-2)+Y(I-1,N-2))/2.0d0
DY2=(Y(I,N-2)+Y(I-1,N-2))/2.0d0-(Y(I,N-3)+Y(I-1,N-3))/2.0d0
ENDIF
PSURF=P(I,N-2)+(P(I,N-2)-P(I,N-3))*DY1/DY2
HNEW=PSURF/9810.0d0
HOLD=y(i,n)
y(I,n)=(1.-RFS)*HOLD+RFS*HNEW
DH=ABS(y(I,n)-HOLD)+DH
10 CONTINUE
DH=DH/(M-1)
DH=DH/y(m,n)
PRINT*,'DH=',DH
return
end
*****************************************************************
*%%%%%%%%%%%%%%%%%%%% SUBROUTINE FOR SOLVING %%%%%%%%%%%%%%%%%%*
*%%%%%%%%%%%%%%%%%%%%%%%% G-TERM IN K-E %%%%%%%%%%%%%%%%%%%%%%*
*%%%%%%%%%%%%%%%%%%%%%%%% EQUATION %%%%%%%%%%%%%%%%%%%%%%%%%%*
*****************************************************************
SUBROUTINE GENTERM (m,n,u,v,xe,xz,ye,yz,jac,gen,tvis,h,z,udsq,tk,
*    vdsq,udvd)
implicit double precision (a-h,o-z)
real U(M,N),V(M,N),ye(m,n),yz(M,N),xe(m,n),xz(m,n),
*    gen(m,n),tvis(m,n),h(m,n),z(m,n),udsq(m,n),tk(m,n),vdsq(m,n),
*    udvd(m,n),jac(m,n)
do 10 i=2,m-1
do 20 j=2,n-1
dh=h(i,j)-h(i,j-1)
```

```
dz=z(i,j)-z(i-1,j)

yep=(ye(i,j)+ye(i,j-1)+ye(i-1,j)+ye(i-1,j-1))/4.0d0
yzp=(yz(i,j)+yz(i,j-1)+yz(i-1,j)+yz(i-1,j-1))/4.0d0
xep=(xe(i,j)+xe(i,j-1)+xe(i-1,j)+xe(i-1,j-1))/4.0d0
xzp=(xz(i,j)+xz(i,j-1)+xz(i-1,j)+xz(i-1,j-1))/4.0d0
pjac=(jac(i,j)+jac(i,j-1)+jac(i-1,j)+jac(i-1,j-1))/4.0d0

dudz=(u(i,j)-u(i-1,j))/dz
dude=(u(i,j+1)+u(i-1,j+1)-u(i,j-1)-u(i-1,j-1))/4.0d0/dh
dudy=(xzp*dude-xep*dudz)/pjac
dudx=(yep*dudz-yzp*dude)/pjac

dvde=(v(i,j)-v(i,j-1))/dh
dvdz=(v(i+1,j)+v(i+1,j-1)-v(i-1,j)-v(i-1,j-1))/4.0d0/dz
dvdy=(xzp*dvde-xep*dvdz)/pjac
dvdx=(yep*dvdz-yzp*dvde)/pjac

udsq(i,j)=2.0d0/3.0d0*tk(i,j)-2.0d0*tvis(i,j)*dudx
vdsq(i,j)=2.0d0/3.0d0*tk(i,j)-2.0d0*tvis(i,j)*dvdy
udvd(i,j)=tvis(i,j)*(dudy+dvdx)

gen(i,j)=((dudy+dvdx)**2+2.0d0*dudx**2+2.0d0*dvdy**2)*tvis(i,j)
20 continue
10 continue
return
end
*****************************************************************
SUBROUTNE DSS (i,j,m,n,td,tk,tvis,xz,yz,xe,ye,jac,z,h,gen,
*   c1,c2,dd,cmu,omegad,ubar,vbar,deltad,ae,aw,an,as,sd,u,v,p)
implicit double precision (a-h,o-z)
real td(m,n),tk(m,n),jac(m,n),h(m,n),z(m,n),tvis(m,n),
* xz(m,n),xe(m,n),yz(m,n),ye(m,n),gen(m,n),u(m,n),v(m,n),p(m,n),
* ubar(m,n),vbar(m,n)
real(kind=8) jacn,jacs,jace,jacw

dh=h(i,j)-h(i,j-i)
dz=z(i,j)-z(i-1,j)
C.....CONVECTIONS..
ce=ubar(i,j)/2.0d0*dh
cw=ubar(i-1,j)/2.0d0*dh
cs=vbar(i,j-1)/2.0d0*dz
cn=vbar(i,j)/2.0d0*dz
C.....DIFFUSIONS..
yew=(ye(i-1,j)+ye(i-1,j-1))/2.0d0
xew=(xe(i-1,j)+xe(i-1,j-1))/2.0d0
tvisw=(tvis(i,j)+tvis(i-1,j))/2.0d0
q1w=yew**2+xew**2
jacw=(jac(i-1,j)+jac(i-1,j-1))/2.0d0
if(i.ne.2)dzw=(z(i,j)-z(i-2,j))/2.0d0
if(i.eq.2)dzw=z(2,j)/2.0d0
dw=tvisw*q1w/jacw/deltad*dh/dzw

tvise=(tvis(i+1,j)+tvis(i,j))/2.0d0
yee=(ye(i,j)+ye(i,j-1))/2.0d0
xee=(xe(i,j)+xe(i,j-1))/2.0d0
q1e=yee**2+xee**2
jace=(jac(i,j)+jac(i,j-1))/2.0d0
dze=(z(i+1,j)-z(i-1,j))/2.0d0
de=tvise*q1e/jace/deltad*dh/dze


tvisn=(tvis(i,j)+tvis(i,j+1))/2.0d0
yzn=(yz(i,j)+yz(i-1,j))/2.0d0
xzn=(xz(i,j)+xz(i-1,j))/2.0d0
jacn=(jac(i,j)+jac(i-1,j))/2.0d0
q3n=yzn**2+xzn**2
dhn=(h(i,j+1)-h(i,j-1))/2.0d0
dn=tvisn*q3n/jacn/deltad*dz/dhn

tviss=(tvis(i,j)+tvis(i,j-1))/2.0d0
jacs=(jac(i,j-1)+jac(i-1,j-1))/2.0d0
xzs=(xz(i,j-1)+xz(i-1,j-1))/2.0d0
yzs=(yz(i,j-1)+yz(i-1,j-1))/2.0d0
q3s=yzs**2+xzs**2
if(j.ne.2)dhs=(h(i,j)-h(i,j-2))/2.0d0
```

```
if(j.eq.2)dhs=h(i,2)/2.0d0
ds=tviss*q3s/jacs/deltad*dz/dhs
C.....SOURCE TERM..
yes=(ye(i,j-1)+ye(i-1,j-1))/2.0d0
yen=(ye(i,j)+ye(i-1,j))/2.0d0
xen=(xe(i,j)+xe(i-1,j))/2.0d0
xes=(xe(i,j-1)+xe(i-1,j-1))/2.0d0
yze=(yz(i,j)+yz(i,j-1))/2.0d0
xze=(xz(i,j)+xz(i,j-1))/2.0d0
yzw=(yz(i-1,j)+yz(i-1,j-1))/2.0d0
xzw=(xz(i-1,j)+xz(i-1,j-1))/2.0d0

q2w=-(yew*yzw+xew*xzw)
q2e=-(yee*yze+xee*xze)
q2n=-(yen*yzn+xen*xzn)
q2s=-(yes*yzs+xes*xzs)

tdne=(td(i+1,j)+td(i+1,j+1)+td(i,j)+td(i,j+1))/4.0d0
tdse=(td(i+1,j)+td(i+1,j-1)+td(i,j)+td(i,j-1))/4.0d0
tdnw=(td(i,j+1)+td(i,j)+td(i-1,j+1)+td(i-1,j))/4.0d0
tdsw=(td(i,j)+td(i,j-1)+td(i-1,j)+td(i-1,j-1))/4.0d0

sd1=tvise*q2e*(tdne-tdse)/jace/deltad
*   -tvisw*q2w*(tdnw-tdsw)/jacw/deltad
*   +tvisn*q2n*(tdne-tdnw)/jacn/deltad
*   -tviss*q2s*(tdse-tdsw)/jacs/deltad

pjac=(jac(i,j)+jac(i,j-1)+jac(i-1,j)+jac(i-1,j-1))/4.0d0
if(tk(i,j).lt.0.001d0)tk(i,j)=0.001d0
sd2=c1*gen(i,j)*td(i,j)/tk(i,j)*pjac*dh*dz
sd=sd1+sd2
c....hybrid scheme
AE=(DE+ABS(CE)+ABS(DE-ABS(CE)))/2.0d0-CE
AW=(DW+ABS(CW)+ABS(DW-ABS(CW)))/2.0d0+CW
IF(I.EQ.2)AW=2.0d0*CW+DW
AS=(DS+ABS(CS)+ABS(DS-ABS(CS)))/2.0d0+CS
AN=(DN+ABS(CN)+ABS(DN-ABS(CN)))/2.0d0-CN
co=c2*td(i,j)/tk(i,j)*pjac*dh*dz
AP=AE+AW+AS+AN+co

C.....FORMING TDMA
AE=AE/AP
AW=AW/AP
AS=AS/AP
AN=AN/AP
Sd=Sd/AP
return
end
*****************************************************************
*%%%%%%%%%%%%%%%%%%% SUBROUTINE FOR SOLVING  %%%%%%%%%%%%%%%%*
*%%%%%%%%%%%%%%%%%%%%%     DISSIPATION      %%%%%%%%%%%%%%%%%*
*%%%%%%%%%%%%%%%%%%%%%%     EQUATION      %%%%%%%%%%%%%%%%%%%*
*****************************************************************
SUBROUTNE TDRE (m,n,td,tk,tvis,xz,yz,xe,ye,jac,z,h,gen,
*  c1,c2,dd,cmu,omegad,ubar,vbar,deltad,temp,u,v,p,u1,y1,y)
implicit double precision (a-h,o-z)
real td(m,n),tk(m,n),jac(m,n),h(m,n),z(m,n),tvis(m,n),
*xz(m,n),xe(m,n),yz(m,n),ye(m,n),gen(m,n),temp(m,n),v(m,n),u(m,n),
*a(250),b(250),c(250),t(250),f(250),ubar(m,n),vbar(m,n),p(m,n),
*y(m,n)


DO 1 I=1,M
DO 1 J=1,n
temp(i,j)=td(i,j)
1 CONTINUE
do 1000 ii=1,1
C==============================
C.....SWEEP IN X-DIRECTION..
C==============================
DO 10 J=2,N-1
DO 20 I=2,M-1
call diss(i,j,m,n,td,tk,tvis,xz,yz,xe,ye,jac,z,h,gen,
*  c1,c2,dd,cmu,omegad,ubar,vbar,deltad,ae,aw,an,as,sd,u,v,p)

IF(I.GT.2)GOTO 50
```

```
A(I-1)=0.0d0
B(I-1)=1.0d0
C(I-1)=-AE
F(I-1)=AW*td(I-1,J)+AS*td(I,J-1)+AN*td(I,J+1)+Sd
GOTO 20
50 IF(I.EQ.M-1)GOTO 60
A(I-1)=-AW
B(I-1)=1.0d0
C(I-1)=-AE
F(I-1)=AS*td(I,J-1)+AN*td(I,J+1)+Sd
GOTO 20
60 A(I-1)=-AW
B(I-1)=1.0d0-ae
C(I-1)=0.0d0
F(I-1)=AS*td(I,J-1)+AN*td(I,J+1)+Sd
20 CONTINUE
C.....CALCULATE FINITE DIFF. EQU...
CALL TRIDAG(A,B,C,F,M-2,T)
C.....UNDERRELAXATION OF td
DO 70 I=2,M-1
td(I,J)=(1.-OMEGAd)*td(I,J)+OMEGAd*T(I-1)
70 CONTINUE
td(m,j)=td(m-1,j)
if(j.ne.n-1)goto 10
do 80 i=2,m
td(i,n)=td(i,n-1)
80 continue
10 continue
c....Sweep in y-direction
do 110 i=2,m-1
do 120 j=2,n-1
call diss(i,j,m,n,td,tk,tvis,xz,yz,xe,ye,jac,z,h,gen,
*   c1,c2,dd,cmu,omegad,ubar,vbar,deltad,ae,aw,an,as,sd,u,v,p)

IF(J.GT.2)GOTO 150
A(J-1)=0.0d0
B(J-1)=1.0d0
C(J-1)=-AN
F(J-1)=AW*td(I-1,J)+AS*td(I,J-1)+AE*td(I+1,J)+Sd
GOTO 120
150 IF(J.EQ.N-1)GOTO 160
A(J-1)=-AS
B(J-1)=1.0d0
C(J-1)=-AN
F(J-1)=AE*td(I+1,J)+AW*td(I-1,J)+Sd
GOTO 120
160 A(J-1)=-AS
B(J-1)=1.0d0-an
C(J-1)=0.0d0
F(J-1)=AE*td(I+1,J)+AW*td(I-1,J)+Sd
120 CONTINUE
C.....CALCULATE FINITE DIFF. EQU...
CALL TRIDAG(A,B,C,F,N-2,T)
C.....UNDERRELAXATION OF td
DO 170 J=2,N-1
IF(I.EQ.2.AND.J.EQ.2) Dd=0.0d0
dOO=td(I,J)
td(I,J)=(1.0d0-OMEGAd)*td(I,J)+OMEGAd*T(J-1)
dd=ABS(td(I,J)-dOO)+Dd
170 CONTINUE
C.....MODIFY NORTH AND SOUTH WALLS..
td(I,N)=td(I,N-1)
IF(I.EQ.M-1)THEN
DO 1111 J=1,N
td(M,J)=td(M-1,J)
1111 CONTINUE
ELSE
ENDIF
110 CONTINUE
1000 continue
Dd=dd/(n-2)/(m-2)
print*,'dd=',dd
do 171 i=2,m
do 171 j=2,n
td(I,J)=(1.0d0-0.2d0)*temp(I,J)+0.2d0*td(i,j)
171 CONTINUE
```

```
return
end
*****************************************************************
SUBROUTINE KNEN(i,j,m,n,td,tk,tvis,xz,yz,xe,ye,jac,z,h,gen,
*   dk,cmu,omegak,ubar,vbar,deltak,ae,aw,an,as,sk,u,v,p)
implicit double precision (a-h,o-z)
real td(m,n),tk(m,n),jac(m,n),h(m,n),z(m,n),tvis(m,n),
* xz(m,n),xe(m,n),yz(m,n),ye(m,n),gen(m,n),
* ubar(m,n),vbar(m,n),u(m,n),v(m,n),p(m,n)
real(kind=8) jacn,jacs,jace,jacw

dh=h(i,j)-h(i,j-1)
dz=z(i,j)-z(i-1,j)
C.....CONVECTIONS..
ce=ubar(i,j)/2.0d0*dh
cw=ubar(i-1,j)/2.0d0*dh
cs=vbar(i,j-1)/2.0d0*dz
cn=vbar(i,j)/2.0d0*dz
C.....DIFFUSIONS..
yew=(ye(i-1,j)+ye(i-1,j-1))/2.0d0
xew=(xe(i-1,j)+xe(i-1,j-1))/2.0d0
tvisw=(tvis(i,j)+tvis(i-1,j))/2.0d0
q1w=yew**2+xew**2
jacw=(jac(i-1,j)+jac(i-1,j-1))/2.0d0
if(i.ne.2)dzw=(z(i,j)-z(i-2,j))/2.0d0
if(i.eq.2)dzw=z(2,j)/2.0d0
dw=tvisw*q1w/jacw/deltak*dh/dzw

tvise=(tvis(i+1,j)+tvis(i,j))/2.0d0
yee=(ye(i,j)+ye(i,j-1))/2.0d0
xee=(xe(i,j)+xe(i,j-1))/2.0d0
q1e=yee**2+xee**2
jace=(jac(i,j)+jac(i,j-1))/2.0d0
dze=(z(i+1,j)-z(i-1,j))/2.0d0
de=tvise*q1e/jace/deltak*dh/dze

tvisn=(tvis(i,j)+tvis(i,j+1))/2.0d0
yzn=(yz(i,j)+yz(i-1,j))/2.0d0
xzn=(xz(i,j)+xz(i-1,j))/2.0d0
jacn=(jac(i,j)+jac(i-1,j))/2.0d0
q3n=yzn**2+xzn**2
dhn=(h(i,j+1)-h(i,j-1))/2.0d0
dn=tvisn*q3n/jacn/deltak*dz/dhn

tviss=(tvis(i,j)+tvis(i,j-1))/2.0d0
jacs=(jac(i,j-1)+jac(i-1,j-1))/2.0d0
xzs=(xz(i,j-1)+xz(i-1,j-1))/2.0d0
yzs=(yz(i,j-1)+yz(i-1,j-1))/2.0d0
q3s=yzs**2+xzs**2
if(j.ne.2)dhs=(h(i,j)-h(i,j-2))/2.0d0
if(j.eq.2)dhs=h(i,2)/2.0d0
ds=tviss*q3s/jacs/deltak*dz/dhs

C.....SOURCE TERM..
yes=(ye(i,j-1)+ye(i-1,j-1))/2.0d0
yen=(ye(i,j)+ye(i-1,j))/2.0d0
xen=(xe(i,j)+xe(i-1,j))/2.0d0
xes=(xe(i,j-1)+xe(i-1,j-1))/2.0d0
yze=(yz(i,j)+yz(i,j-1))/2.0d0
xze=(xz(i,j)+xz(i,j-1))/2.0d0
yzw=(yz(i-1,j)+yz(i-1,j-1))/2.0d0
xzw=(xz(i-1,j)+xz(i-1,j-1))/2.0d0

q2w=-(yew*yzw+xew*xzw)
q2e=-(yee*yze+xee*xze)
q2n=-(yen*yzn+xen*xzn)
q2s=-(yes*yzs+xes*xzs)

tkne=(tk(i+1,j)+tk(i+1,j+1)+tk(i,j)+tk(i,j+1))/4.0d0
tkse=(tk(i+1,j)+tk(i+1,j-1)+tk(i,j)+tk(i,j-1))/4.0d0
tknw=(tk(i,j+1)+tk(i,j)+tk(i-1,j+1)+tk(i-1,j))/4.0d0
tksw=(tk(i,j)+tk(i,j-1)+tk(i-1,j)+tk(i-1,j-1))/4.0d0

sk1=tvise*q2e*(tkne-tkse)/jace/deltak
*   -tvisw*q2w*(tknw-tksw)/jacw/deltak
*   +tvisn*q2n*(tkne-tknw)/jacn/deltak
```

```
*   -tviss*q2s*(tkse-tksw)/jacs/deltak

pjac=(jac(i,j)+jac(i,j-1)+jac(i-1,j)+jac(i-1,j-1))/4.0d0
sk2=(gen(i,j)-td(i,j))*pjac*dh*dz
sk=sk1+sk2
c.....Hybrid Scheme
AE=(DE+ABS(CE)+ABS(DE-ABS(CE)))/2.0d0-CE
AW=(DW+ABS(CW)+ABS(DW-ABS(CW)))/2.0d0+CW
IF(I.EQ.2)AW=2.0d0*CW+DW
AS=(DS+ABS(CS)+ABS(DS-ABS(CS)))/2.0d0+CS
AN=(DN+ABS(CN)+ABS(DN-ABS(CN)))/2.0d0-CN
AP=AE+AW+AS+AN
c.....  if(ap.lt.0.001d0)ap=0.001d0
C.....FORMING TDMA
AE=AE/AP
AW=AW/AP
AS=AS/AP
AN=AN/AP
Sk=Sk/AP
return
end
*****************************************************************
*%%%%%%%%%%%%%%%%%%%%  SUBROUTINE FOR SOLVING  %%%%%%%%%%%%%%%%%*
*%%%%%%%%%%%%%%%%%%%%%%%%  KINETIC ENERGY  %%%%%%%%%%%%%%%%%%%%*
*%%%%%%%%%%%%%%%%%%%%%%%%  EQUATION  %%%%%%%%%%%%%%%%%%%%%%%%*
*****************************************************************
SUBROUTINE TKEE (m,n,td,tk,tvis,xz,yz,xe,ye,jac,z,h,gen,
*   dk,cmu,omegak,ubar,vbar,deltak,temp,u,v,p,u1)
implicit double precision (a-h,o-z)
real td(m,n),tk(m,n),jac(m,n),h(m,n),z(m,n),tvis(m,n),
*xz(m,n),xe(m,n),yz(m,n),ye(m,n),gen(m,n),temp(m,n),v(m,n),u(m,n),
*a(250),b(250),c(250),t(250),f(250),ubar(m,n),vbar(m,n),p(m,n)

DO 1 I=1,M
DO 1 J=1,n
temp(i,j)=tk(i,j)
1 CONTINUE
do 1000 ii=1,1
C=================================
C.....SWEEP IN X-DIRECTION..
C=================================
DO 10 J=2,N-1
DO 20 I=2,M-1
call kinen(i,j,m,n,td,tk,tvis,xz,yz,xe,ye,jac,z,h,gen,
*   dk,cmu,omegak,ubar,vbar,deltak,ae,aw,an,as,sk,u,v,p)

IF(I.GT.2)GOTO 50
A(I-1)=0.0d0
B(I-1)=1.0d0
C(I-1)=-AE
F(I-1)=AW*tk(I-1,J)+AS*tk(I,J-1)+AN*tk(I,J+1)+Sk
GOTO 20
50 IF(I.EQ.M-1)GOTO 60
A(I-1)=-AW
B(I-1)=1.0d0
C(I-1)=-AE
F(I-1)=AS*tk(I,J-1)+AN*tk(I,J+1)+Sk
GOTO 20
60 A(I-1)=-AW
B(I-1)=1.0d0-ae
C(I-1)=0.0d0
F(I-1)=AS*tk(I,J-1)+AN*tk(I,J+1)+Sk
20 CONTINUE
C.....CALCULATE FINITE DIFF. EQU...
CALL TRIDAG(A,B,C,F,M-2,T)
C.....UNDERRELAXATION OF tk
DO 70 I=2,M-1
tk(I,J)=(1.0d0-OMEGAk)*tk(I,J)+OMEGAk*T(I-1)
!  if(tk(i,j).lt.0.0d0)tk(i,j)=0.001d0
! if(tk(i,j).gt.0.01d0)tk(i,j)=0.01d0
70 CONTINUE
tk(m,j)=tk(m-1,j)
if(j.ne.n-1)goto 10
do 80 i=2,m
tk(i,n)=tk(i,n-1)
80 continue
```

```
10 continue

C....Sweep in y-direction
do 110 i=2,m-1
do 120 j=2,n-1
call kinen (i,j,m,n,td,tk,tvis,xz,yz,xe,ye,jac,z,h,gen,
*   dk,cmu,omegak,ubar,vbar,deltak,ae,aw,an,as,sk,u,v,p)

IF(J.GT.2)GOTO 150
A(J-1)=0.0d0
B(J-1)=1.0d0
C(J-1)=-AN
F(J-1)=AW*tk(I-1,J)+AS*tk(I,J-1)+AE*tk(I+1,J)+Sk
GOTO 120
150 IF(J.EQ.N-1)GOTO 160
A(J-1)=-AS
B(J-1)=1.0d0
C(J-1)=-AN
F(J-1)=AE*tk(I+1,J)+AW*tk(I-1,J)+Sk
GOTO 120
160 A(J-1)=-AS
B(J-1)=1.0d0-an
C(J-1)=0.0d0
F(J-1)=AE*tk(I+1,J)+AW*tk(I-1,J)+Sk
120 CONTINUE
C.....CALCULATE FINITE DIFF. EQU...
CALL TRIDAG(A,B,C,F,N-2,T)
C.....UNDERRELAXATION OF tk
DO 170 J=2,N-1
IF(I.EQ.2.AND.J.EQ.2) Dk=0.0d0
dOO=tk(I,J)
tk(I,J)=(1.0d0-OMEGAk)*tk(I,J)+OMEGAk*T(J-1)
Dk=ABS(tk(I,J)-dOO)+Dk
170 CONTINUE
C.....MODIFY NORTH AND SOUTH WALLS..
tk(I,N)=tk(I,N-1)
IF(I.EQ.M-1)THEN
DO 1111 J=1,N
tk(M,J)=tk(M-1,J)
1111 CONTINUE
ELSE
ENDIF
110 CONTINUE
1000 continue
Dk=dk/(n-2)/(m-2)/0.1d0
print*,'dk=',dk

do 171 i=2,m
do 171 j=2,n
tk(I,J)=(1.0d0-0.2d0)*temp(I,J)+0.2d0*tk(i,j)
171 CONTINUE
return
end
*****************************************************************
SUBROUTINE WALSHR (M,N,U,V,TK,TD,TW2,Ce,Ck,VIS,CMU,DW,x,y)
implicit double precision (a-h,o-z)
real U(M,N),V(M,N),TK(M,N),TD(M,N),y(m,n),x(m,n),TW2(m,n)


RFW=0.2d0
uw1=U(1,1)
DW=0.0d0
DO 10 I=2,M-1
dx1=(x(i,1)-x(i-1,1))/2.0d0
dx2=(x(i+1,1)-x(i,1))/2.0d0
du1=u(i+1,1)-u(i,1)
du2=u(i+1,2)-u(i,2)
r=dx1/(dx1+dx2)
UC1=U(I,1)+r*du1
UC2=U(I,2)+r*du2

TW=1000.0d0*CK*UC2*CMU**0.25*TK(I,1)**.5/LOG(CE*abs(y(i,1)-
*   y(i,3))*CMU**.25*TK(I,1)**.5/VIS)

USTARO=SQRT(TK(I,1)*CMU**.5)
USTARN=SQRT(abs(TW/1000.0d0))
```

```
USTAR=(1.0d0-RFW)*USTARO+RFW*USTARN
TKOLD=TK(I,1)
TK(I,1)=USTAR**2/SQRT(CMU)
DTKW=ABS((TK(I,1)-TKOLD)/TK(I,1))
TDOLD=TD(I,1)
TD(I,1)=USTAR**3/CK/abs(Y(I,1)-y(i,2))
DTDW=ABS((TD(I,1)-TDOLD)/TD(I,1))
UOLD=UC1
UC1=USTAR/CK*LOG(CE*abs(y(i,1)-y(i,2))*USTAR/VIS)
DUW=ABS((UC1-UOLD)/UC1)
U(I,1)=(UW1+UC1)/2.0d0
UW1=UC1
DWMAX=DMAX1(DTKW,DTDW,DUW)
DW=DW+DWMAX
TW2(i,1)=TW
10 CONTINUE
TW2(m,1)=TW2(m-1,1)
u(m,1)=u(m-1,1)
tk(m,1)=tk(m-1,1)
td(m,1)=td(m-1,1)
DW=DW/(M-2)
DO 20 I=2,M-1
DY=y(i,1)
DX=(x(I+1,1)-x(I-1,1))/2.0d0
V(I,1)=dy/dx/2.0d0*(U(I,1)-U(I+1,1))
20 CONTINUE
V(M,1)=V(M-1,1)
RETURN
END
*************************************************************************
*            SUBROUTINE FOR GRID GENERATION                             *
*            SIMPLE TRANSFORMATION IS USED                              *
*************************************************************************
SUBROUTINE GRID (ii,m,n,x,y,h,z,xz,xe,yz,ye,jac,a,b,c,tol,y1,y2,Fr,
* Subm,L,yt)
implicit double precision (a-h,o-z)
real x(m,n),y(m,n),h(m,n),z(m,n),xz(m,n),xe(m,n),
* a(m,n),b(m,n),c(m,n),jac(m,n),L,ye(m,n),yz(m,n)

if(ii.ne.1)goto 11
x(1,1)=0.0d0
x(M,1)=L
y(M,1)=0.0d0
x(1,N)=0.0d0
y(1,N)=yt
x(M,N)=L
y(M,N)=yt

dx=L/(M-1)
Do j=1,N
Do i=2,M
x(i,j)=x(i-1,j)+dx
Enddo
Enddo
Do j=1,N
Do i=1,M
z(i,j)=x(i,j)
Enddo
Enddo
do i=1,m
y(i,n)=yt
enddo
11  do i=1,M
y(i,1)=(0.00086d0)+ (-0.537d0*x(i,1))+(1.205d0*x(i,1)**2)+
* (-0.93d0*x(i,1)**3)+(0.25d0*x(i,1)**4)
enddo
do i=1,m
IF(y(i,1)<0.) THEN
dy=(y(i,n)+ABS(y(i,1)))/(N-1)
do j=2,n
y(i,j)=y(i,j-1)+dy
Enddo
else
dy=(y(i,n)-y(i,1))/(N-1)
do j=2,N
y(i,j)=y(i,j-1)+dy
```

```
Enddo
endif
Do j=2,N
h(i,j)=(y(i,j)-y(i,1))/(y(i,n)-y(i,1))
Enddo
Enddo
call coeff(m,n,x,y,a,b,c,jac,xe,ye,xz,yz,z,h)
end
*****************************************************************
SUBROUTNE COEFF (m,n,x,y,a,b,c,jac,xe,ye,xz,yz,z,h)
implicit double precision (a-h,o-z)
real a(m,n),b(m,n),c(m,n),jac(m,n),x(m,n),y(m,n),
*    xz(m,n),xe(m,n),yz(m,n),ye(m,n),z(m,n),h(m,n)

do 10 i=2,m-1
do 20 j=2,n-1
dz=z(i+1,j)-z(i-1,j)
de=h(i,j+1)-h(i,j-1)
xe(i,j)=(1.0d0/de)*(x(i,j+1)-x(i,j-1))
ye(i,j)=(1.0d0/de)*(y(i,j+1)-y(i,j-1))
xz(i,j)=(1.0d0/dz)*(x(i+1,j)-x(i-1,j))
yz(i,j)=(1.0d0/dz)*(y(i+1,j)-y(i-1,j))
20 continue
10 continue

do 30 j=2,n-1
dz=z(3,j)-z(1,j)
xz(1,j)=(1.0d0/dz)*(-x(3,j)+4.0d0*x(2,j)-3.0d0*x(1,j))
yz(1,j)=(1.0d0/dz)*(-y(3,j)+4.0d0*y(2,j)-3.0d0*y(1,j))
dz=z(m,j)-z(m-2,j)
xz(m,j)=(1.0d0/dz)*(x(m-2,j)-4.0d0*x(m-1,j)+3.0d0*x(m,j))
yz(m,j)=(1.0d0/dz)*(y(m-2,j)-4.0d0*y(m-1,j)+3.0d0*y(m,j))
de=h(1,j+1)-h(1,j-1)
xe(1,j)=(1.0d0/de)*(x(1,j+1)-x(1,j-1))
ye(1,j)=(1.0d0/de)*(y(1,j+1)-y(1,j-1))
de=h(m,j+1)-h(m,j-1)
xe(m,j)=(1.0d0/de)*(x(m,j+1)-x(m,j-1))
ye(m,j)=(1.0d0/de)*(y(m,j+1)-y(m,j-1))
30 continue

do 40 i=2,m-1
de=h(i,3)-h(i,1)
xe(i,1)=(1.0d0/de)*(-x(i,3)+4.0d0*x(i,2)-3.0d0*x(i,1))
ye(i,i)=(1.0d0/de)*(-y(i,3)+4.0d0*y(i,2)-3.0d0*y(i,1))
de=h(i,n)-h(i,n-2)
xe(i,n)=(1.0d0/de)*(x(i,n-2)-4.0d0*x(i,n-1)+3.0d0*x(i,n))
 ye(i,n)=(1.0d0/de)*(y(i,n-2)-4.0d0*y(i,n-1)+3.0d0*y(i,n))
dz=z(i+1,1)-z(i-1,1)
xz(i,1)=(1.0d0/dz)*(x(i+1,1)-x(i-1,1))
yz(i,1)=(1.0d0/dz)*(y(i+1,1)-y(i-1,1))
dz=z(i+1,n)-z(i-1,n)
xz(i,n)=(1.0d0/dz)*(x(i+1,n)-x(i-1,n))
yz(i,n)=(1.0d0/dz)*(y(i+1,n)-y(i-1,n))
40 continue

de=h(1,3)-h(1,1)
xe(1,1)=(1.0d0/de)*(-x(1,3)+4.0d0*x(1,2)-3.0d0*x(1,1))
ye(1,1)=(1.0d0/de)*(-y(1,3)+4.0d0*y(1,2)-3.0d0*y(1,1))
dz=z(3,1)-z(1,1)
xz(1,1)=(1.0d0/dz)*(-x(3,1)+4.0d0*x(2,1)-3.0d0*x(1,1))
yz(1,1)=(1.0d0/dz)*(-y(3,1)+4.0d0*y(2,1)-3.0d0*y(1,1))
de=h(1,n)-h(1,n-2)
xe(1,n)=(1.0d0/de)*(x(1,n-2)-4.0d0*x(1,n-1)+3.0d0*x(1,n))
ye(1,n)=(1.0d0/de)*(y(1,n-2)-4.0d0*y(1,n-1)+3.0d0*y(1,n))
dz=z(3,n)-z(1,n)
xz(1,n)=(1.0d0/dz)*(-x(3,n)+4.*x(2,n)-3.*x(1,n))
yz(1,n)=(1.0d0/dz)*(-y(3,n)+4.*y(2,n)-3.*y(1,n))
de=h(m,3)-h(m,1)
xe(m,1)=(1.0d0/de)*(-x(m,3)+4.0d0*x(m,2)-3.0d0*x(m,1))
ye(m,1)=(1.0d0/de)*(-y(m,3)+4.0d0*y(m,2)-3.0d0*y(m,1))
dz=z(m,1)-z(m-2,1)
xz(m,1)=(1.0d0/dz)*(x(m-2,1)-4.0d0*x(m-1,1)+3.0d0*x(m,1))
yz(m,1)=(1.0d0/dz)*(y(m-2,1)-4.0d0*y(m-1,1)+3.0d0*y(m,1))

de=h(m,n)-h(m,n-2)
xe(m,n)=(1.0d0/de)*(x(m,n-2)-4.0d0*x(m,n-1)+3.0d0*x(m,n))
```

```
ye(m,n)=(1.0d0/de)*(y(m,n-2)-4.0d0*y(m,n-1)+3.0d0*y(m,n))
dz=z(m,n)-z(m-2,n)
xz(m,n)=(1.0d0/dz)*(x(m-2,n)-4.0d0*x(m-1,n)+3.0d0*x(m,n))
yz(m,n)=(1.0d0/dz)*(y(m-2,n)-4.0d0*y(m-1,n)+3.0d0*y(m,n))

do 50 i=1,m
do 50 j=1,n
a(i,j)=xe(i,j)**2+ye(i,j)**2
b(i,j)=xz(i,j)*xe(i,j)+yz(i,j)*ye(i,j)
c(i,j)=xz(i,j)**2+yz(i,j)**2
jac(i,j)=xz(i,j)*ye(i,j)-xe(i,j)*yz(i,j)
50 continue
return
end
*****************************************************************
SUBROUTINE  TRIDAG (A,B,C,F,N,T)
 implicit double precision (a-h,o-z)
real A(250),B(250),C(250),F(250),T(250)
DO 5 I=2,N
D=A(I)/B(I-1)
B(I)=B(I)-C(I-1)*D
F(I)=F(I)-F(I-1)*D
5 CONTINUE
T(N)=F(N)/B(N)
DO 6 I=1,N-1
J=N-I
T(J)=(F(J)-C(J)*T(J+1))/B(J)
6 CONTINUE
RETURN
END
*****************************************************************
```